Spring 1-1-2011

# Probabilistic Models for Uniform and Non-Uniform Snow Loading on Roofs

Kyle Allen Jackson
*University of Colorado at Boulder*, kyle.jackson@colorado.edu

# PROBABILISTIC MODELS FOR UNIFORM AND NON-UNIFORM SNOW LOADING ON ROOFS

by
KYLE JACKSON

B.S. Colorado School of Mines, 2009

M.S. University of Colorado, 2010

A thesis submitted to the
Faculty of the Graduate School of the
University of Colorado in partial fulfillment
of the requirement for the degree of
Masters of Science
Department of Civil, Environmental and Architectural Engineering

November 30, 2010

This thesis entitled:
Probabilistic Models for Uniform and Non-Uniform Snow Loading on Roofs
Written by Kyle Jackson
Has been approved for the Department of Civil, Environmental and Architectural Engineering

_____
(Abbie Liel)

_____
(Ross Corotis)

_____
(George Hearn)

Date_____

The final copy of this thesis has been examined by the signatories, and we
Find that both the content and the form meet acceptable presentation standards
Of scholarly work in the above mentioned discipline.

## ABSTRACT

Jackson, Kyle Allen (M.S., Structural Engineering, Department of Civil, Environmental and Architectural Engineering)

Probabilistic Models for Uniform and Non-Uniform Snow Loading on Roofs

Thesis directed by Assistant Professor Abbie Liel

Snow loads account for a majority of roof damage and associated losses in the United States. The significant impact that snow related failures can have on the safety of people and the economic losses associated with business closures and repair costs make the design and mitigation of snow related failures very important. The purpose of this thesis is to develop models to predict roof snow loads, for use in performance-based engineering. Performance-based snow engineering can provide decision makers with a better, quantitative understanding of snow related risks.

Two probabilistic models were developed to have an understanding of the factors that affect the magnitude and distribution of roof snow load. The models developed are different from building codes and standards, where the model predicts the roof snow load for a single snow event instead of a 50-year maximum roof snow load used in design standards. The first model predicts uniform roof snow loads, given a ground snow load and roof characteristics; the second model predicts non-uniform drifting snow loads for multilevel roofs, given ground snow load, ground snow density and roof characteristics.

Ground snow load hazard curves, or predictions of the probability that a specified ground snow load level will be exceeded in a particular year, are available from weather data. The probabilistic load models can be used in a performance-based engineering framework to predict

the likelihood that certain critical deflections or stresses will be exceeded. In this study, the models are used to predict deflections and stresses in an open walkway roof structure. Hazard curves were developed to show the probability of exceedance of a critical deflection for different ground snow loads. Hazard curves of this type can be used in analysis of other light-weight steel structures to develop metrics of structural failure and collapse that can help building owners decide whether to invest in retrofitting roofs.

## ACKNOWLEDGMENTS

I would like to thank my advisor, Professor Abbie Liel, for her assistance, advice and experience throughout the process of this project. In addition, I would like to thank the other members of my committee, Professor George Hearn and Professor Ross Corotis, for their advice and guidance.

I would also like to thank Professor Michael O'Rourke at Rensselaer Polytechnic Institute, who provided much of the data and publications used in this project. His assistance and great intellectual thought in snow load design and hazard mitigation was of great help in the development of this thesis. In addition I would like to thank Shedd Webster, property manager at Copper Mountain, Colorado for his time in discussing the snow load failures that occurred at Copper Mountain.

In addition, I would like to thank the University of Colorado and my classmates for their assistance in programing, modeling and research efforts. In particular I would like to thank Jamie Geis, Kristen Strobel and Natasha Ayala for their assistance in this research project. I would also like to thank the National Science Foundation and the research program, Hazard Mitigation and Structural Engineering, who provided funding for this research project. It is greatly appreciated.

Lastly, I would like to thank my friends and family for their continued support throughout my graduate and undergraduate studies. In particular I would like to thank my grandfather, Bruce Riggs, Ph.D. in metallurgical engineering, for his support, advice and critique of my writing and research. I would also like to thank my parents, Dallas and Susan Byers for their continued support.

**CONTENTS**

## TABLES

## FIGURES

# 1. INTRODUCTION

## *1.1 Background*

Snow loads are a consideration in the design of almost all roof systems in the United States. The importance of accurately determining the design snow load is made apparent by previous snow related roof collapses in the United States and worldwide. According to statistics compiled by the insurance industry, snow loads account for approximately 55% of all roof losses reported to insurance companies, and of these 75% are due to drift loads on multilevel roofs (O'Rourke et al. 1986). Snow related failures can have significant impact on not only the safety of people who occupy snow-damaged buildings, but also on communities and businesses. Repairs due to snow related failures can lead to business closures, which result in millions of dollars in lost revenue. According to a study by Geis et al. (2010), snow induced building failures caused business closure lasting for four months on average and costing up to $200 million in repair costs and economic losses for a single building failure. Interestingly, Geis et al. (2010) reported many of the snow induced failures in new construction, i.e., buildings constructed in the last ten years, indicating that buildings designed to new snow design provisions are still at risk. This thesis describes work to develop roof snow load estimating methods that may be incorporated in a performance-based design methodology, which can be used to provide decision makers with a quantitative understanding of snow related risks.

Performance-based engineering is a methodology that has been mainly used in seismic analysis to analyze building performance under normal and extreme loading (Moehle and Deierlein 2004). Performance-based methodology has not yet been applied to snow engineering, but the principles used in seismic engineering can be applied to snow loading in a similar manner. A performance-based design and assessment framework can be used to make decisions

about the design to reduce life cycle costs and mitigate risks. Performance-based engineering differs from conventional design in that it looks at the performance of a building in terms of metrics of interest to building owners, such as the probability of collapse in a certain time frame, economic losses associated with repairing the structure or the likelihood of interrupting business due to building closure. By informing building owners of the consequences and the likelihood of economic loss, their decision to invest in upgrading the design is based on a quantifiable estimate of the reduction in future risk. The importance of mitigating snow risk is evident based on the recent failures both nationally and internationally of large structures, where the large number of occupants or the large amounts of lost revenue due to business interruption leads to substantial consequences. By using a performance-based methodology, decisions about the structural design can account for the risks of snow induced failure.

*1.2 Objectives and Scope*

In this study, probabilistic roof snow load models were developed, which can be used in the context of performance-based design and assessment to improve decision making in snow design. To develop a probabilistic model for the magnitude and distribution of roof snow loads, two models were developed: one to convert ground snow load value to a uniform roof snow load value and another to convert a ground snow load to a drift snow load on multilevel roofs. In the first model, the uniform roof snow load was predicted from a given ground snow load and several structural parameters, such as exposure, thermal, slope, material, etc. The model is probabilistic and predicts the roof snow load distribution using a Monte Carlo simulation that samples the probability distribution of each of the underlying factors that affect the conversion of ground snow load to roof snow load. Current design standards estimate a maximum roof snow load for a 50-year period based on a 50-year maximum ground snow load and structural

parameters; the model developed estimates the roof snow load at a particular time from a ground snow load at the same time (single event). By predicting the roof snow load on an event-by-event basis we can use the data to develop a probabilistic representation of snow-related risk, which will be discussed later. The second model predicts a drift load based on a given ground snow load and different structural parameter that affect the drift load, including, exposure, thermal, roof length, snow density, etc.

Finally, a case study roof structure is modeled to examine its failure under extreme snow loading. Using the model for uniform loads, the structural model will be loaded reporting different failure mechanisms, such as, exceedance of deflection limits. Hazard curves showing the risks of collapse for different ground snow loads can be used to inform decision makers of possible risks of collapse.

*1.3 Thesis Organization*

The following is an outline of each of the chapters in this thesis. Chapter 2 is a literature review that describes past research on ground snow load data in the United States and methods for predicting roof snow loads on the basis of ground snow loads. The first part of Chapter 3 reviews how American design standards account for different conditions on the roof, such as wind, thermal, slope and material, affect the uniform roof snow load design. In addition, it reviews existing literature to determine the factors that affect roof snow loads and how this differs from ground snow loads. As part of this review, case studies and other relevant publications on snow load structural failures in the United States are included. The second part describes the development of the uniform probabilistic roof snow load model and how the model differs from typical standard-based estimates of roof snow loads for design purposes. The

probabilistic model considers roof conditions such as, exposure, thermal, slope and material to estimate a roof snow load from a ground snow load for a particular snow event.

Chapter 4 first describes how drifting snow loads occur and how they are accounted for in roof snow load design in American standards. This information provides the basis for the probabilistic model developed here for predicting drift formation and size. The drifting model considers roof conditions that affect the size of the drift load, such as exposure, thermal, roof length and snow density in order to predict a maximum drift load for a particular snow event.

Chapter 5 is a literature review of case studies of past structural failures due to snow. Chapter 5 also describes the case study used in Chapter 6 and why this structure was chosen to model. Chapter 6 describes the analytical model of the case study building, loading applied and the results of the structural model in terms of deflections, stresses, and risk of snow-related damage. The structure is modeled under three distinct loading conditions: (1) code design load levels, (2) snow loads estimated on the day of failure and (3) the probabilistic uniform load models developed in Chapter 3. Using the results, a hazard curve was developed for the structure showing the risk of excessive deflection or stresses for different ground snow loads.

Lastly, Chapter 7 is a discussion of the results found in this study and how these results differ from snow design standards in the United States. In addition, it is shown how the results can be used to reduce the probability of snow induced failures, reducing life cycle costs and mitigating risk. Finally, how these results can be used to further develop the performance-based methodology in snow load engineering.

## 2. GROUND SNOW LOADS

Ground snow loads provide the basis for roof snow load used in structural design. The variability in snow conditions make scientists and engineers uncertain of the amount of snow for which to design. Snow levels also vary from year to year and season to season. In addition, snow density can vary, making the loads different from year to year or even storm to storm. Due to these uncertainties, building code committees and structural designers must try to stay ahead by continuously monitoring snow depths and adjusting ground snow load maps and design equations. Engineers must then use these provisions and engineering judgment so roofs are designed economically, but effective in preventing snow induced failures. This section discusses the history of ground snow load data, the methodology for calculating maximum ground snow loads and the methods by which the current design standard uses ground snow loads to predict roof snow loads.

### *2.1 History of Development of Ground Snow Load Provisions*

The design snow load for a particular structure, using American standard and building code provisions in ASCE 7-10 and IBC (2006), is determined from a ground snow load estimate that is then adjusted to predict roof snow load, based on the exposure of the site, the thermal characteristics of the structure, the slope of the roof and the importance of the structure. The ground snow loads in current American standards were developed after many years of collecting weather data including snow depth and snow density. The snow data is continuously changing and standards must be updated to accommodate these changes.

The ground snow loads for U.S. snow design were first determined by Thom in 1955 based on data of annual maxima of the water equivalent of ground snow. Annual maxima water equivalent values are obtained from weather stations that report the amount of snow in either

water equivalents of snow or simply as the snow depth. Water equivalent values are preferred over snow depth measurements because water equivalent values can be uniformly converted to a ground snow load using the relationship:

$$P_g = \frac{62.4}{12} d_w \qquad (1)$$

where $P_g$ is the ground snow load (psf), 62.4 is the density of water (lb/ft$^3$) and $d_w$ is the water equivalent depth (in.). Snow depth measurements, on the other hand, must be converted using the density of the snowpack. Density can vary by time of year or geographic location, making it difficult to gather consistent ground snow load data. Using a lognormal distribution of the maximum water equivalents for a given year, the ground snow load for design was computed to have a mean recurrence interval of 50 years. In other words, the design ground snow loads developed in the design standard would have a 2% probability of being exceeded in any given winter. These values, obtained by Thom, for the 50-year recurrence interval were used to develop the ground snow load map in the 1972 American National Standard (O'Rourke and Stiefel 1983).

The ground snow load map was updated in the 1982 American National Standard based on work done by Tobiasson and Redfield (1983) who also used a similar lognormal distribution, but with a longer historical record of data. A similar form of developing design ground snow loads for building standards has continued over the past 30 years, but it is continuously updated as more ground snow load data become available and more station instruments are included.

The lognormal probability density function used to develop the 50-year mean recurrence interval for ground snow loads is obtained from the equations below:

$$F_{p_g}\ p_g = \Phi\ \frac{ln\, p_g - \lambda_g}{\zeta_g} \qquad (2)$$

$$F_{p_g} = 1 - \frac{1}{N} \qquad (3)$$

$F_{p_g}$ - cumulative distribution function of the yearly maximum ground snow load
$p_g$ - the N-year ground snow load
$\lambda_g = E[\ln(P_g)]$
$\zeta_g = \mathrm{Var}[\ln(P_g)]$
$\Phi$ = the standard normal integral
$N$ = the return period for the ground snow load level of interest (e.g., 50 years)

Equations *(2)* and *(3)* can be used to determine ground snow loads. Based on snow data from the National Weather Service (NWS) the expected value of the natural logarithm of the maximum ground snow ($\lambda_g$) and the variance of the natural logarithm of the maximum ground snow ($\zeta_g$) can be determined. After determining the expected value and variance and using a standard normal probability table the N-year ground snow load can be determined (Equation *2*). To determine the ground snow load with a 50-year recurrence, the probability of exceedance is computed from Equation *(3)*, i.e., $F(p_g) = 0.98$, implying there is a 98% chance that the snow load is lower than the 50-year level in a given year and a 2% chance the 50-year snow load is exceeded. The 50-year ground snow load has been used as the basis for design since the 1972 standard. The ground snow load value with 2% chance of exceedance was calculated for many different locations across the country where weather service data were available. A ground snow load map could then be developed within a 5 psf range for most territories in the United States.

To demonstrate how the 50-year maximum ground snow load is calculated, snow data for Copper Mountain, CO were taken from the National Water and Climate Center (2010). The data are reported in water equivalent values from January, 1979 through December of 2010. Water equivalents were reported daily and the maximum value was taken for each year. Using MATLAB the annual maximum values were lognormally distributed using 10,000 observations.

The histogram of the lognormally distributed data is shown in Figure 2.1. On average the maximum water equivalent of snow at Copper Mountain is 16.6 in., corresponding to 86.3 psf, in a given year. Using the lognormal probability density function, as shown in Equation *2*, the 50-year mean recurrence interval of water equivalent value for Copper Mountain, CO was found to be 25.6 in. Using Equation *(1)*, the 50-year mean water equivalent value was converted to a 50-year ground snow load of 133 psf. This is a very high value for ground snow loads compared to many parts of the country, but this is expected since the station is located at approximately 10,000 feet elevation and in the middle of the Rocky Mountains.

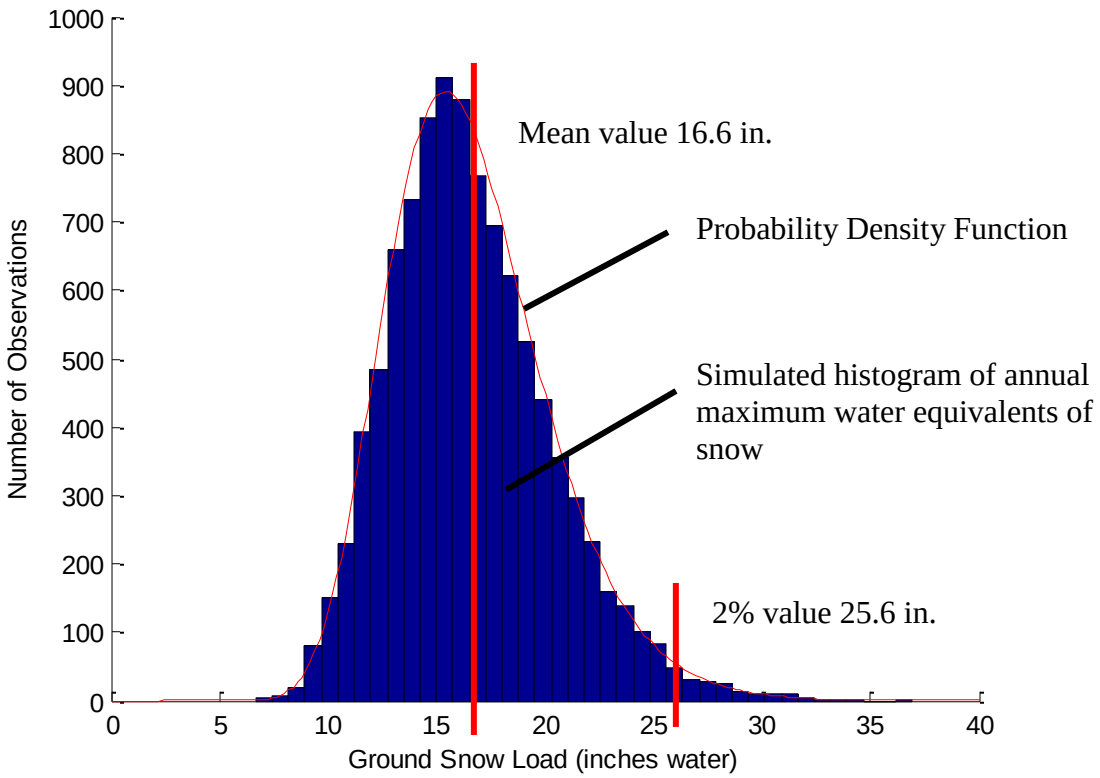


**Figure 2.1-** Annual maximum ground snow load for Copper Mountain, CO in inches of water

*2.2 ASCE 7-10 Ground Snow Load*

The current design standard, ASCE 7-10, uses a similar procedure of using a lognormal distribution to develop the ground snow load map. Data of the depth and load of snow (i.e., the

water equivalent) on the ground were used from 204 National Weather Service (NWS) locations each having a minimum of 11 years of data, called first order locations; second order locations only reported the depth of the snow (Tobiasson and Greatorex 1996). The average period of record for the locations was 33 years and the data was taken through the winter of 1991-1992. A lognormal distribution (Equation *2*) was used to obtain 2% probability of exceedance snow depths and 2% probability of exceedance snow loads for the first order locations. Then a nonlinear relationship was used to estimate the 50-year mean recurrence interval ground snow load at the 9,200 other locations where only the snow depth was measured (Equation *4*).

$$p_g = 0.279 h_g^{1.36} \qquad (4)$$

$p_g$- 50-year maximum ground snow load in psf
$h_g$- 50-year maximum ground snow depth in inches

Tobiasson and Greatorex (1996) used Equation *(4)* to tabulate 50-year ground snow load data for the 9,200 second order NWS locations across the United States. In general, the loads from Equation *(4)* and loads reported at first order locations were in agreement and, where they were not, the first order location was considered to be more valuable. The data was then used to construct the snow load map in ASCE 7-95. Even with the addition of record winters in areas in the east coast from the winter of 1992-1993 the 50-year maximum ground snow loads changed by very little from past standards. This is due to many NWS locations having over 20 years of snow data, making the 50-year maxima a consistent value that will not really change even with record snow falls. For that reason, the ground snow map has not changed since the ASCE 1995 standard.

In the ground snow loads map of ASCE 7-10, the ground snow load is given in 5 psf increments. The ground snow load depends on locations the latitude, distance from the coast and elevation. For example, the 50-year ground snow load for Eastern Colorado (East of Denver) is

20 psf and the value increases to as much as 50 psf in North Dakota near the Canadian border. In many regions, the ground snow is only applicable if the site's elevation is below a specified limit. If the site of a structure is above this elevation the ground snow load must be determined from case studies in that region. Regions on the map with "CS" indicate that specific case studies for a particular site must be used to determine the ground snow load, since "the extreme local variations in ground snow loads in these areas preclude mapping at this scale" (ASCE 7-10). In these regions Equation *(4)* may no longer be an accurate relationship of ground snow depth to ground snow load and having additional statistical data could improve the accuracy of the ground snow loads in these regions. In many of the states that have case study regions, the local structural engineers' association develops a snow load map using the methods described above, but in much greater detail (Tobiasson and Greatorex 1996). For example, over half the state of Colorado is labeled as CS in the ASCE 7-10 ground snow load map so the Structural Engineering Association of Colorado (SEAC) developed a more detailed ground snow load map based on site-specific case studies.

As an example of how state structural engineering associations develop ground snow load maps for case study regions, Lee and Rosowsky (2005) determined 50-year ground snow load values for case study areas in Oregon. The state of Oregon was split into 23 regions with similar trends between ground snow load and elevation. A hazard curve for one of the counties in Oregon is shown in Figure 2.2 (a), which shows the probability of exceeding a particular ground snow level, depending on the elevation. Lee and Rosowsky (2010) used these same curves to develop a ground snow load hazard curve, which could be used in performance-based design of structures, as shown in Figure 2.2 (b). Figure 2.3 shows a hazard curve developed for the Copper Mountain, CO site described above and used in the case study in Chapter 6.

These curves can be combined with fragility curves for roof capacity, where the probability of roof collapse can be determined from a ground snow load. Relating the ground snow load to the roof snow load and determining the probability of roof collapse is one of the goals of the Monte Carlo roof snow load model developed in the next chapter.

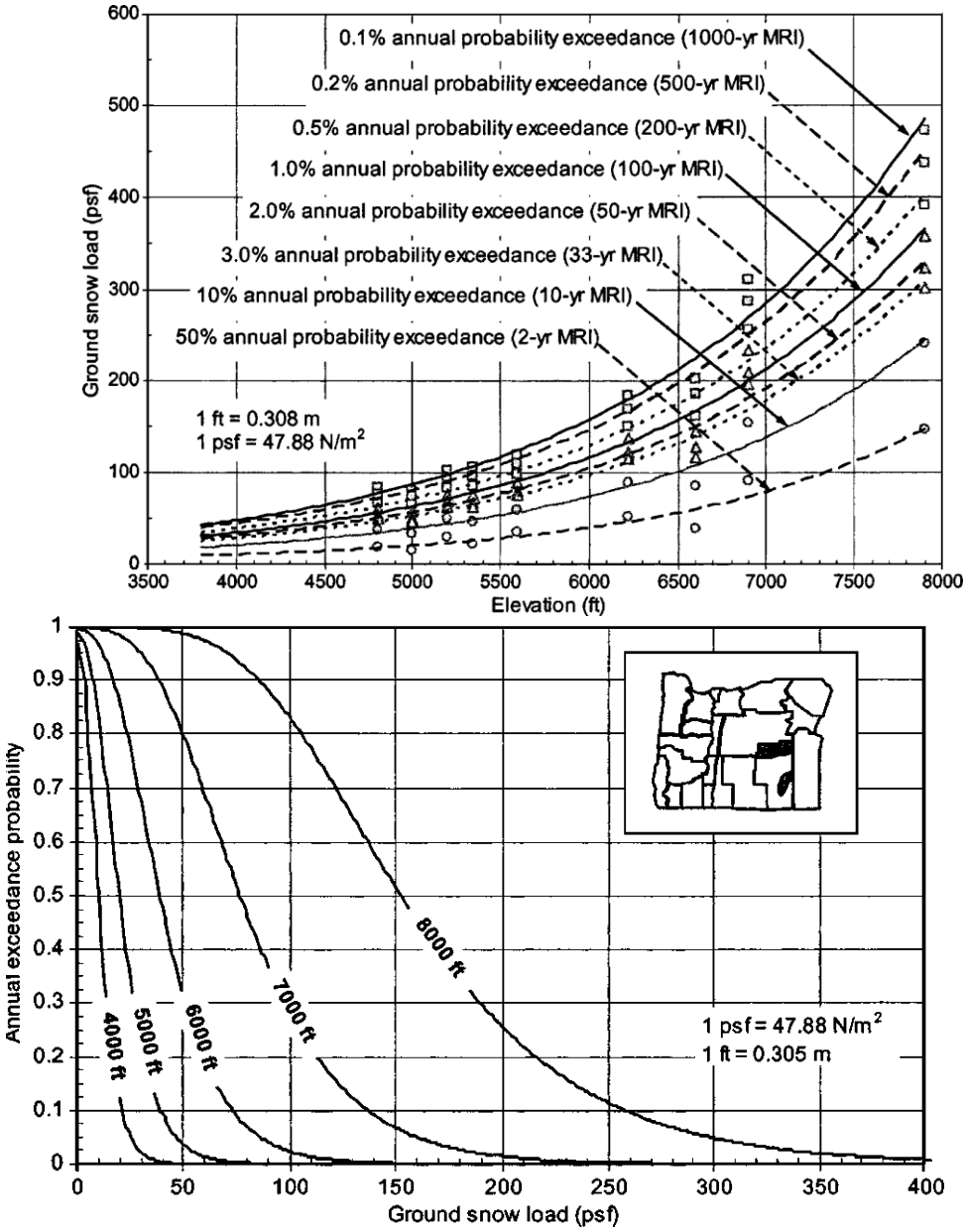


**Figure 2.2-** (a) Probability of the ground snow load being exceeded as a function of elevation for one of the counties in Oregon. Figure 2.2 (b) Ground snow hazard curves for the same county in Oregon as a function of ground snow load (Lee and Rosowsky 2005).

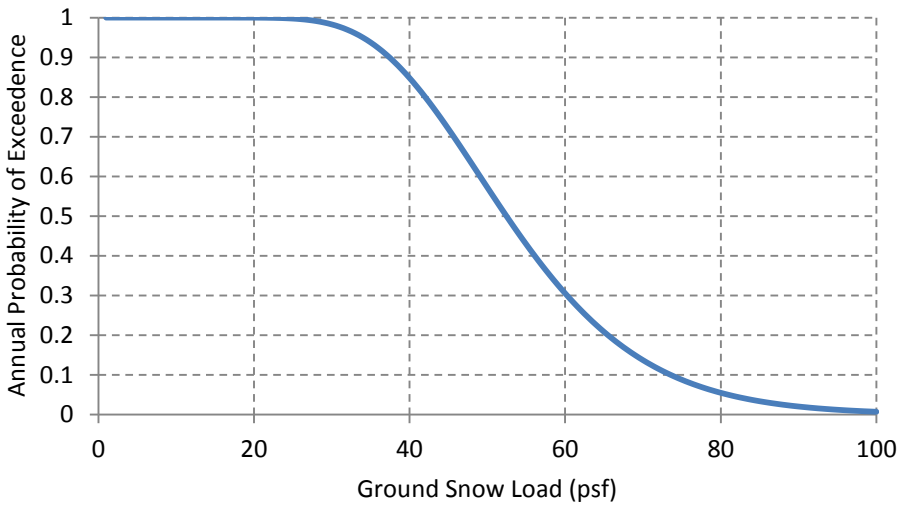


**Figure 2.3-** Ground snow hazard curve for Copper Mountain, CO.

## 3. UNIFORM ROOF SNOW LOAD PROBABILISTIC MODEL

Roof snow load design is a function of the ground snow load and the factors that affect the amount of snow that will accumulate on the roof. For example, if a structure is heated, a portion of the snow on the roof will melt, reducing the roof snow load in relation to that on the ground. Scientists and engineers have over 60 years of ground snow load data and have a fairly good understanding of snow patterns and snow accumulation across the country. On the other hand, roof snow loads are inherently more complicated because of the varying roof properties for different structures, such as structure heating parameters, roof exposure, etc. In addition, there is more limited data on roof snow loads, and therefore conversion factors for ground to roof snow loads are used to develop roof snow load estimates.

ASCE 7-10's snow load provisions have several factors that reduce or increase the roof snow load for a particular structure in a particular climate or region. In this Chapter, the conversion factors that are currently in design standards and the factors that are not included in the standard that could also affect roof snow load estimates are discussed (Section 3.1). In Section 3.2, a computer program using MATLAB software was developed to give a probabilistic model of the conversion of ground snow load to roof snow load given a set of input parameters about the structure and past measurements of roof snow loads. This model was developed to obtain a prediction of the roof snow load from a ground snow load for a site-to-site basis. The model allows one to determine the roof snow load given the ground snow load, thermal and exposure conditions of the structure, roof material, and roof slope. These values can later be used to develop ground snow load hazard curves for a specific case study and location where weather data are available.

### 3.1 Roof Snow Load Factors Used in Design

The roof snow load for design is determined using Equation *(5)* from ASCE 7-10.

$$P_r = 0.7(C_s)(C_e)(C_t)(I)P_g \qquad (5)$$

In Equation *(5)*, $P_r$ is the roof snow load, *0.7* is the ground to roof conversion factor, $C_s$ is the roof slope conversion factor, $C_e$ is the exposure conversion factor, $C_t$ is the thermal conversion factor, $I$ is the importance Factor and $P_g$ is the design ground snow load (50-year mean recurrence interval). The factors $C_s$, $C_e$ and $C_t$ describe conditions on the roof and will either increase or decrease the amount of snow on the roof in relation to the ground snow load although in general the design roof snow load, $P_r$, is smaller than the ground snow load, $P_g$, due to factors such as wind and thermal properties of the structure. The importance factor, $I$, is a design adjustment factor based on the importance of the structure (hospitals and schools with many occupants are designed to withstand high loads -- greater $I$ -- than a residential structure). The $C_e$ factor accounts for the effects of wind either blowing a portion of the snow off the roof, or surrounding buildings/roofs, trees or other obstructions that limit the amount of snow removal due to wind, and varies from 0.8 to 1.2 for windswept and sheltered roofs, respectively. The $C_t$ factor relates to the reduction in snow load that may occur due to the amount of heat flux radiating through the roof or the limited heat flux in an unheated structure, and varies from 0.85 to 1.2 for heated greenhouses and unheated structures, respectively. Lastly, the $C_s$ factor accounts for the amount of snow that will slide off the roof due to the slope and this value varies from 0 to 1.0 depending on the thermal parameter, roof material and slope.

Roof design values are then used in either Allowable Stress Design (ASD) or Load and Resistance Factor Design (LRFD) load combinations for structural design. The LRFD [ASD] load combinations that account for snow load are:

$1.2D + 1.6L + 0.5(L_r \text{ or } S)$ [in ASD, $D + (L_r \text{ or } S)$]

$1.2D + 1.6(L_r \text{ or } S) + 0.8L$ [$D + 0.75L + 0.75(L_r \text{ or } S)$]

$1.2D + 1.6W + L + 0.5(L_r \text{ or } S)$ [$D + .75(W \text{ or } 0.7E) + 0.75L + 0.75(L_r \text{ or } S)$ ]

$1.2D + 1.0E + L + 0.2S$

In these equations, D is the dead load, L is live load, S is snow load ($P_r$ in Equation *5*), and $L_r$ is the roof live load. The snow load is to be used instead of the roof live load when the snow load is larger than the live roof load of 20 psf defined in ASCE 7-10. Design roof snow loads *($P_r$)* are based on a 50-year mean recurrence interval, meaning that the design ground snow load has a 2% probability of being exceeded in any given winter season for a particular location. In the following sections, the development of factors for snow load design, based on studies of ground and roof snow data are described.

*3.1.1 CRREL Study of Uniform Roof Snow Loads*

Over the past 50-60 years a substantial amount of data have been collected for ground snow loads, but many fewer have been collected on roof snow loads. The report, "Analysis of roof snow load case studies: Uniform loads", prepared on behalf of the US Army Corps of Engineers, Cold Regions Research & Engineering Laboratory (CRREL) was done to have a better understanding of roof snow loads in different areas of the country (O'Rourke et al. 1983). The data collected in the report would have a substantial influence on snow load design in U.S. design standards. Over the three year study, a total of 199 structures were analyzed in different regions of the country, making it the largest collection of roof snow load information in the United States. Data were collected on both the ground and roof to determine the conversion factor for uniform roof snow load for flat and sloped roofs. Specifically, the data collected show how thermal, wind and slope of the roof affect the conversion of ground snow load to uniform roof snow load. Although roof snow load data for both uniform loads and drifting loads were

gathered, the findings focused on the uniform roof snow loads, being limited to roof geometries that do not form drifts, leaving out parapet roofs and multilevel roofs. The following paragraphs describe the findings of the report and how the results influenced snow design standard changes in the 1980's.

Each researcher from the participating universities was assigned to select a number of structures in their area. Structural characteristics encompassed a range of roof exposures, geometries and thermal characteristics. Researchers measured snow density and were given instructions on how to measure ground and roof snow to ensure uniformity in data results. In addition, the contract manager from CRREL visited all the universities and a number of the structures to maintain consistency in the exposure rating and collection of data. In the CRREL data, some buildings were visited over two or three winter seasons, therefore providing as many as three case studies for the same building. In addition, each building may be been visited several times within a single season. From the data, a conversion factor that related the roof snow load to the ground snow load was developed. The conversion factor was determined based on exposure, thermal and slope effects (O'Rourke et al. 1983).

Two conversion factors were proposed. $C_v$ is the ratio of roof to ground snow load for a particular event or data collection visit:

$$C_v = \frac{h_r * \gamma_r}{h_g * \gamma_g} \qquad (6)$$

$C_m$ is the ratio of maximum roof load to maximum ground load in a single winter season:

$$C_m = \frac{(h_r \gamma_r)_{max}}{(h_g \gamma_g)_{max}} \qquad (7)$$

In Equations *(6)* and *(7)*, $h_r$ is the depth of snow on the roof (ft.), $h_g$ is the depth of snow on the ground (ft.), $\gamma_r$ the roof snow density (pcf) and $\gamma_g$ is the ground snow density (pcf). Values of $C_v$ and $C_m$ are not the same because the maximum ground and roof snow loads may not occur at the

same time. In about half of the case studies in the report, the maximum roof load occurred at some time during the winter before the maximum ground load. In 40% of the case studies, the maximum roof and ground loads occurred at the same visit, and in about 10% of the case studies, the maximum roof load occurred at some time after the maximum ground load. The pattern of seasonal snowfall has an effect on the timing of maximum ground and roof snow loads, as well. For buildings located in regions where there are a few large snowstorms separated by warmer temperatures, the maximum ground and roof snow loads occur just after the largest snowfall, making the conversion factor close to 1. For buildings located where snowstorms are closely spaced and temperatures stay below freezing, both the ground snow load and roof snow load will accumulate throughout the winter and the roof load will be affected by wind, thermal and other effects. Most of the CRREL buildings are in regions with closely spaced snowstorms and low temperatures (O'Rourke et al 1983).

The data from the 1982 CRREL report was used in the development of the conversion factor between ground and uniform roof snow loads in the 1982 American National Standard. The maximum conversion factor ($C_m$) was used in the analysis since standards are concerned in the design of a 50-year mean recurrence interval or a 2% probability that the roof snow load will be exceeded in any given winter season. Using an expected value relationship an expected value of $C_m$ was developed using the exposure and thermal parameters:

$$C_m = 0.47 * E * T \qquad (8)$$

In Equation *(8)*, $E$ is the exposure rating, $T$ is the thermal parameter and 0.47 is a mean conversion factor. The equation is similar in form to Equation *(5)* where parameters are used to convert ground to roof snow loads. Proposed values for the conversion factors, $E$ and $T$, based on the CRREL report and other findings by researchers are described in the following sections.

*3.1.2 Roof Conversion Factor (C)*

The conversion factor is a ratio used to convert the ground snow load to a design roof snow load, specifically relating a 50-year mean recurrence interval ground snow load to the design roof snow load, also implicitly a 50-year mean recurrence load. ASCE 7-10 defines this factor to be 0.7, as shown in Equation *(5)*. The conversion factor is the percentage of the ground snow load that will be present on a typical roof (i.e., the roof is flat $C_s$=1, the roof is heated $C_t$=1 and the exposure rating is semi-sheltered $C_e$=1). The factor was developed based on a lognormal distribution of data on the ratio of maximum roof snow loads to maximum ground snow loads $C_m$ in Equation *(6)*. The conversion factor was changed in the 1982 standard based on the previously described CRREL report and the substantial improvement in ground snow load data. In the 1982 American National Standard, the conversion factor *C* was lowered to 0.7 from its previous 0.8, where it remains today in ASCE 7-10. This reduced the design roof load by 14%, leading some engineers to question the reliability of roofs designed with the lower 0.7 factor (Bennett 1988). However, the CRREL data suggests that a conversion factor of 0.47 is appropriate in Equation *(8)*; both the ASCE 7-10 value of 0.7 and the National Building Code of Canada 1977 value of 0.6 are higher, reflecting the conservative intent of codes and standards to overestimate loads (O'Rourke et al. 1983).

*3.1.3 Exposure Conversion Factor ($C_e$)*

Exposure to wind plays a key role in the conversion of ground to roof snow loads. Wind can reduce the amount of snow load on the roof if the structure is exposed to high winds, or in areas with dense trees or other obstructions the snow load on the roof is closer in value to the ground snow load. In some regions, wind can form snow drifts, making the roof snow load substantially larger than the ground snow load. In ASCE 7-10, the effect of wind and exposure

is accounted for in the roof snow load design through an exposure conversion factor, $C_e$. The $C_e$ conversion factor is arguably the most difficult factor for which to assign a value because exposure factors must encompass a wide range of exposure conditions and variability of weather conditions. A study by Meloysund et al. (2007) discusses the difficulty in determining the exposure factor $C_e$ in Norway. Snow load design in the Norway building code is slightly different from U.S. design standards, but the factors influencing the exposure factor for roof snow load design are the same. Meloysund et al. (2007) showed that the exposure factor should be a function of the climate. In other words, temperature variation and snowfall patterns differ from place to place and will have a large effect on the wind speed needed to remove snow from the roof. It was noted in the study that snow with a higher density, usually associated with higher temperatures, will require a larger wind speed to be removed from the roof than less dense snow, associated with colder temperatures (Meloysund et al. 2007). Accounting for snow density and wind speeds that occur at a particular location could improve the accuracy of roof snow load estimates.

In ASCE 7-10 the exposure factor is not a function of temperature, nor does it account for the changes in snow density based on climatic variation. Values for exposure in ASCE 7-10 depend on three different exposure conditions (i.e., sheltered, partially exposed and fully exposed) and several different terrain categories. For example, structures in areas with high wind exposure, such as places in Alaska where trees are limited, the exposure factor, $C_e$, reduces the design snow load on the roof by 30% with a factor of 0.7. For other structures that are sheltered, located tight in among trees, the snow load on the roof would be increased by a factor of 1.2. Values for $C_e$ can be found in Table 7.2 of ASCE 7-10 for different terrain categories and exposure conditions (ASCE 2010).

The exposure factors in ASCE 7-10 were determined in part by the data collected in the 1982 CRREL report. Roof exposure conditions were ranked as sheltered, semi-sheltered or windswept. The average conversion factor ($C_m$) for sheltered was found to be 0.78, 0.59 for semi-sheltered, and 0.53 for windswept roofs. It was noted from the data that exposure conditions had the largest impact on the ground to roof conversion factor. The mean exposure factors were adjusted in order to make a comparison with design exposure factors in design standards. The semi-sheltered exposure was used as the base where the factor was assigned to be *E=1.00*. The values for windswept and sheltered were found by taking the average $C_m$ value for each category and relating it to the base exposure condition. Relating these values, a sheltered roof has a value of *E=1.32*, semi-sheltered roof has a value of *E=1.00* and a windswept roof has a value of *E=0.95*. The ratio in factors between windswept and sheltered is 1.4 (1.32/0.95), a much lower value than had been previously reported in earlier standards. This encouraged the changing of the exposure factor in the 1982 standard to 1.2 for sheltered and 0.8 for windswept making the ratio 1.5 (O'Rourke et al. 1983).

*3.1.4 Thermal Factor ($C_t$)*

In general, structures that radiate heat like a greenhouse will reduce the snow load. Structures that are well-insulated or structures that are kept intentionally below freezing will melt little to no snow from the roof. The thermal factor, $C_t$, has remained the same since the changes in the 1982 ANSI standard and is defined in ASCE 7-10 as 0.85, 1.0, 1.1, 1.2 and 1.3 for heated greenhouses, standard structures, structures kept just above freezing, unheated and open air structures, and structures kept intentionally below freezing, respectively. Several characteristics of the roof affect the $C_t$ value, including the material on the roof, the effectiveness of the insulation in the roof, the drainage system and the purpose of the structure. The purpose of the

structure must be that anticipated during the winters for the life of the structure, so if the structure is intended to be a refrigerated structure the $C_t$ value should be determined accordingly. The amount of insulation used and whether the roof is ventilated or not ventilated affect the heat flow through the roof, quantified by the R-value in U.S. units as $^{\circ}F \times h \times ft^2/Btu$ (where h is the time in hours).

Data collected in the CRREL report were used to verify $C_t$ values used in snow design. In that report, structures were categorized as heated or unheated. These categories were defined such that unheated structures were those that were intentionally kept below freezing or the structure had no heating system, all other structures were considered as heated. For example, an open walkway roof system like the one used in the case study in Chapter 6 would be considered an unheated roof structure. For the CRREL data, the mean value of the thermal coefficient is 0.70 for unheated structures and 0.55 for heated structures. The calculation of mean and variance was repeated for subsets of the data falling in the three exposure categories (sheltered, semi-sheltered and windswept) and the values are summarized in Table 3.1. The thermal condition was modified by making the heated structure the base case and assigning a value of *T=1.00*. Using *1.00* for heated structures, and multiplying by the ratio of the mean for unheated structures by the mean for heated structures, yields a *T* value of *1.22* for unheated structures.

**Table 3.1-** Average $C_m$ for various combinations of thermal and exposure conditions CRREL Report

| $C_m$ | sheltered | semi-sheltered | windswept |
|---|---|---|---|
| unheated | 0.84 | 0.66 | 0.55 |
| heated | 0.66 | 0.48 | 0.52 |

Comparing the values for $C_t$ in ASCE 7-10 with those in the CRREL study, it can be concluded that the values match fairly well. An average conversion factor of 1.22 for unheated structures corresponds to a factor of 1.2 found in ASCE 7-10 Table 7.3, for unheated or

intentionally kept below freezing structures. Additional factors for greenhouses and structures kept just above freezing were not included in the report and therefore could not be compared. In a later study by Irwin et al. (1995), several flat roof buildings varying in size and thermal rating showed the effects of heat transfer on roof snow loads. In the study, a finite area element method was used to simulate weather patterns in several Canadian cities. The program uses historical meteorological data to superimpose weather data onto finite element models of heat transfer of a hypothetical roof system. Making some assumptions about the amount of insulation in the roof and an internal temperature of the structure the effects of heat transfer on roof snow load could be studied. The report showed a 14% reduction in roof snow load for buildings that are not well insulated, compared with buildings with very large thermal resistance. This observation compares to a 16.6% reduction in ASCE 7-10 for a normal insulated building versus an unheated building. Irwin et al. (1995) concluded that the results found are similar in magnitude to American standards for flat roofs and that reductions might be even larger for sloped roofs (Irwin et al. 1995).

*3.1.5 Roof Material and Slope ($C_s$)*

In general, sloped roofs accumulate less snow than flat roofs because of wind action, the ability of snow to slide off sloped roofs, and improved drainage of melted snow on sloped roofs. The ability of snow to slide off the roof is dependent on the absence of obstructions on the roof and below the roof, the slipperiness of the surface, and the temperature of the roof. Reductions in the design roof snow load due to slope and material are accounted for through the $C_s$ factor in ASCE 7-10.

The roof material, which may be shingle, concrete, gravel, tar, metal, or some other type of specialty roofing material, can be an important consideration affecting the snow load on the

roof. Some roof materials, such as fabric or glass and plastic, may have little or no snow accumulation because of their geometric characteristics and slippery surface. Slippery materials such as some concrete roofs and metal roofs are more likely to have snow sliding occur, depending on the slope, making the $C_s$ value smaller for these roof materials (ASCE 7-10). Roof sliding can lead to the formation of drifts or sliding loads on lower roofs, as will be discussed later.

The value of $C_s$ is found according to Figure 3.1 (which is based on Figures 7-2 in ASCE 7-10). Analysis of data from controlled field experiments conducted in Canada and the United States, showed that roofs with a slope less than 25˚ the $C_s$ factor is 1.0 and roof slopes steeper than 70˚ the snow load is not considered ($C_s = 0$) regardless of the roof surface or thermal condition of the roof (Ellingwood and O'Rourke 1985). For roofs with slopes less than 70° and greater than 25˚ the value of $C_s$ varies depending on the temperature of the roof and the slipperiness of the surface. Ellingwood and O'Rourke (1985) reported that in addition to slope, roof surface and ambient temperature, the roof orientation will also have an effect on the conversion of ground to roof snow loads. Roofs with southern sun exposure would in general have a smaller roof snow load than north facing roofs, which would have less exposure to sunlight. Figure 3.1 accounts for the roof surface condition and ambient temperature by relating $C_s$ to $C_t$ as suggested by Ellingwood and O'Rourke (1985), however it does not account for roof orientation which one would assume would have an effect on the slope conversion factor due to additional melting snow.

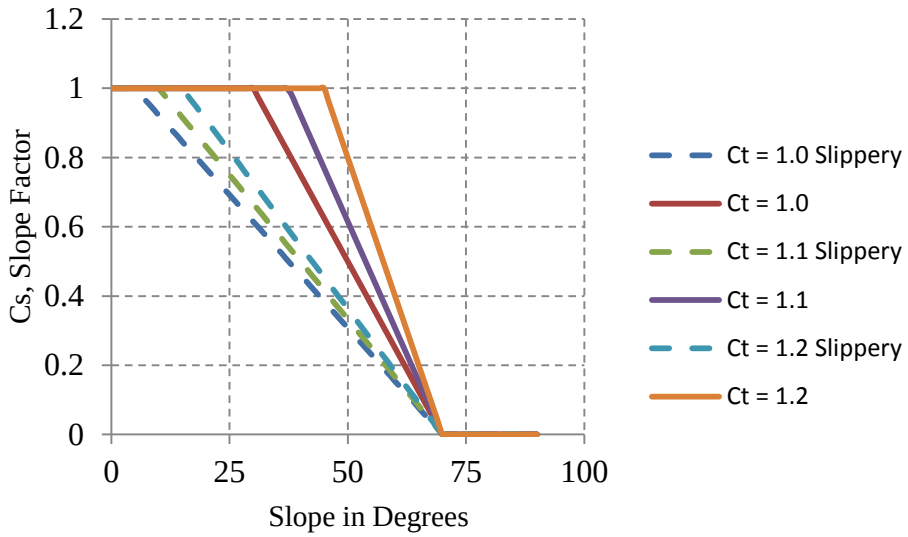


**Figure 3.1-** $C_s$ value in ASCE 7-10 based on the slope, the material and the thermal parameters of the structure (ASCE 7-10).

In ASCE7-10, the roof material is to be considered when determining the $C_t$ value and the $C_s$ value, but there is not a specific conversion factor for different roofing materials. According to ASCE 7-10, slippery roofs are those that have a metal, slate, glass, bituminous, rubber, or a plastic membrane with a smooth surface. Roofs that contain an imbedded aggregate or mineral granule surface, as well as asphalt shingles, wood shingles and shakes are not to be considered as smooth surfaces. In addition, a slippery surface must not have any obstructions and have sufficient space below the eaves to collect sliding snow. Sloped roofs that have obstructions such as valleys where additional snow can accumulate due to drifting and snow sliding will not have a reduction in $C_s$ due to slope.

The drainage system is also important when considering the slope factor and assuming sliding snow will occur. If sliding snow is being assumed, preventing the formation of ice dams, icicles and other forms of increased local loading that may occur due to improper drainage is important in preventing local damage or collapse. Many roof structures will have colder and warmer areas on the roof, and this thermal variation must also be considered in the snow load

design. Ice dams may form along the eaves of the roof where water is unable to drain, particularly in warm structures that are poorly insulated and located in cold regions (Ellingwood and O'Rourke 1985). This can be prevented by having a well-insulated roof and providing ventilation at the eaves. Providing heat tape at the eaves or snow guards to prevent the movement of snow would also prevent excessive build up in snow load and prevent ice dams from forming at the eaves (Buska and Tobiasson 2001).

*3.1.6 Reliability of Snow Loads in Building Codes and Standards*

The conversion of ground to roof snow loads is a key component in the reliability of the design of structures. Since there is limited data on roof snow loads, ground snow loads must be converted to roof snow loads. The design roof snow load is intended to have a 50-year mean recurrence interval or a 2% probability of being exceeded. However, since the annual maximum roof load probability distribution is unknown, the 50-year ground snow load is converted to an estimated 50-year roof load. Several researchers have addressed the problems encountered in developing a ground to roof conversion factor for design that provides uniform reliability in roof snow load design.

In O'Rourke and Stiefel (1983), 128 weather stations were used to establish a probability density function of roof snow loads based on lognormal probability functions of both the ground snow load and the ground to roof load conversion factor. The lognormally distributed 50-year ground snow load values from the weather station data were converted to a 50-year roof snow loads using the conversion factor relationship developed in O'Rourke et al. (1983), shown in Equation *(8)*. Having a 50-year roof load and a 50-year ground snow load for each of the 128 weather stations a 50-year conversion factor for the various weather stations could be determined. Based on this analysis, an average conversion factor of 0.61 was found for a 50-

year recurrence interval. Since ASCE 7-10 uses a value of 0.70, it is 16% higher (on average) than the 50-year roof snow load. For most of the sites studied, O'Rourke and Stiefel (1983) showed that the flat roof snow loads obtained using snow design equations have a mean recurrence interval of about 80 years. The data contributed to the decision to lower the average ground-to-roof conversion factor from 0.8 to 0.7 in the 1982 ANSI standard.

However, there are concerns about the data used to develop the ground-to-roof conversion factors in design standards. Some researchers mention that the model may not provide adequate statistical data because the roof snow load data used to develop the conversion factor were from a three year project, and many of the structures were studied only for one year. Bennett (1988) points out that the high coefficient of variability in the conversion of ground snow loads to roof snow loads causes inconsistencies in the reliability of snow load design. The conversion factor is site independent and consequently is not a function of the ground snow load. Bennett (1988) proposed to diminish the variability by using direct measurements of roof snow loads instead of converting ground snow loads to roof snow loads and, for example, a 50-year mean recurrence roof snow load map. The decrease in uncertainty by eliminating some of the conversion factors would allow for a decrease in snow load factors and lead to a more uniform reliability among structures, but there is limited statistical data on roof snow loads making this virtually impossible.

Since roof snow loads must be converted from a ground snow load, Bennett (1988) proposed a change in the LRFD snow load factor. Bennett's study of the same conversion factors for ground to roof snow loads for the 128 sites used in O'Rourke and Stiefel (1983) found that structures were less reliable where the snow load combination controls the design over dead, wind or other loads. Using the design equation for flexural design of compact simply supported

steel beams in the 1986 AISC manual (0.9R=1.2D+1.6S) and keeping the factors constant for the dead load and the resistance. Reliability indices are one possible metric related to the probability of failure for a reference period of years. Mathematically, the reliability index, denoted $\beta$, is related to the probability of failure by $P_f=\Phi(-\beta)$ where $\Phi$ is the standard normal integral found in a probability table. In other words, $P_f$ is the area under the probability of failure curve at a given reference period. A higher reliability index indicates a safer design, i.e., lower probability of failure. An LRFD factor of 2.05 applied to the snow load was found on the average to obtain a reliability index of 2, compared to a reliability index of 1.6 with the current load combination and reliability index of 2.6 for buildings where the snow load does not control. As a result, Bennett (1988) argued for increasing the load factor on S in the load combination in design standards.

Other studies have also looked at the reliability of snow load design, most recently by Takahashi and Ellingwood (2004). Their study compared Japanese building codes and standards to American standards, showing that there is a concern in the reliability of structures designed to the Japanese Building Code, 2000 (JBC) for snow loads. Existing building codes in Japan were developed under the assumption that heavy snows would be removed from the roof, making the JBC unconservative, compared to US, Canadian and European codes and standards. This is shown in Figure 3.2 (a) where the reliability decreases as the snow load to dead load ratio increases in very snowy regions of Japan (snow depth of 2 meters on a 50-year mean recurrence interval). The reliability index of roof structural members designed using JBC were considerably less than using ASCE 7 for load and resistant factored design, as shown in Figure 3.2 (b). In this study, the reliability indexes ($\beta$) were calculated using a service life for structures of 50 years and using a distance to a failure point to determine the mean and standard deviation of the

variables in the analysis, flexural strength, dead load and snow load. In addition, Takahashi and Ellingwood (2004) found that $\beta$, for snowy regions vary from 3 to 2.5 as the ratio of snow load to dead load increases using ASCE 7 design standards.

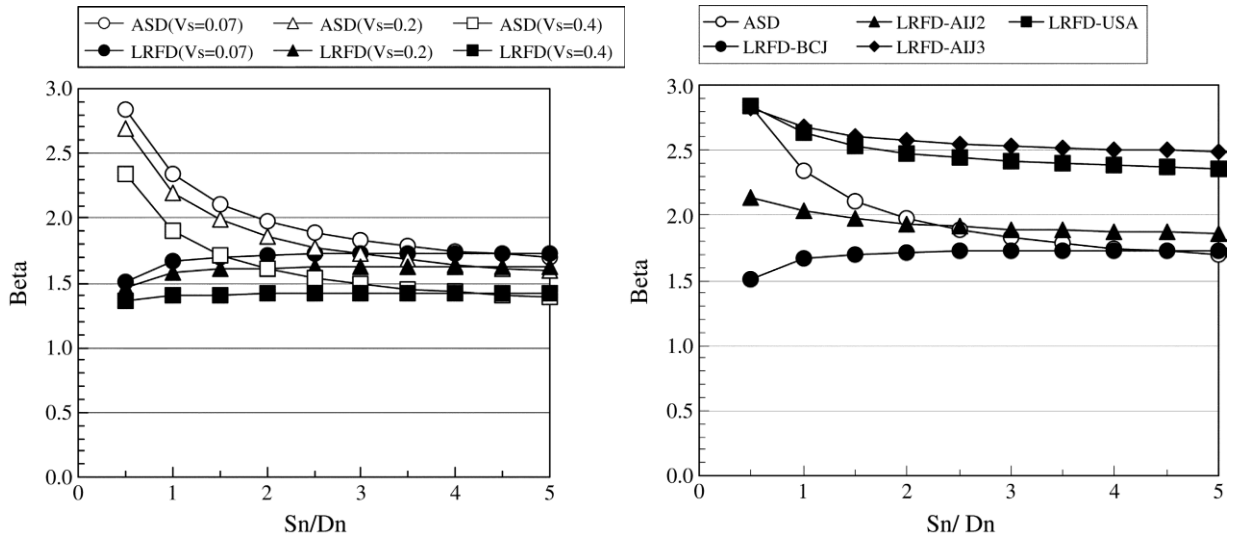


**Figure 3.2-** a) Reliability indices of members designed to ASD and LRFD using the Japanese Building Code for snowy regions (d = 2 m). b) Reliability indices of members designed to ASD and LRFD using JBC and US design standards (Takahashi and Ellingwood 2004).

These numerical values are different than the reliability index found by Bennett however the idea is similar in that the snow to dead load ratio has a critical impact on the value of the reliability index. There are several differences in the computed reliability indices by Bennett (1988) and Takahashi and Ellingwood (2004) for several reasons. First, the ground snow loads used to develop the reliability indexes were from two different countries encompassing very different climates and snowfall patterns. Second, methods for converting ground snow loads to roof snow loads were different in the two studies and involved different design standards. However, Takahashi and Eillingwood (2004)'s comparison of a number of different international standards shows that the U.S. LFRD load standards has the highest reliability and, therefore, a reasonable probability of failure.

### 3.2 Probabilistic Model Factors

Previous research has shown that where snow loads are the controlling factor in the gravity load design of a structure, the reliability of the structure is reduced (Bennett 1988). The goal of the model developed in the following section is to develop probabilistic models that predict the roof snow load, at a given time or event, based on structural parameters on the roof and the ground snow load at that same point in time. These roof snow load predictions can then be used to develop hazard curves for deflections and stresses in a building at a particular site useful in the context of performance-based engineering.

In order to develop a probabilistic model for predicting uniform roof snow loads from a ground snow load a list of factors affecting roof snow loads had to be identified. Using the data from the CRREL study and other sources (ASCE 2010 and Meloysund et al. 2007), the factors were organized in order of importance. The following shows the list of factors that we would expect to have an effect on the conversion of ground to roof snow loads for uniform snow loads:

- Exposure Factor ($K_e$): Exposure factors include fully exposed, partially exposed and sheltered, with fully exposed roofs tending to have less snow accumulation on the roof.
- Roof Temperature ($K_t$): Cold structures such as refrigerated structures, or well-insulated structure, will have a larger roof snow load compared to smaller roof loads in heated structures.
- Slope ($K_{sm}$): Increased roof slope can lead to greater amounts of sliding snow and lower snow loads.
- Materials ($K_{sm}$): Snow may slide off metal roofs onto the ground or lower roofs. Other, less slippery roofs will not tend to have sliding snow, therefore a larger roof snow load.
- Climatic Factor ($K_{gs}$): As the ground snow load increases the conversion factor between ground and roof snow loads decreases. The reason for this relationship is discussed in more detail below.

Exposure, thermal conditions, roof material, slope, and ground snow load would have the largest effects on the overall conversion factor. The development of the uniform roof snow load model is described in the following section. Depending on the geometry of the structure drifting can also have a large effect on the roof snow load. A non-uniform drifting model will be discussed in Chapter 4.

*3.2.1 Development of the Uniform Roof Snow Load Model*

A total of 467 measurements of roof and ground snow loads from 110 structures from the CRREL report were used to develop the model. For each data point, a conversion factor for each event was found using the following relationship:

$$K_v = \frac{RSL}{GSL} \qquad (9)$$

where $K_v$ is the conversion of Roof Snow Load (*RSL*) to Ground Snow Load (*GSL*) for one event. The conversion factors are therefore determined on the basis of a single event, or specific measurement visit. The conversion between ground and roof snow loads in this study, which relate ground snow load at a particular time to roof snow load at the same time, are different from those used in building codes and other design documents, which relate the maximum ground snow load in a given season to the maximum roof load in the same season.

Of the 110 buildings included in the dataset, 65% are heated and 35% are unheated. In terms of exposure conditions, 23% of the data set is categorized as sheltered, 32% as semi-sheltered and 45% as windswept. Roof materials include 14% metal roofs and 86% shingle or other non-slippery material roofs. The roof slopes varied from 0˚ to 65˚ and were not considered for shingle and other non-slippery roofs. The complete dataset is provided as an appendix to this thesis.

The following sections describe the parameters used in the model and how they were developed. Combining all the factors used in the model the uniform roof snow load can be predicted using:

$$RSL = K * K_e * K_t * K_{sm} * K_{gs} * GSL \qquad (10)$$

where *RSL* is the predicted value of roof snow load (in psf, or other consistent units), *GSL* is the ground snow load, *K* is the mean conversion factor, $K_e$ is the factor relating to roof exposure, $K_t$ is the factor relating to building thermal properties and insulation, $K_{sm}$ relates to the roof slope and roofing material and $K_{gs}$ relates to the amplitude of the ground snow load. The equation takes this form in order to be consistent with past research and other building codes and standards, which use a multiplicative series of conversion factors for different parameters to relate a ground snow load to a roof snow load.

The factors determined in Equation *(10)* are assumed to be lognormally distributed with statistical parameters as shown:

$$\lambda = \ln \mu - \frac{1}{2}\zeta^2 \qquad (11a)$$

$$K_{log} = \exp(\lambda) \qquad (11b)$$

where μ is the factor's mean value, λ is the lognormally distributed mean and ζ is the lognormally distributed coefficient of variation; $K_{log}$ is the median or the exponent of the lognormal mean for each factor. Two standard deviations are of interest: (1) the standard deviation in non-log space, i.e., $\sigma = \mu\delta$, and (2) the lognormal standard deviation, i.e., $\sigma_{ln} = \lambda\,\zeta$. The parameters of the lognormal distribution are summarized in Table 3.2 and used in developing a Monte Carlo simulation tool to predict the distribution of roof snow loads. The Monte Carlo simulation and a comparison of predicted roof snow loads using the model to

measured roof snow loads in the CRREL report will be discussed later. The following sections describe the steps used to develop the coefficients in the uniform model.

**Table 3.2-** Statistical parameters for different factors used in the probabilistic model for uniform snow loads

| Factor | Description | Mean Value (μ) | Standard Deviation (σ) | Lognormal mean ($K_{log}$) | Lognormal Standard Deviation ($\sigma_{ln}$) |
|---|---|---|---|---|---|
| $K$ | Average Ground to Roof Conversion | 0.57 | 0.39 | 0.47 | 0.62 |
| $K_e$ | Sheltered | 1.31 | 0.63 | 1.18 | 0.46 |
| | Semi-sheltered | 1.04 | 0.65 | 0.88 | 0.57 |
| | Windswept | 0.82 | 0.68 | 0.63 | 0.72 |
| $K_t$ | Unheated Roof | 1.07 | 0.67 | 0.91 | 0.57 |
| | Heated Roof | 0.96 | 0.71 | 0.77 | 0.66 |
| $K_{sm}$ | Metal Roof (0-20º) | 0.95 | 0.76 | 0.74 | 0.70 |
| | Metal Roof (>20 º) | 0.87 | 0.49 | 0.76 | 0.52 |
| | Shingle Roof | 1.01 | 0.70 | 0.83 | 0.63 |
| $K_{gs}$ | GSL≤35 psf | K=-0.022xGSL + 1.44 | 0.73 | 0.872 | 0.62 |
| | GSL >35 psf | 0.70 | 0.47 | 0.583 | 0.61 |

The first step in the process was to determine the mean and standard deviation of the factors related to exposure, thermal conditions, roof material and slope independently of one another. Plots of each of the factors were made to determine the importance of each of the factors to the overall conversion factor of ground to roof snow load. As shown in Figure 3.3, the exposure rating, which categorized buildings as sheltered, semi-sheltered and windswept, has the largest effect on the ground to roof conversion factor. The importance of the exposure factor is further validated by combining exposure factors with thermal and slope/material parameters. Table 3.3 shows that the exposure parameter decreases from sheltered to windswept regardless of the other parameters, therefore indicating a larger effect than the other parameters in this study. In addition, the ratios of the average $K_v$ values for sheltered to windswept (exposure parameter) was found to be 1.6 compared to a 1.1 ratio for unheated to heated (thermal parameter), showing

exposure has the largest effect and then the thermal parameter. Lastly, slippery roof to non-slippery roof (slope and material parameter) was found to be 1.02, therefore having the smallest effect on the overall conversion factor. Past publications such as O'Rourke and Redfield (1982), and a number of building codes and standards, have also shown that exposure has the largest effect on the overall conversion factor for ground to roof snow loads.

**Table 3.3-** Average $K_v$ values for roof snow load data with various combinations of thermal, material and slope parameters, and the exposure rating (numbers in parenthesis are the number of data points in each category).

| | Exposure Category | | |
|---|---|---|---|
| Other Parameters | Sheltered | Semi-sheltered | Windswept |
| Heated | 0.73 (35) | 0.58 (108) | 0.55 (159) |
| Unheated | 0.75 (70) | 0.62 (43) | 0.44 (52) |
| Non-Slippery | 0.78 (81) | 0.58 (137) | 0.47 (186) |
| Slippery with Slope 0-20˚ | 0.63 (24) | 0.68 (8) | 0.53 (18) |
| Slippery with Slope >20˚ | 0 | 0.74 (6) | 0.31 (7) |

To begin the regression model, $K$ is computed as the average conversion factor for all the dataset buildings. This data gives $K$ = 0.57, which is similar to the 0.7 in Equation *(5)* used in American design standards and the 0.47 in Equation *(8)* found using ground and roof snow load data. A value of 0.57 gives a reasonable estimate since the value used in design standards is a conservative design value and we would expect our value to be slightly larger than the value found in the CRREL data because our dataset includes ground snow loads smaller than 20 psf where the CRREL dataset left these data out. In general, we would expect values under 20 psf to have a higher conversion factor. Of the roof events considered, the maximum K was 2.44 and the minimum was 0. Variation in K depends on the other characteristics of the roof, as described below.

Accordingly, the development of the stepwise regression model starts, and $K_e$ is calculated here as:

$$K_e = \frac{ARS}{K\ GSL} \qquad (12)$$

The mean of conversion factors between was determined by averaging the actual reported snow load (ARS) divided by the estimated roof snow load, which already accounts for the average conversion, i.e., $GSLxK$. Three exposure categories are considered: (1) sheltered if the building is surrounded by dense trees or other large and confined obstructions, (2) semi-sheltered if there are some obstructions, and (3) windswept if there are little or no obstructions. The mean exposure factor decreases from 1.31 to 0.82 as the amount of shelter decreases from the sheltered category to the windswept category. This trend is in line with previous research and our intuition about wind effects on roofs.

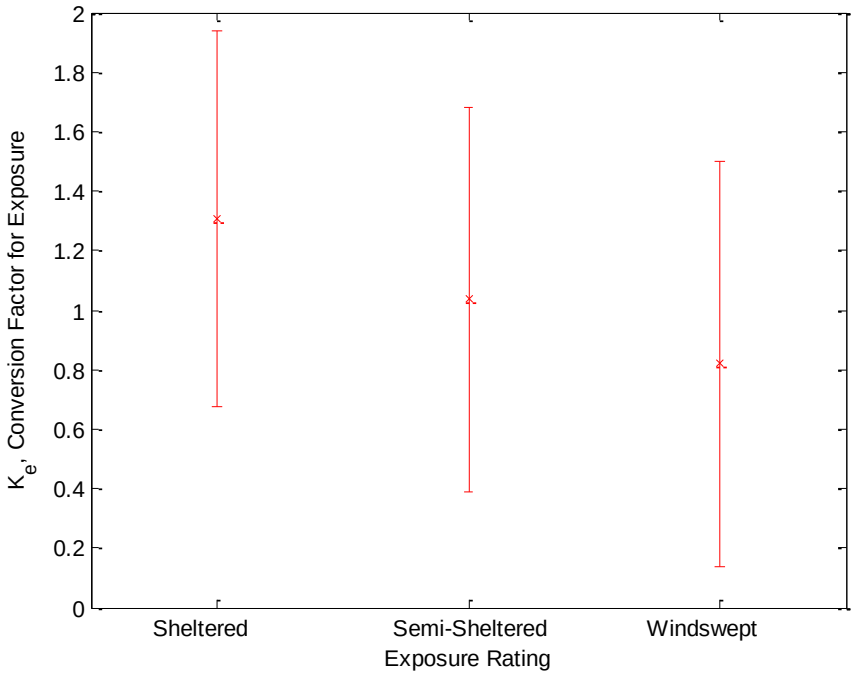


**Figure 3.3-** Event-based ground to roof snow load conversion factor as a function of the exposure rating of the structure. Error bars show mean +/- one standard deviation.

The thermal parameter is the next most influential factor on the conversion of ground to roof snow loads.

$$K_t = \frac{ARS}{K\ K_e GSL} \qquad (13)$$

Roofs were classified as unheated or heated. Approximately 65% of the data were from heated structures. Roofs were considered to be unheated based on the internal temperature of the building and the amount of insulation in the roof, i.e., very well insulated roofs were unheated. The mean and standard deviation for heated and unheated structures are shown in Figure 3.4. The conversion factor is smaller for heated structures versus unheated structures, indicating that heated buildings will lead to melting of some of the snow on the roof.

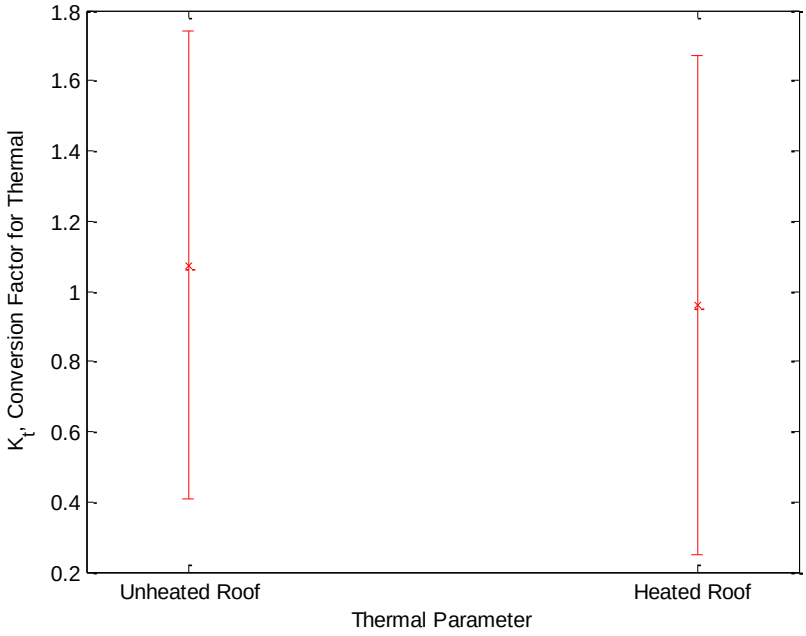


**Figure 3.4-** Event-based ground to roof snow load conversion factor as a function of the thermal parameter of the structure.

In order to refine the definitions of heated and unheated roofs and improve predictions of the effects of temperature on the ground to roof conversion factor, von Bradsky (1980) used the same CRREL data and classified roofs as hot, warm, cool or cold, defined as follows:

1. Hot Roof - $R \leq 10$, no vents or airspace between rooms and roofs
2. Warm Roof- $10 < R \leq 20$, no vents or airspace or $R \leq 10$, vents and airspace
3. Cool Roof- $20 < R \leq 30$, no vents or airspace or $10 < R \leq 20$, vents or airspace or no insulation and building inside temperature kept between 32-50°F or $R \leq 10$, double roofed, eave and end or ridge vented

4. Cold Roof- 30<R, no vents or airspace or 20<R vents and airspace or unheated buildings or R<10, double roofed, eave and end or ridge vented

Figure 3.5 shows how the mean and standard deviation vary for these four refined categories of thermal conditions on roofs. Although we would expect the conversion factor to increase as the temperature of the roof decreases, a different trend is apparent in Figure 3.5. One reason why this does not occur is because of the large effect exposure has on the conversion factor. Since thermal factors have a lesser effect, separating thermal parameters into four separate categories no longer shows a trend of thermal effects on the conversion factor. Due to the inconsistency in the data and the tendency for wind to have a larger effect on the conversion factor, structures could not be separated into categories based on R-values of the roof (O'Rourke et al. 1983). Therefore, the thermal parameters in this study were only separated into heated roofs or unheated roofs, as shown in Figure 3.4.

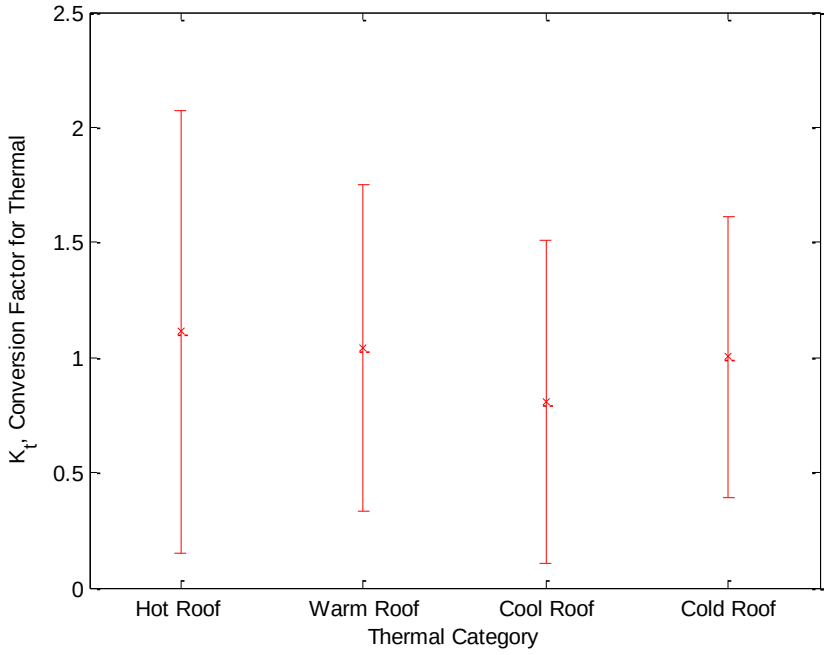


**Figure 3.5-** Event-based ground to roof snow load conversion factor as a function of revised thermal parameter categories.

Roof slope and roof material also have an influence on the conversion factor of ground to roof snow load. The conversion factor $K_{sm}$ is therefore a function of both the roof slope and material and is computed from:

$$K_{sm} = \frac{ARS}{K\, K_e K_t GSL} \qquad (14)$$

Initially, the factors were separated into a slope parameter categorized into groups of 11˚ (i.e., roof slopes ranging from 0-11º, roof slopes ranging from 12-23 º, etc.). The plot of the average conversion factor, $K_{sm}$, (adjusted for thermal and exposure effects such that $K_{sm} = \frac{ARS}{K\, K_e\, K_t GSL}$) for these roof slope categories in Figure 3.6 does not show a clear trend. In addition, the adjusted conversion factor is plotted as function of slope, as shown in Figure 3.7. This plot also shows a flat trend line, showing slope has no effect.. However, when roof slope parameter and material are considered together a trend is found.

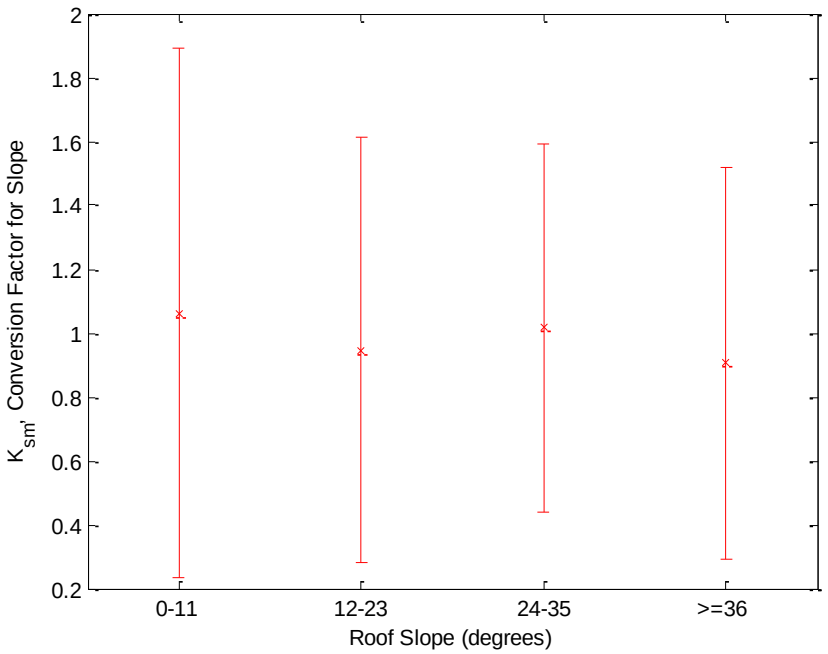


**Figure 3.6-** Event-based ground to roof snow load conversion factor as a function of roof slope

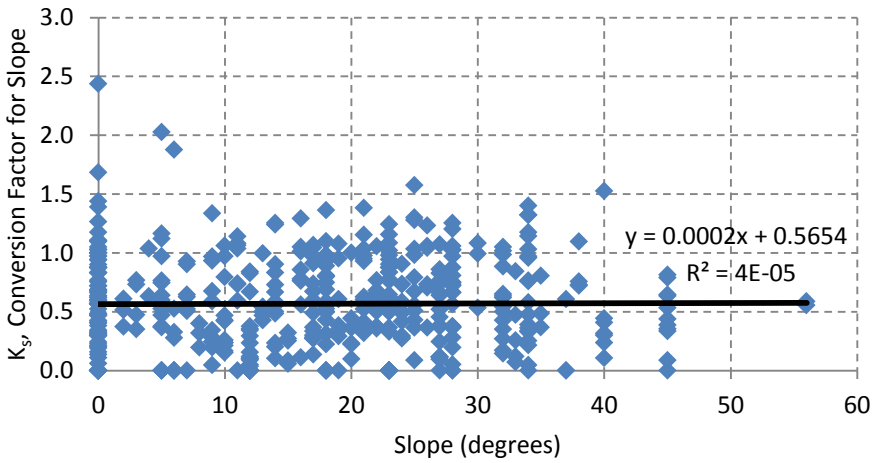


**Figure 3.7-** Scatterplot of the adjusted conversion factor (including exposure and thermal) as a function of the roof slope. The flat trend line shows that there is no effect with slope.

Figure 3.8 shows the mean and standard deviation of the adjusted roof conversion factor for the different roof materials found in the CRREL dataset. This plot shows that there is no clear trend in material either, but knowing that metal roofs should have a lower conversion factor than shingle roofs, especially for greater roof slopes, roof slope and material were considered together. First, tar roofs and gravel roofs were combined into the same category as shingle roofs since all these materials are non-slippery materials and snow is less likely to slide off roofs of these materials, regardless of slope. Second, roof slope was classified into two categories; less than 20º or greater than 20 º. The results are shown in Figure 3.9, showing that that metal roofs have a lower conversion factor ($K_{sm}$) than shingle or other non-slippery roofs, especially for greater slopes, indicating more snow slides off. Roof slope does not affect the conversion factor for shingle or non-slippery roofs. We note that the dataset did not have many very steep roofs, i.e., only 27 data points from buildings with slopes greater than 36˚.

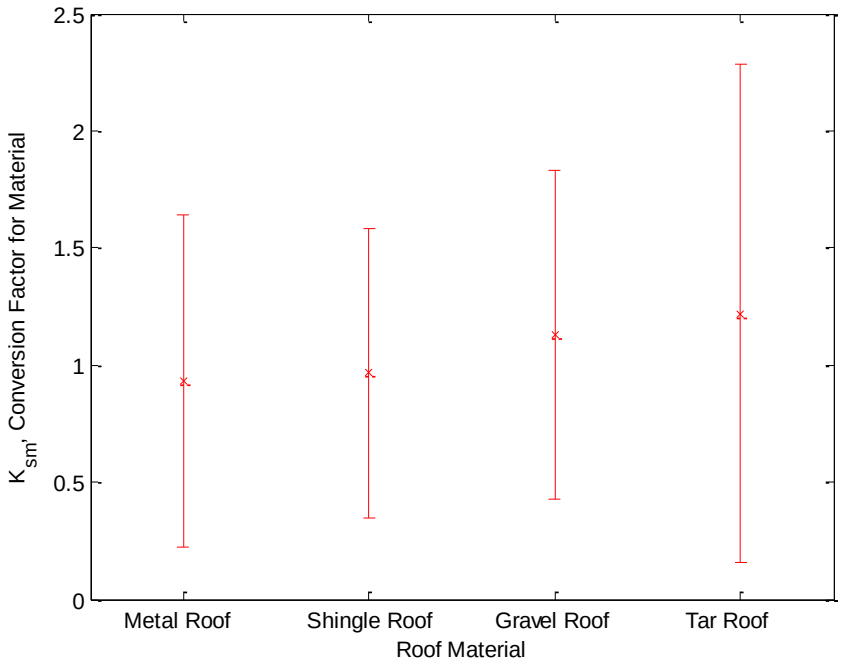


**Figure 3.8-** Event-based ground to roof snow load conversion factor as a function of roof material.

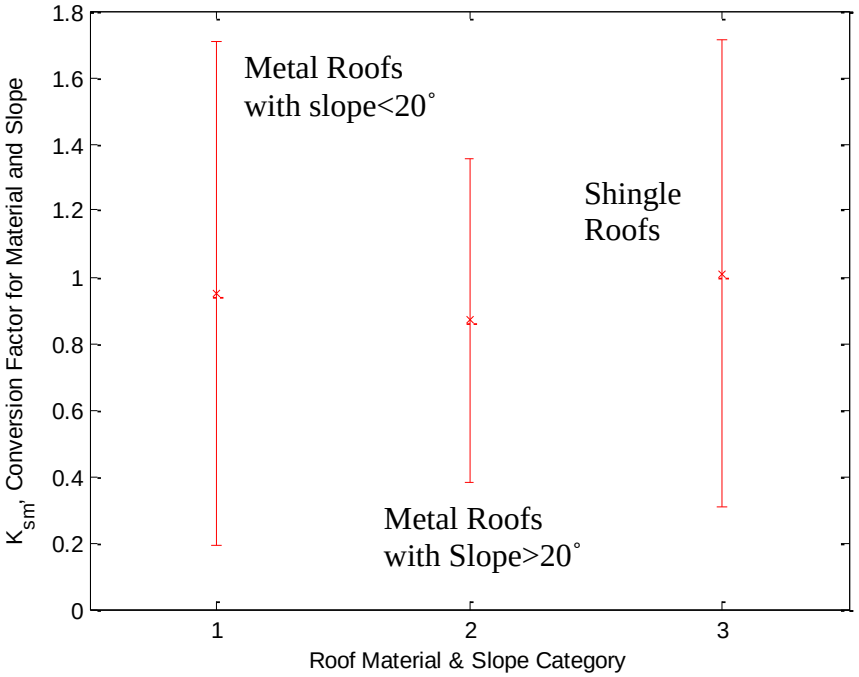


**Figure 3.9-** Event-based ground to roof snow load conversion factor as a function of both the roof material and slope of the structure.

In addition to the parameters described above, snow density and ground snow load were studied to determine if this had an effect on the conversion factor. As previously discussed,

lower snow roof loads tend to occur when few snowfalls are separated by warmer temperatures. In addition, higher snow density that occurs in warmer temperatures will reduce the amount of snow removed from the roof due to wind action. Figure 3.10 shows the effect the time of year can have on the density of the snow. The best-fit lines indicate a general increase in both the roof snow density and the ground snow density as the winter season progresses indicating that snow falling in spring months tends to be denser than snow falling in winter. We also note that that the roof snow density appears to be slightly higher than the ground snow density on the average. However, since the two best-fit lines for roof snow density and ground snow density are close to parallel, density will not have a significant effect on the ground to roof load-based conversion factor. The month of the year seems to have an effect on the density of the snow, but since both the ground and roof snow densities increase as the weather gets warmer (late winter and spring seasons), this was not included in the overall conversion factor.

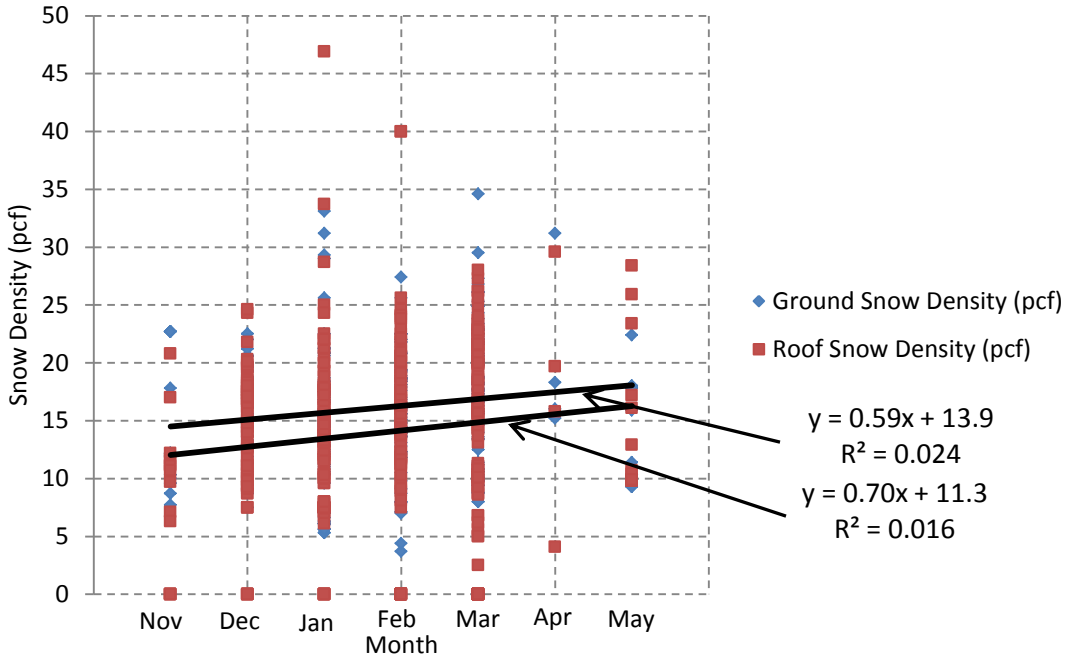


**Figure 3.10-** Roof and ground snow density versus month of the year

We also thought that location in the country might have an effect on snow density because of different climatic regions in the U.S. The snow density plotted with location in the country is shown in Figure 3.11. The hope was to show that snow density in the Northeastern part of the U.S. is different than the Rocky Mountain regions or Cascade Regions, etc., therefore having a different conversion factor. However, since only the name of the school was reported and not the actual locations of the buildings it was difficult to determine if snow density varies in different regions of the country and results were inconclusive. Having additional data for different regions might show that region or snow density has an effect on the conversion factor, but it was not included in this study. However, for non-uniform drifting loads, which are discussed in the next chapter, density is shown to have an effect on the size of the drift.

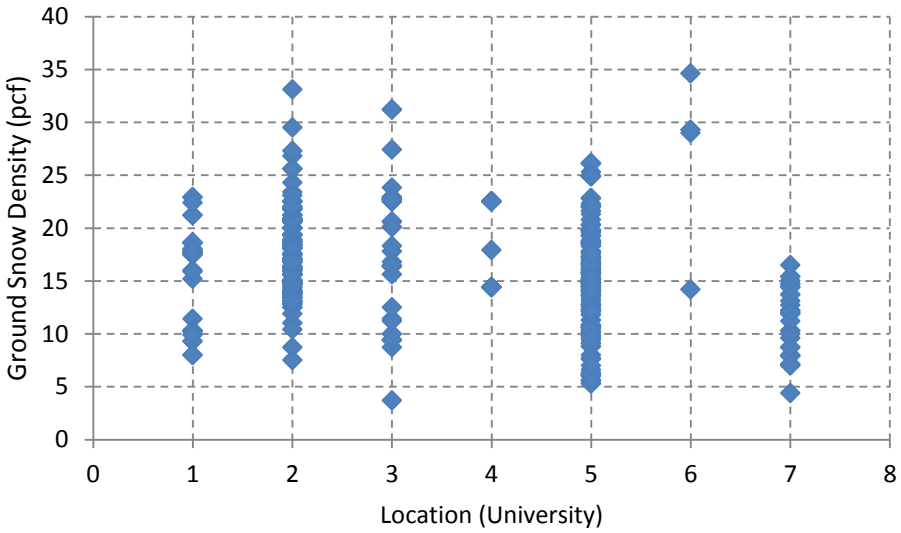


**Figure 3.11-** Ground snow density as a function of location. The locations are numbered according to the University that provided data for the CRREL study: 1) University of Colorado, 2) Michigan Tech, 3) University of Oregon, 4) Rochester Institute of Technology, 5) Rensselaer Polytechnic Institute, 6) University of South Dakota and 7) University of Washington.

The final conversion factor, $K_{gs}$ is a climatic conversion factor that takes into account the frequency of snowfalls by accounting for the ground snow load. The factor has a general negative slope as the ground snow load increases, as shown in Figure 3.12. The trend shows that

areas with a smaller ground snow load have a conversion factor closer to one, meaning the ground and roof snow load will be closer in value when the ground snow load is smaller. Conversely, larger ground snow loads tend to have roof loads that are relatively lower. This is attributed to the density of the snow, where snow that accumulates throughout the year is less dense due to consistently lower temperatures in these regions and therefore is affected by wind, thermal and other roof parameters more so than smaller ground snow loads. The functional form developed is:

$$K_{gs} = 0.70 \text{ for } GSL > 35 \text{ psf} \quad (15a)$$

$$K_{gs} = -0.022 \times GSL + 1.44 \text{ for } GSL \leq 35 \text{ psf} \quad (15b)$$

Current building code provisions do not consider the variation in the conversion of ground snow loads to roof snow loads with ground snow load.

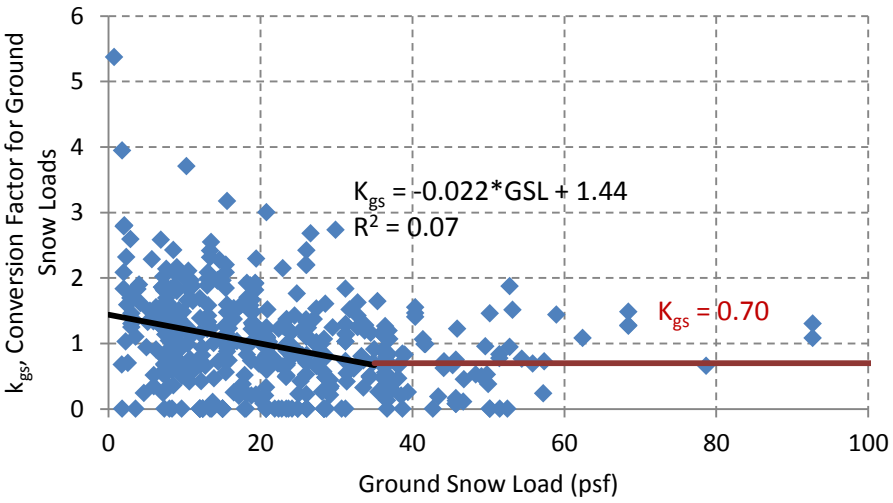


**Figure 3.12-** Event-based ground to roof snow load conversion factor as a function of the ground snow load

*3.2.2 Results of the Uniform Roof Snow Load Model*

The following discussion shows the accuracy of the uniform roof snow load model by comparing the predicted roof snow load using the model to the actual roof snow loads in the

CRREL report. The 467 roof snow load data points from the CRREL report were used to evaluate bias in the uniform roof snow load model. Unfortunately, the data set used in forming the model, also had to be used to check the model because this was the only measured data available of both ground and roof snow loads. Appendix A shows the roof snow load predicted using the model and the corresponding structural parameters from the CRREL dataset. The maximum and minimum $K_v$ values were 1.05 and 0.30, respectively, compared to actual maximum and minimum $C_v$ values of 2.44 and 0. The empirical model developed predicts smaller variation in ground-to-roof conversion factors than that actually observed, reducing the lognormal standard deviation for all buildings from 0.62 to 0.28. The bias was calculated as the ratio of actual to predicted as shown:

$$\text{Bias} = \frac{Actual\ Roof\ Snow\ Load}{Predicted\ Roof\ Snow\ Load} \qquad (16)$$

For all buildings, the mean of the bias using Equation *(16)*, where the predicted roof snow load was found using Equation *(10)*, was found to be 1.01. Table 3.4 summarizes the bias in the conversion factor among the building subcategories. Three categories of roofs were found to have a large bias in the conversion factor: (1) windswept, unheated, non-slippery roofs, with a slope greater than 20º and (2) semi-sheltered, unheated, metal roofs with small slopes (less than 20˚) and (3) semi-sheltered, unheated metal roofs with large slopes (greater than 20˚). In all three of these roof categories, the model is under predicting the roof snow load, and the actual roof load is 50% to 100% higher. This bias may be due to the relatively small number of buildings in these subcategories (fewer than 10% of the total data set) such that they were not weighted heavily in the simplified regression undertaken. However, assuming these types of buildings are not common in the real building stock either, these biases may not have a large

effect on the accuracy of the model. Further data should be analyzed for these categories in order to have a better understanding of the ground to roof conversion factor.

**Table 3.4-** Comparison of predicted $K_v$ values to actual $C_v$ values found in the CRREL study for various structural parameters

| Group Description | No. of Structures in Group | Mean $K_v$ Predicted | Standard Deviation $K_v$ | Mean $C_v$ Actual | Standard Deviation $C_v$ | Mean Bias Ratio |
|---|---|---|---|---|---|---|
| Windswept Heated | 159 | 0.47 | 0.10 | 0.44 | 0.39 | 0.94 |
| Windswept Unheated Metal | 17 | 0.45 | 0.12 | 0.47 | 0.44 | 1.02 |
| Windswept Unheated Other Slope ≤ 20º | 9 | 0.51 | 0.10 | 0.57 | 0.43 | 1.14 |
| Windswept Unheated Other Slope >20 º | 26 | 0.43 | 0.09 | 0.59 | 0.31 | 1.51 |
| Semi-sheltered Heated | 108 | 0.61 | 0.14 | 0.58 | 0.35 | 0.97 |
| Semi-sheltered Unheated Metal Slope ≤ 20˚ | 8 | 0.51 | 0.10 | 0.68 | 0.36 | 1.32 |
| Semi-sheltered Unheated Metal Slope>20 º | 6 | 0.42 | 0.07 | 0.74 | 0.23 | 2.11 |
| Semi-sheltered Unheated Other | 29 | 0.56 | 0.12 | 0.58 | 0.47 | 1.04 |
| Sheltered Heated | 35 | 0.67 | 0.15 | 0.73 | 0.31 | 1.11 |
| Sheltered Unheated | 70 | 0.76 | 0.13 | 0.75 | 0.38 | 1.03 |

It is also important to note that stepwise regression undertaken assumed that the conversion factors are independent of one another, i.e., $K_t$ for a heated roof does not depend on the exposure parameter, the slope or material. To understand the implications of these assumptions, we used a hypothesis (t-test) to compare the mean conversion factors for different groups of data, e.g., sheltered and unheated roofs vs. windswept and unheated roofs. If the independence assumption is reasonable, the mean $K_t$ value for unheated roofs should be the same regardless of exposure. The t-test performs a paired t-test of the hypothesis that the two samples

come from distributions with equal means; the hypothesis is rejected if the means are significantly different. T-tests were conducted at the 5% significance level such that a rejection of the hypothesis implies 95% confidence that the means of the two samples are not equal.

The t-test was repeated for each combination of exposure, thermal, slope and material parameter. All groups considered resulted in a failure to reject the hypothesis, indicating that means of a particular roof group (i.e., unheated) did not vary as a function of other roof parameters.

*3.2.3 Uniform Roof Snow Load Model: Applications in Performance-Based Engineering*

After comparing the calculated roof snow load from the modal to the actual roof snow loads measured in the study, the underlying lognormal parameter distributions model can be used in a Monte Carlo simulation to predict the probability of the roof snow load given a ground snow load and other structure parameters. In Monte Carlo simulation, a random number is generated with respect to an underlying probability distribution. In this study, the coefficients converting ground to roof snow load have each been described probabilistically (Table 3.2) and are statistically independent of one another. Using 10,000 repetitions, a histogram is generated showing the possible values for the roof snow load based on the coefficients inputted for roof and ground snow load parameters. In Figure 3.13, the Monte Carlo model was used for a ground snow load of 10 psf and 25 psf for an unheated structure with a semi-sheltered exposure a metal roof with a slope of 3/12 or 14˚. In this scenario, the mean roof snow load is 15 psf with a median of 5.4 psf for a ground snow load of 25 psf with a logarithmic standard deviation of 1.4; the mean roof load is approximately 60% of the ground snow load. Using the same building properties, but reducing the ground snow load to 10 psf results in average predicted roof snow load of 8 psf with a median of 2.6 psf and a logarithmic standard deviation of 1.5. Not

surprisingly, the average roof snow load is smaller for 10 psf ground snow loads. However, a larger percentage of the ground snow load (80%) remains on the roof, reflecting the change in the climatic factor, $K_{gs}$.

If Monte Carlo simulation is used to predict many realizations of roof snow load, the logarithmic standard deviation provides a measure of the overall uncertainty in the model. For the load cases considered above, we compute a logarithmic standard deviation of 1.55 in the first load case and 1.48 in the second load case. These measures of dispersion can be compared to the standard deviation in the reported CRREL $C_v$ values within the group with the same roof characteristics, i.e., semi-sheltered, unheated, metal roof with a relatively small slope, of 0.36. Ideally, the uncertainties would be close in value. Even though uncertainty in the overall conversion factor is smaller for the model, the Monte Carlo simulation does not show this because the factors are combined in a step by step form such that the variance increases at each step in the model. This is a limitation in this portion of the model and should be considered when using the Monte Carlo simulation. Further research will improve the prediction of uncertainty in the model.

Current U.S. design standards would predict the design roof snow load to be 21 psf for a design ground snow load of 25 psf. The conversion between ground and roof snow loads in this study, which relate ground snow load at a particular time to roof snow load at the same time, are fundamentally distinct from those used in building codes and other design documents, which relate the maximum ground snow load with 2% probability of exceedance to a corresponding maximum roof load in the same season. U.S. building standards base design on the ground snow load with 2% probability of exceedance in 50-years to ensure that roofs across the country are designed to comparable reliability levels. In addition to converting from ground to roof snow

loads, factors used in design standards tend to be conservatively estimated, thereby increasing, rather than reducing safety.

While the use of annual maxima with 2% probability of exceedance is consistent with reliability goals in modern building codes and standards, a performance-based engineering paradigm requires prediction of the maximum loads and the deflections and damage that may occur, but also the magnitude of more frequent and more rare loading scenarios than the code level and the damage that may occur under these loads. Accounting for all roof snow loads, not only yearly maxima, allows one to combine roof snow load models with the probabilistic characterization of ground snow hazard to predict structural response under any level of snow load in assessing risk. In later chapters of this thesis, the probabilistic uniform load model developed here will be used in a case study of an actual roof failure where deflection limits and stress requirements can be quantified as the probability of exceedance for different ground snow loads.

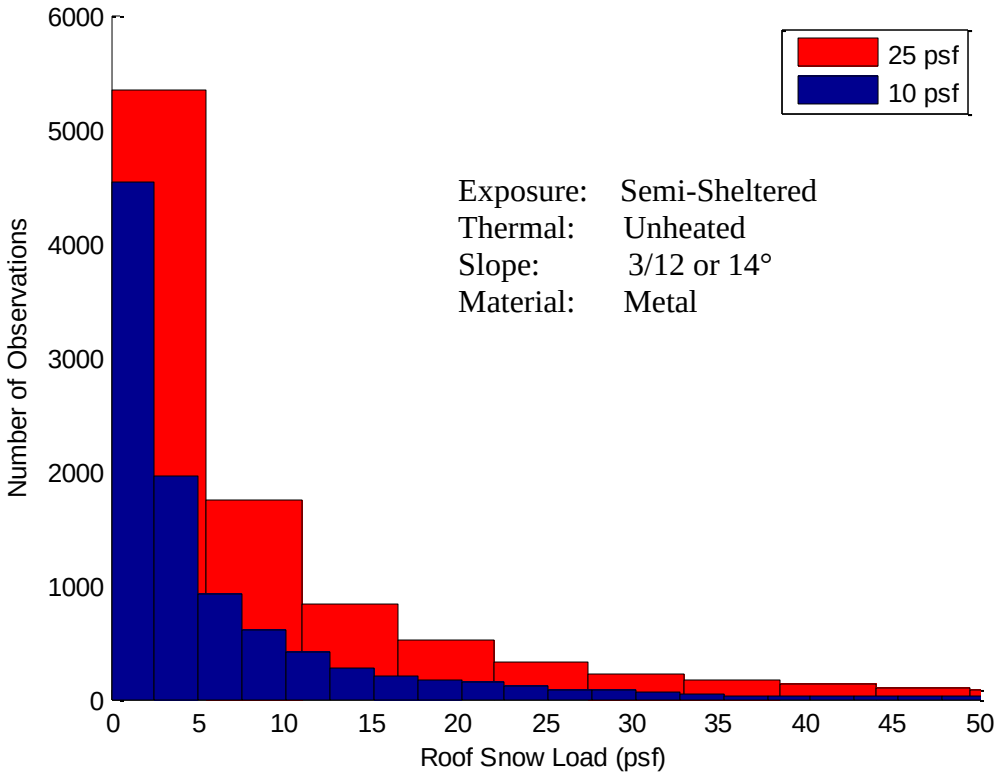


**Figure 3.13-** Monte Carlo simulations for 10,000 realizations of roof snow load, based on ground snow loads of 10 psf and 25 psf. These simulations assume uniform load, *i.e.*, no drifting.

# 4. NON-UNIFORM ROOF SNOW LOADS

Based on information from the insurance industry, approximately 75% of all structural losses from snow have historically been caused by drifting snow. These damages contributed to $210,000,000 in insured damage between 1977 and 1989 in 1990 dollars (O'Rourke & Auren 1997). In this section, snowdrift will be discussed in two parts. The first part describes research on snow drifts and how drift is included in U.S. design standards. The second part describes the development of a non-uniform probability model that predicts drift loads. The non-uniform model was developed to estimate the drift snow load that typically forms at the base of multilevel roofs. As with the uniform roof load model, non-uniform loads will be determined on an event by event basis making the predictions different from what design equations estimate in the design of drift loads. In addition to predicting the peak drift load, a drift height is also predicted in the model. The drift height, along with the peak drift load, allows the user to estimate a triangular distributed drift load at the base of multilevel roofs.

## 4.1 Past Research on Snowdrift Loading and Application in U.S. Design Standards

Snowdrift occurs where roof structures are uneven and wind can carry snow from one portion of the roof to another. Drifting happens when high winds transfer snow particles to areas of low winds. Roofs with steps, gables, valleys and other obstructions are likely candidate structures that may form drift loads. The drifting surcharge must be accounted for in the roof snow load design in areas where drifts are likely to occur. Drifting causes an unbalanced snow load and can lead to local failure if not properly accounted for in the structural design. Drifts can occur on either the leeward or the windward roofs.

It is important to first consider the conditions under which a snow drift may or may not occur in order to asses drift snow load design. In order for drifting to occur, (1) a source of snow must be present to be moved, (2) a geometric irregularity must exist in the roof and (3) a source of wind must be present (O'Rourke & Auren 1997). The roof size has also been shown to have a large effect on the size of the drift (O'Rourke et al. 2005). In addition, based on meteorological data and transport theory, drifts will not occur if any one of the following three conditions is present. First, snow does not drift after the rain, sleet or freezing rain. Second, drift will not happen if the temperature is greater than 32˚F. Last, drifting does not occur if more than three days have elapsed since the last occurrence of snowfall (DeGaetano et al 2003). Any of these three conditions make the snow denser and less likely to be transported by winds. Snow density is a function of air temperature and depends also on how long the snow has been on the ground.

Wind speed also has an important influence on drift formation. DeGaetano et al. (2003) states that wind speeds less than 10 miles per hour (mph) are insufficient to transport snow. However, Meloysund et al. (2007) finds that drifts have been found to form at wind speeds as low as 1-3 mph. As wind speed increases up to 12 mph, the snow blows more horizontally than vertically, causing large redistributions of snow. However, even greater wind speeds will often blow the snow vertically off the roof leaving roofs bare (Meloysund et al. 2007).

Climate, therefore, has an important influence on the formation of drifts on multilevel and gable roofs. In Canada and the North Eastern part of the United States, heavy snowfalls often coincide with high wind speeds and freezing temperatures. As a result, drift-load ratios are the greatest in the Northern Plains and the Eastern Great Lakes regions of the United States (O'Rourke et al. 2005). However, in other locations, such as Norway and the mountain regions

of the Western U.S., heavy snowfalls occur with lower wind speeds, reducing the likelihood that drifts will form.

Over the years, many changes have been made to the snowdrift provisions in design standards and continue to be updated based on an improved understanding of snow density, wind speeds and transport theory. The ASCE 7 load standard has provisions for snow drift for gable roofs, multilevel flat roofs, parapets and arch roofs. In this section, it will be discussed how ASCE 7 has changed over the years to develop the provisions for snowdrift design in the current ASCE 7-10 standard.

*4.1.1 Drift Loading on Gable Roofs*

Gable roofs are very common, particularly on residential structures, and are likely to form snow drifts on one side of the roof. Figure 4.1 shows a low-sloped gable roof structure before and after the formation of snow drift; in the figure, *W* is the distance from the ridge to the eave. The figure shows how the depth of snow can become very small on the windward side and very heavy on the leeward side, especially at the eave. The surcharge due to snowdrift must be considered if the slope of the roof exceeds ½ on 12 (2.4˚) and is less than 7 on 12 (30.2˚) (ASCE 2010).

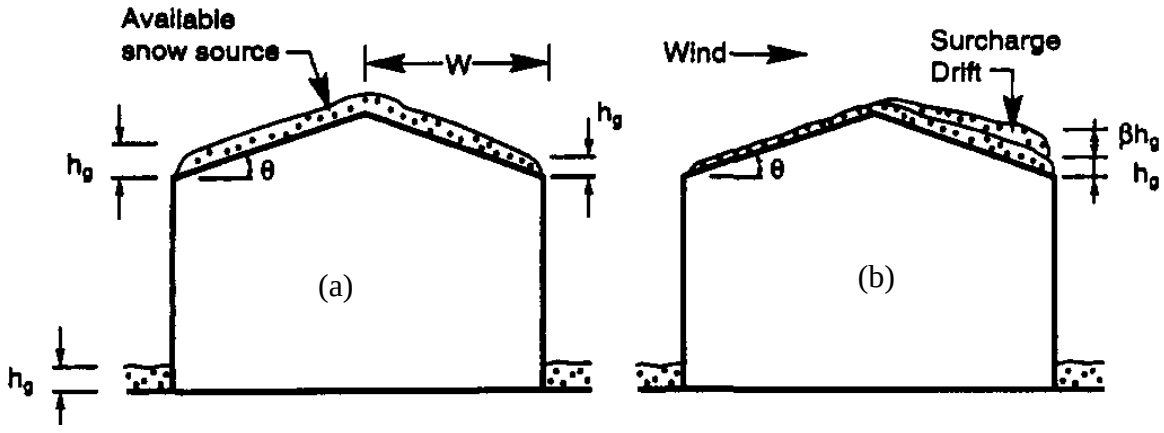


**Figure 4.1-** Snow loads on leeward gable roofs (a) before and (b) after drift formation (O'Rourke and Auren 1997)

The development of the ASCE 7-02 snow load provisions for gable roofs used information gathered from 28 case studies reviewed by O'Rourke and Auren in the 1997 report "Snow Loads on Gable Roofs". In these case studies, the majority of the snow failures due to snow drift were found to be on structures with large widths and low design ground snow loads. O'Rourke and Auren (1997) proposed that the snow drift coefficient, $\beta$, be revised for low sloped gable roofs symmetric about the ridge line to consider the length to width ratio. The snowdrift coefficient, $\beta$ based on the length-to-width ratio is shown here:

$$\beta = \begin{matrix} 0.5 & L/W \leq 1 \\ 0.333 + 0.167L/W & 1 < \frac{L}{W} < 4 \\ 1.0 & L/W \geq 4 \end{matrix} \qquad (17)$$

In Equation *(17)* $L$ is the length of the roof or the dimension going into the page in Figure 4.1 In the 2002 standard (Equation *18*), the length-to-width dependence, $\beta$ was not included, but $\beta$ did become a function of the ground snow load, $P_g$. Based on meteorological data drift heights are based on the ground snow load and wind speed. Lower ground snow loads will form larger drifts, whereas heavier snowfalls will need a larger wind speed to form drifts and, therefore are less likely to form drifts.

$$\beta = \begin{Bmatrix} 1.0 \\ 1.5 - 0.025P_g \\ 0.5 \end{Bmatrix} \begin{matrix} P_g \leq 20 \\ 20 < P_g < 40 \\ P_g \geq 40 \end{matrix} \qquad (18)$$

The current design standard, ASCE 7-10, provides guidelines for snowdrift design on gable roofs in a slightly different manner than the previous standards presented. In ASCE 7-10 the $\beta$ term is no longer used. Instead, the surcharge drift load is based on a length and width equation, where $h_d$ is the drift height in feet and is calculated according to the equation below:

$$h_d = 0.43 \sqrt[3]{l_u} \sqrt[4]{p_g + 10} - 1.5 \qquad (19)$$

where $l_u$ is the eave to ridge distance in feet (i.e., the same as *W* above) and $p_g$ is the ground snow load in psf. The magnitude (Equation *20*) and horizontal extent (Equation *21*) of the drift load is based on $h_d$:

$$D = \frac{h_d \gamma}{\bar{S}} \qquad (20)$$

$$w = \frac{8\ \overline{Sh_d}}{3} \qquad (21)$$

where $h_d$ is the drift height in Equation *(20)*, $\gamma = 0.13p_g + 14$ is the snow density in pcf and *S* is the roof slope, the run in feet for a rise of one foot. When $l_u$ is less than 20 ft., the surcharge is found by multiplying the importance factor, *I*, by the ground snow load $p_g$ and the drift height, $h_d$, is no longer used (ASCE 7-10). Appendix C shows the design snow load for the same roof structure in accordance with ASCE 7-95, ASCE 7-02 and ASCE 7-10 editions; the provisions in ASCE 7-05 and ASCE 7-10 are very similar for unbalanced snow loads on gable roofs.

O'Rourke et al. (2005) evaluated design equations for snow drift on gable roofs, on the basis of 40 years of drift ratio data from 53 U.S. stations. In this data set, the drift ratio (*DR)* was determined as:

$$DR = L_d / (P_g * F) \qquad (22)$$

where $L_d$ is the total drift surcharge with units of lbs/ft; $P_g$ is the annual maximum ground snow with units of psf; and *F* (i.e., the same as W above) is the fetch or along wind plan dimension of the windward snow source area with units of feet. In order to determine the drift ratio, the total drift surcharge, $L_d$, must be calculated. O'Rourke (2005) simulated the drift formation at each station location for a hypothetical gable roof building with a slope of 2.5˚, 5˚ and 10˚ using transport theory and wind speed (eight directional wind speeds) and ground snow load. Annual maximum drift loads were calculated for the period of 1951-1995 for most of the stations included in the report. Using a Gumbel distribution the annual maxima could be used to

determine a 50-year drift snow load. Comparing the simulated 50-year drift ratios to ASCE 7 standards, O'Rourke (2005) determined that ASCE7-02 is overly conservative in predicting snowdrift for gable roofs, as shown in Figure 4.2. The revised gable equations in ASCE 7-05 were found to more accurately predict snowdrift without being overly conservative (O'Rourke et al. 2005).

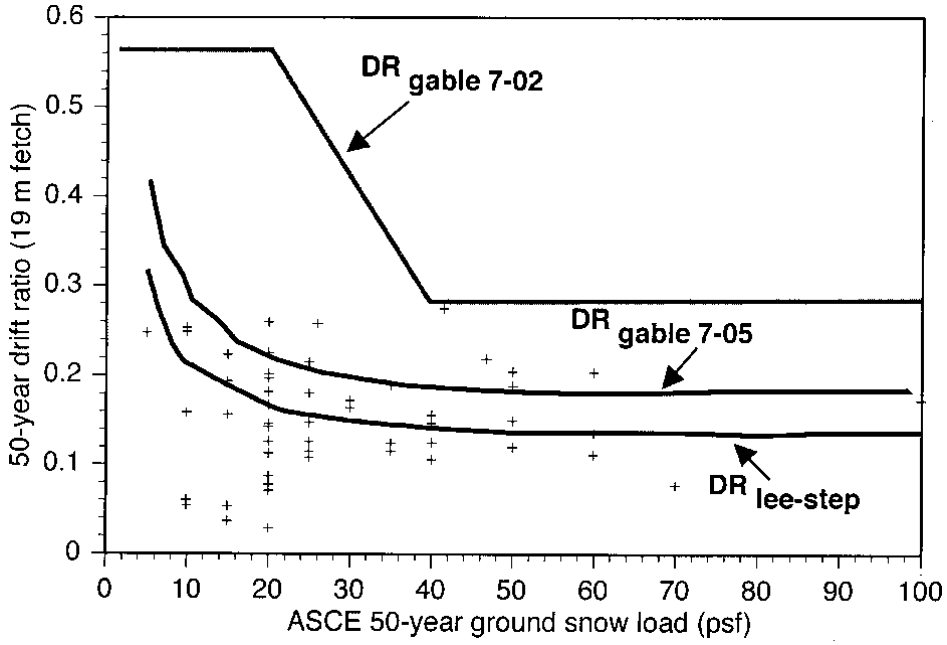


**Figure 4.2-** 50-year drift load ratios for 53 sites in the U.S. compared to the provision in ASCE 7-02 and ASCE 7-05. *DR* is determined using Equation *(22)* with a fetch distance, *F*, of 19 meters (O'Rourke et al. 2005).

*4.1.2 Drift Loading on Multilevel Roofs*

As with gable roofs, snowdrifts can form on multilevel flat roofs where the wind blows the snow off the upper roof and onto the lower roof forming a drift at the step of the upper roof, as shown in Figure 4.3. Based on a number of case studies involving snowdrift on multilevel flat roofs, O'Rourke et al. (1985) developed changes to the 1982 ANSI design standard for this form of snow drifting. The drift load was found to be most influenced by the length of the upper roof, roof elevation difference, ground snow load and lower roof length, in that order. The surcharge snowdrift load used in ASCE 7-10 is a function of both the length of the upper roof, $l_u$, and the

50-year recurrence ground snow load, $p_g$. In Figure 4.4, the surcharge load due to drifting is shown where $h_d$ is the height of the triangular surcharge load and $w$ is the width. The surcharge is assumed to have a slope of 1:4 (rise of 1 foot per 4 feet of run) and the peak surcharge load is the product of $h_d$ and the unit weight of snow, γ. O'Rourke and De Angelis (2002) showed through case studies and dirft formation aerodynamic studies, that drift formations at a roof step tend to be either triangular or quadrilateral in shape; if the total drift height is comparable to the difference in roof height, the wind streamlines will form a triangular drift formation. Therefore, a triangular distribution is assumed in the design of drift loads at the step of a multilevel roof. Equation *(19)* shows the calculation for surcharge height, $h_d$ and Equation *(23)* shows the surcharge width, $w$, in the ASCE 7-10 standard.

$$w = 4h_d \qquad (23)$$

where $h_d$ is the drift height in feet and $w$ is the surcharge width in feet. The surcharge load is added to the balanced snow load predicted by design equations for uniform roof loads.

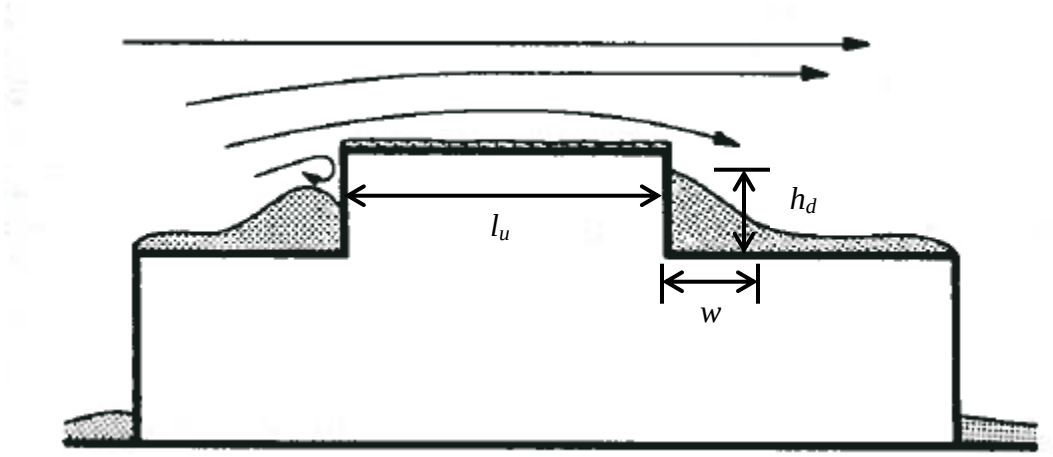


**Figure 4.3-** Snowdrift formation on multilevel flat roof (O'Rourke et al. 1985).

Based on 53 snowdrift case studies, O'Rourke et al. 2005 concluded that ASCE 7-02 accurately predicts the snowdrift formed on the leeward roof, as shown in Figure 4.2. It was also found that the drift loads are slightly more conservative as the fetch distance increases and the

ground snow load decreases. The snow drift load in ASCE 7-10 has only a slight variation from that of ASCE 7-02 and ASCE 7-05. Appendix C shows a comparison for the snow drift on a roof with a leeward step for ASCE 7-02 and ASCE 7-10. The drift load surcharge varies by 0.2 psf or less than half a percent. Multilevel roofs will be the concentration of the non-uniform model developed in the next section.

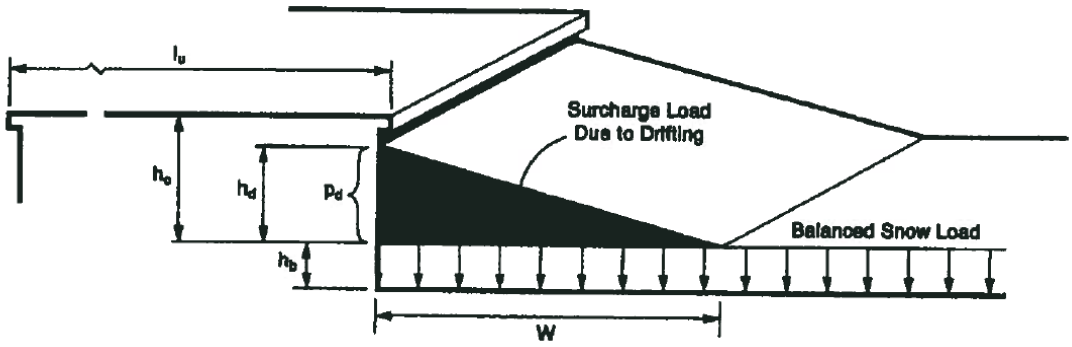


**Figure 4.4-** Surcharge load due to drifting in ASCE 7-10 (O'Rourke et al. 2005).

## 4.2 Probabilistic Drift (Non-Uniform) Load Model

The non-uniform drift load model developed here predicts the total drift load and drift height for multilevel roof structures. As with the uniform load model described in Chapter 3, the probabilistic model developed here is different from load standards in the way that it predicts loads for an event (i.e., measuring the ground snow load and ground snow density and predict the drift load on the roof for that same time). The model uses similar parameters to those in ASCE 7-10.

### *4.2.1 Probabilistic Model Factors*

The model was developed using the data from the CRREL 1982 research project and von Bradsky (1980). Structures included in the dataset have multilevel roofs and non-uniform drifting loads. The data include 18 buildings, encompassing 70 data sets of drift and ground

snow loads of which, 53 are from heated buildings and 17 from unheated buildings, and 49 are windswept and 21 are semi-sheltered. Exposure parameters, thermal parameters, upper roof length, roof snow load, ground snow load, ground snow density and roof snow density for each measurement are reported. Data are only available for multilevel roofs; multilevel roofs are the most common form of structural collapse due to drifting. The model can also be used for parapet roofs where the formation of a drift is similar to multilevel roofs. The complete dataset is provided in Appendix B.

The drift model developed here will predict the maximum drift snow load and the height of the drift for an event where there is ground snow load and ground snow density data available and some structural parameters are known. The maximum drift snow load is defined as the largest snow load in the drift, forming at the step of the lower roof. Unlike the drift load predicted in design standards, which is added to the uniform snow load, the drift load predicted using the model includes the uniform and the drifting load. Factors considered to affect drift loading include the following:

- Obstructions *(D)*: In order for the snow load on a roof structure to form a drift, an obstruction such as a gable roof, a multilevel roof, roof parapets or other must be present to inhibit the wind's movement of snow.
- Exposure Factor ($D_e$): Exposure factors include fully exposed, partially exposed and sheltered, with fully exposed roofs tending to have larger drift formations.
- Roof Thermal ($D_t$): Cold structures such as refrigerated structures will have a smaller drift load whereas heated structures will have a larger drift load.
- Roof Length *($D_l$)*: The upper roof length provides a source of snow to be transported to form snow drifts. Drift loads tend to increase as the upper roof length increases.
- Density of Snow *($D_{gd}$)*: Cold temperatures are associated with less dense snow, therefore forming smaller drift loads. High temperatures are associated with denser/heavier snow forming larger drifts.

To begin the drift model, *D* is computed as the average conversion factor for all the dataset buildings. This data gives *D =4.7*. This value can be compared to design drift loads as obtained by codes and standards, which are based on the drift height, $h_d$, in Equation *(20)*, which varies based on ground snow load and roof length. Of the roof events considered, the maximum *D* was 25 and the minimum was 0. Variation in *D* depends on the other characteristics of the roof, as described below.

Combining the terms, described above, the non-uniform drift load for multilevel roofs can be predicted using:

$$DSL = D * D_e * D_t * D_l * D_{gd} * GSL \qquad (24)$$

In Equation *(24)*, *DSL* is the maximum drift snow load predicted in psf and *GSL* is the ground snow load in psf. The factors used and the steps used to develop the model are described below.

Roof exposure is the first factor in the model, since it has the largest effect. The amount of shelter surrounding the roof has the largest effect on the size of drifts compared to the other factors used in the model. The ratio in mean value between the two categories of exposure is 4, nearly 3 times the size as in the uniform model showing the large effect wind and exposure have on the formation of drift loads. The exposure factor for the non-uniform model only has two categories, windswept or semi-sheltered. Since there were only 2 data points for sheltered roofs, the sheltered exposure roofs were combined with the semi-sheltered roofs, with both having similar effects on the drift conversion factor. It should be noted that it is relatively rare that drifts form on sheltered roofs. Figure 4.5 shows the mean conversion factor for the two exposure parameters. As expected, windswept roofs will have a much larger snow drift load than semi-

sheltered, having a mean conversion factor of 1.3, compared to 0.3 for semi-sheltered. The drift exposure coefficient is determined from:

$$D_e = \frac{ADS}{D*GSL} \quad (25)$$

where *ADS* is the actual (measured) drift snow load in psf, *D* is the drift coefficient, and *GSL* is the ground snow load in psf. The drift conversion factors for exposure are much larger than the uniform conversion factors for exposure, and may be as large as 5.

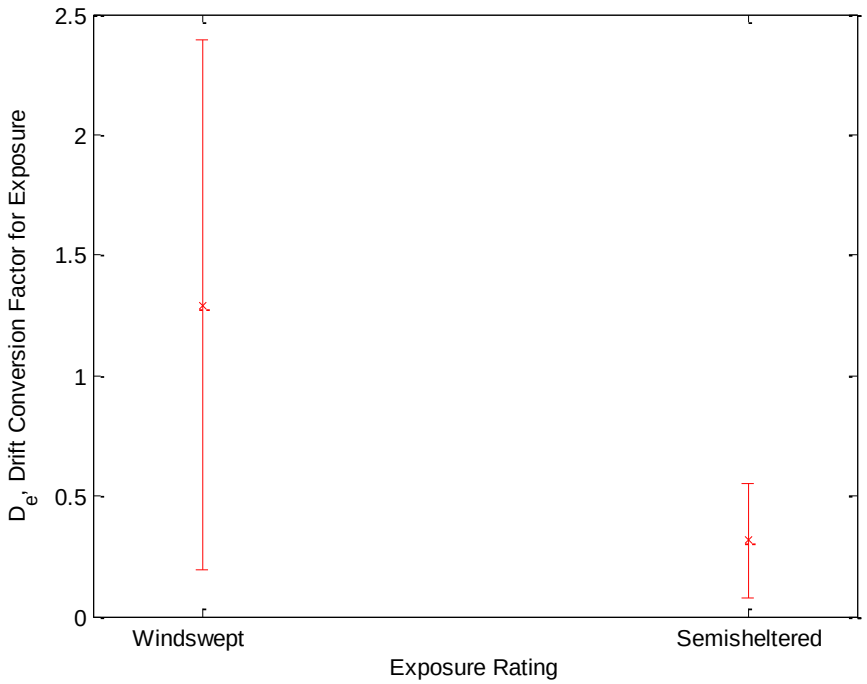


**Figure 4.5-** Event-based ground to roof drift load conversion factor as a function of the exposure rating of the structure. Error bars show mean +/- one standard deviation.

The thermal parameter was determined to have the second largest effect on the drift snow load. In comparison to the uniform model, the thermal parameters had the opposite effect on the predicted conversion factor of ground to roof snow loads due to the relationship between building thermal characteristics, the density of the snow, and the role of snow density in drift formation. Unheated structures will have less dense snow. When the wind blows the less dense snow, it is more likely that it will be completely removed from the roof instead of forming a

drift. Figure 4.6 reports the thermal conversion factor for drift loads, $D_t$, where the mean conversion factor for heated is 1.2 compared to 0.5 for unheated roofs. The conversion factor for thermal $D_t$ is adjusted for exposure and takes the form:

$$D_t = \frac{ADS}{DD_e GSL} \qquad (26)$$

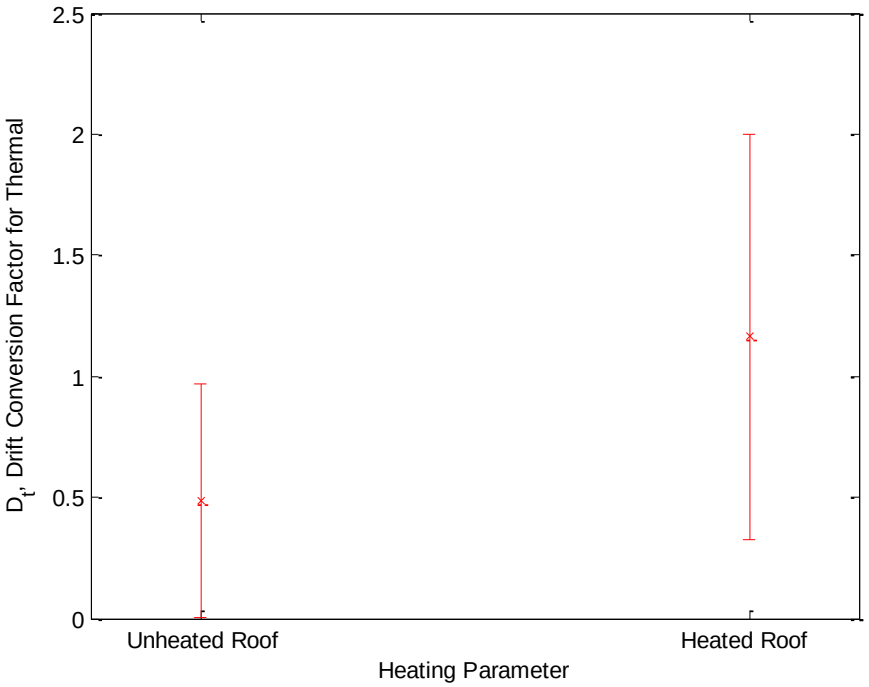


**Figure 4.6-** Event-based ground to roof drift load conversion factor as a function of the heating parameter of the structure.

The upper roof length *(UL)* in Figure 4.7 was considered next in the model. The length conversion factor is determined from:

$$D_l = \frac{ADS}{DD_e D_t GSL} \qquad (27)$$

As shown in Figure 4.7, the upper roof length is modeled as causing a linear increase in conversion factor as the length of the upper roof increases. For upper roof lengths of 100 ft. or longer, the roof conversion factor becomes constant. The functional form is as follows:

$$D_l = 0 \text{ for } UL<5 \text{ ft.}$$

$$D_l = 0.0062 \times UL + 0.59 \text{ for } UL<100 \text{ ft.} \qquad (28a)$$

$$D_l = 1.20 \text{ for } UL \geq 100 \text{ ft.} \qquad (28b)$$

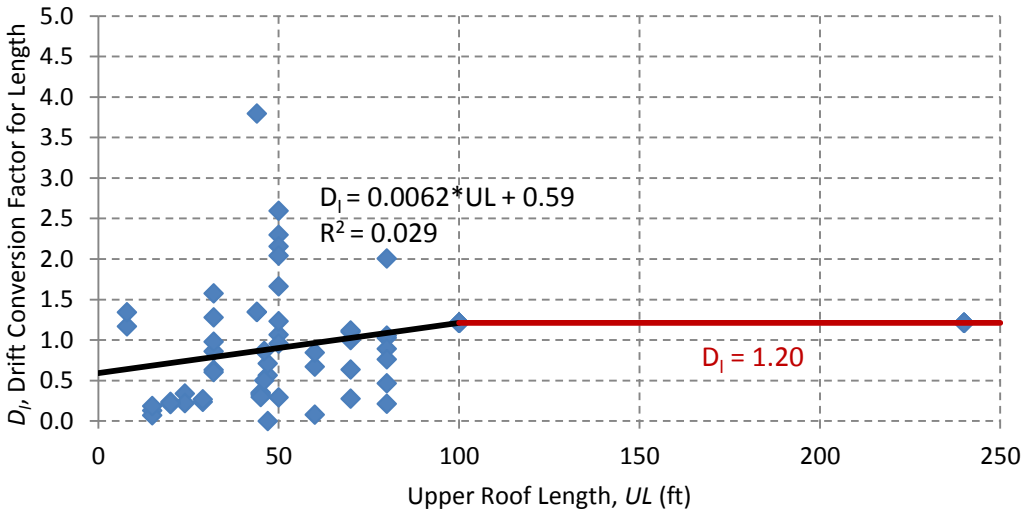


**Figure 4.7**- Drift conversion factor $D_l$ in Equation *(27)* as a function of the upper roof length, *UL*.

The last factor in determining the drift snow load was a ground snow density term where

$$D_{gd} = \frac{ADS}{DD_e D_t D_l GSL} \qquad (29)$$

The ground snow density has a similar decreasing affect as the climate term in the uniform snow load model, where a higher ground density indicates a smaller drift load, as shown in Figure 4.8. As the ground density increases, the wind will transport less snow to form a drift, making the conversion factor smaller. Drifts are less likely to occur as the ground snow load becomes heavy, therefore there is no upper limit on the linear equation for practical values of ground snow density. The ground density factor, $D_{gd}$, can be determined using Equation *(30)* where *GSD* is the ground snow density:

$$D_{gd} = -0.03 \times GSD + 1.38 \qquad (30)$$

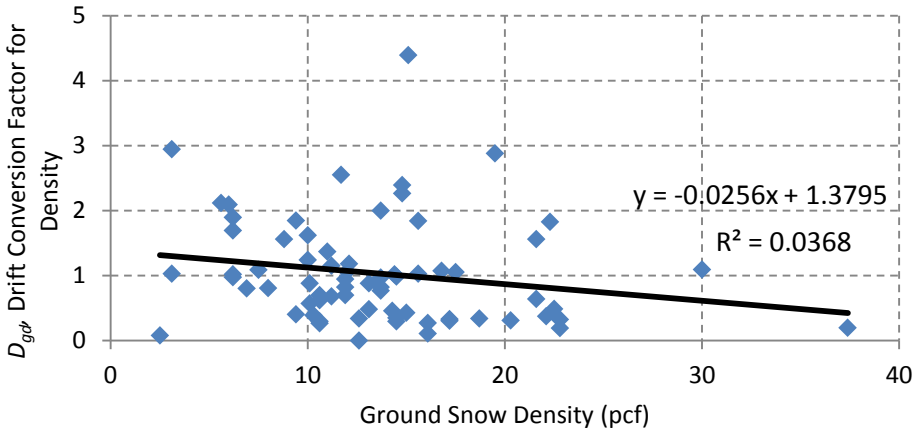


**Figure 4.8-** Event-based ground to roof drift load conversion factor as a function of the ground snow density.

Lastly, in order to determine the drift height and thus the spatial distribution of the drift on a particular roof a factor relating the ground snow density to roof density had to be developed. Since roof conditions are different than the ground, a linear equation was developed to relate the roof drift *(RSD)* and ground snow densities *(GSD)* by

$$RSD = 0.42 \times GSD + 10.6 \qquad (31)$$

As shown in Figure 4.9, the linear equation obtained from regression relates roof density to ground snow density fairly well, though there is still significant dispersion in the prediciton having an $R^2$ value is 0.18. For lower ground snow densities the roof drift density is much higher, whereas for large ground densities the roof density is similar in value. Higher ground densities will be less affected by roof thermal radiation, whereas lower ground densities will be denser on the roof due to thermal effects. Using the drift height and the predicted maximum drift load, a 1:4 triangular distribution of the drift snow load can be calculated at the roof step. A 1:4 relationship is assumed based on previous research (O'Rourke and De Angelis, 2002) using drift fromation aerodynamics and previous assumptions made in building codes and standards for drift load formation.

If the ground density is unknown for the site, the ASCE 7-10 density equation should be used:

$$\gamma = 0.13P_g + 14 \qquad (32)$$

where $\gamma$ is the snow density in pcf and $P_g$ is the ground snow load in psf. When the CRREL data is used, ground snow density is related to ground snow load by $\gamma = 0.23P_g + 14$, a similar relationship.

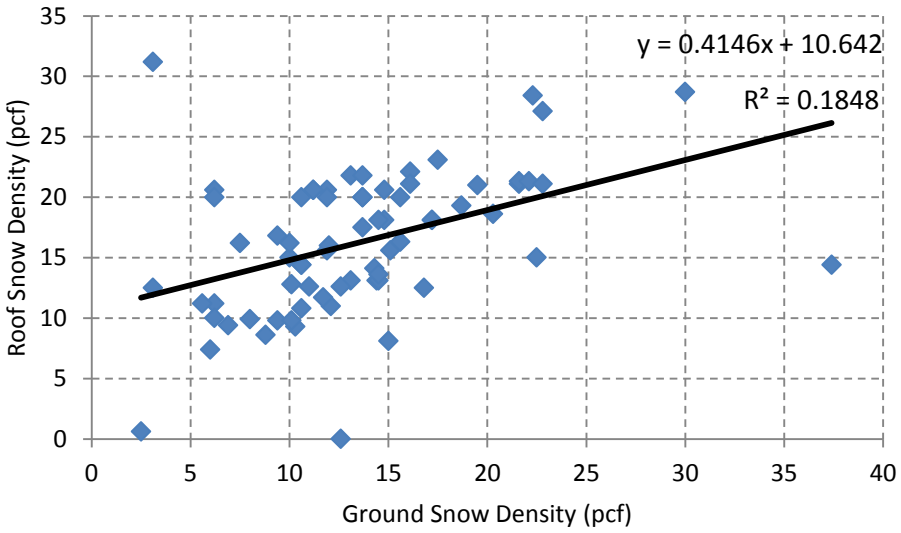


**Figure 4.9-** Ground snow density versus roof (drift) snow density

*4.2.2 Results of the Drift Load Model*

Predicted drift snow loads and drift snow heights were compared to the actual reported in the CRREL report. A complete comparison of the predictions is shown in Appendix B. The maximum and minimum $K_d$ values are 11.2 and 0.38, respectively, showing a much wider variation than the $K_v$ values for the uniform roof snow load model. The average predicted drift load compared to the average actual drift load was found to be 1.0 using the mean drift conversion values found in Table 4.1 and using Equation *(24)*. Drift heights were also calculated by dividing the maximum roof snow load (Equation *24*) by the ground snow density (Equation *31*), and the mean bias ratio for drift height, i.e., ratio of actual to predicted,was found to be 1.05.

This larger varience in the prediciton of $K_d$ compared to $K_v$ (corresponding to a lognormal standard devation among all buildings of 0.62, compared to 0.28 in the uniform model) is due to larger natural variability in drift loading and occurrence and, consequently, greater difficulty in predicting drift loads.

**Table 4.1-** Drift load conversion factor mean values and lognormal standard deviations.

| Factor | Description | Value ($\mu$) | Standard Deviation ($\sigma_{ln}$) |
|---|---|---|---|
| $D$ | Average Ground to Drift Conversion | 4.73 | 0.85 |
| $D_e$ | Windswept | 1.29 | 0.74 |
| | Sheltered | 0.32 | 0.67 |
| $D_t$ | Unheated | 0.49 | 0.69 |
| | Heated | 1.16 | 0.54 |
| $D_l$ | Roof Length <100 ft. | y = 0.0062x+0.60 | 1.00 |
| | Roof Length ≥ 100 ft. | 1.21 | 0.56 |
| $D_{gs}$ | Ground Snow | y = -0.026x + 1.38 | 0.68 |

Structures in the report were split into subcategories to further evaluate the accuracy of the model. Table 4.2 shows the mean bias in drift conversion factor for the different subcategories. The most accurate category is semi-sheltered/heated roofs, which has a mean bias ratio of 1.06. There is more significant bias for both groups of unheated roofs. Unheated roofs account for less than 25% of the structures used in the study. Therefore, it is recommended that further data be used to determine the accuracy of drift snow load and drift height predictions using this model.

**Table 4.2-** Comparison of predicted $K_d$ values to actual $C_d$ values found in the CRREL study for various structural parameters

| Group Description | No. of Structures in Group | Mean $K_d$ Predicted | Standard Deviation $K_d$ | Mean $C_d$ Actual | Standard Deviation $C_d$ | Mean Bias Ratio |
|---|---|---|---|---|---|---|
| Windswept Heated | 40 | 7.31 | 5.06 | 7.91 | 2.04 | 0.89 |
| Windswept Unheated | 9 | 0.82 | 0.16 | 2.34 | 0.41 | 0.35 |
| Semi-sheltered Heated | 13 | 1.61 | 1.34 | 1.53 | 0.18 | 1.06 |
| Semi-sheltered Unheated | 8 | 1.32 | 0.67 | 0.61 | 0.12 | 2.18 |

*4.2.3 Drift Snow Load Model Case Study*

The model can be used in a Monte Carlo simulation to predict possible drift snow loads, given some structural parameters and climatological data on ground snow loads and ground snow densities for a given site. For a multilevel roof structure that is heated, has a semi-sheltered exposure, upper roof length of 50 ft., ground snow density of 18 pcf and a ground snow load of 30 psf, the probabilistic drift load is shown in Figure 4.10. The magnitude and distribution of the drift load is shown in Figure 4.11.

A comparison of the mdel and ASCE 7-10 drift loads show that design standards are conservative in estimates of drift loads. According to the probabilistic model, the mean value for the maximum drift load on the case study roof is 42 psf, corresponding to a mean drift height of 2.3 ft. The uniform snow load predicted for this structure is 14 psf. If the same roof and loading parameters are inputted into ASCE 7-10 provisions, the surcharge drift load is 43 psf for a surcharge height of 2.4 ft. Adding the surcharge to the uniform snow load (21 psf) the maximum design snow load at the step is 64 psf. As described at the end of Chapter 3, the uniform model tends to underpredict what building codes and standards require for design, primarily because load standards are conservative in this estimate. The non-uniform drifting model developed here

also underpredicts the maximum drift load compared to design requirements in ASCE 7-10 (42 psf from the model and 64 psf in ASCE 7-10). The model uses an event-based conversion factor versus building codes and standards which predict a 50-year maximum value so values may not be directly comparable.

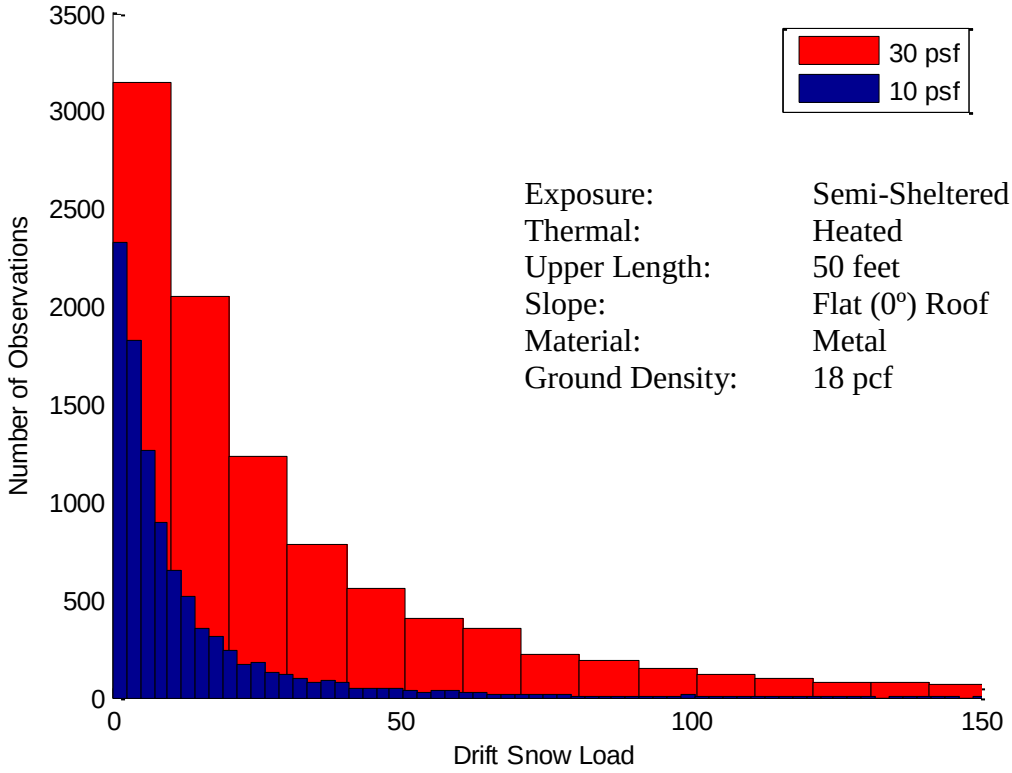


**Figure 4.10-** Monte Carlo simulations for 10,000 realizations of maximum drift load, based on ground snow loads of 10 psf and 30 psf.

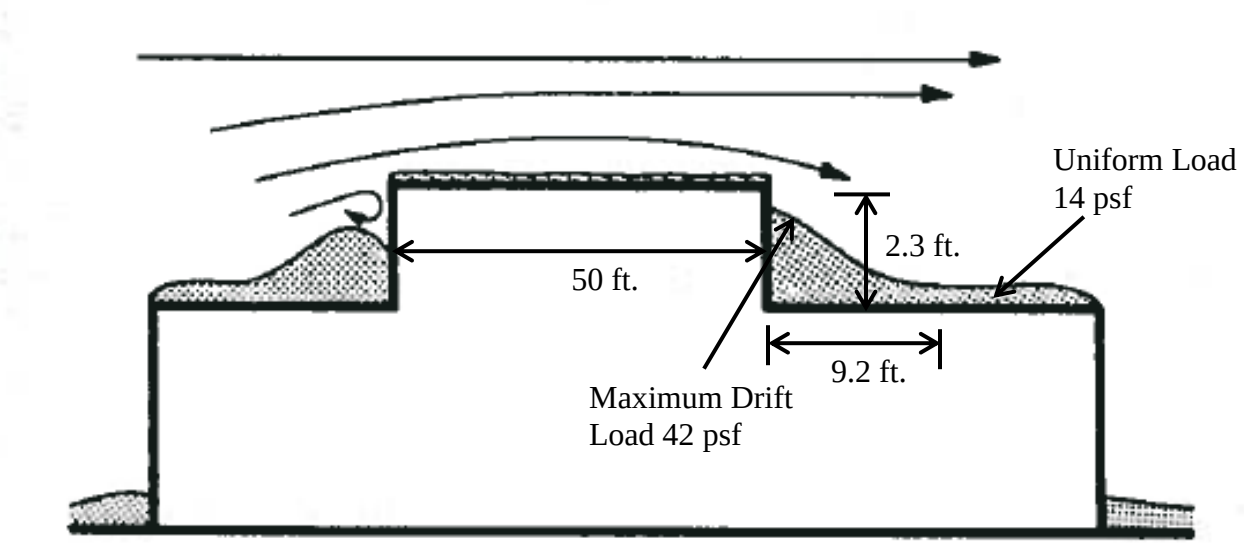


**Figure 4.11-** Mean maximum drift snow load, drift height and uniform snow load predicted using Monte Carlo simulation for a semi-sheltered heated roof structure with an upper roof length of 50 ft.

## 5. SNOW LOAD FAILURE CASE STUDIES

In this section, case studies and other publications discussing structural failures due to excessive snow loads were reviewed to determine common failure mechanisms. This section will outline the problems that occurred with past roof collapse due to extreme snow loads and provide background information on the Village Square walkway roof collapse at Copper Mountain that is analyzed in the next section.

### *5.1 Hartford Civic Center*

The Hartford Civic Center in Hartford, Connecticut is one of the most famous roof failures due to snow loading in U.S. history. The roof collapsed on January 18, 1978 after a heavy snowfall. The coliseum was at full occupancy just hours before the collapse but, fortunately, when the space roof truss system fell 83 feet at 4:19am, the building was vacant. As described by Delatte and Martin (2001), several design flaws, as well as careless construction practice led to this collapse. A primary cause of the failure was the underestimation of the dead load in the design of the coliseum by 20%. In addition, members in the space frame were insufficiently braced, causing compression members in the top layer of the space frame system to be overstressed by as much as 852%. The load on the day of failure was approximately 70 psf and the structure should have had a design capacity of 140 psf (Delatte and Martin, 2001). The structural engineering firm responsible for the design used state-of-the art (at the time) computer software to check the design, but failed to check the analysis with hand calculations or other methods. This technology was new and the engineers felt it would save the client substantial money in material costs. The computer model was so heavily relied upon that even during construction, when inspectors witnessed deflections significantly greater than predicted deflections and allowable limits, engineers chose not to reevaluate or change their design. In

addition, the architect suggested that a structural engineer be on site at all times during construction to ensure that the design was being constructed as intended but, in reality, a structural engineer was rarely present during construction. After the event, many engineers believed that if the Hartford Center had been peer reviewed, as is recommended for large structures, many of the design flaws would have been spotted and potentially corrected. Since the Hartford Center collapse, the state of Connecticut became one of the few states that require large occupancy structures be peer reviewed (Delatte and Martin, 2001). The Hartford Civic Center is a lesson learned on the importance of using more than one method to check designs. This is especially true today with the high reliability that engineers place in software for structural analysis.

*5.2 East Coast Snow Loads*

The evaluation of the January 1996 snow storm that exceeded the 50-year return period ground snow loads in many areas along the Philadelphia, PA to Newark, NJ corridor showed that many of the roof failures had loads exceeding 50-year minimum design standards (DeGaetano et al, 1997). Even so, relatively few roof failures occurred in the Philadelphia to Newark corridor, where snow levels exceeded even the 100-year return period ground snow loads. This was due to local building codes in these areas having additional snow load requirements such that design levels exceeded the 50-year recurrence interval values specified in ASCE Standards. Many of the snow-related roof collapses during this storm were associated with snow loads consistent with return intervals in the 50 to 75 year range. Snow related roof failures that occurred in due to snow loads with recurrence intervals less than the 50-year period were most likely due to other factors, including large drifting loads or deterioration of members in older structures. In a study by O'Rourke et al. (1995), it was found that the minimum requirements for drift height are under

predicted by ASCE 7-95 making it likely that design drift loads were exceeded even in areas where the ground snow load was less than the 50-year return period (DeGaetano et al, 1997).

*5.3 Roof Collapse of a Single Story Steel Factory*

Pidgeon et al. (1986) presented a case study single-story steel factory building, arguing that the failure of the structure was caused by the unintended consequences of progress in the overall understanding of structural behavior. Three different phases of the factory, located in the United Kingdom, were designed by the same engineer over a 10-year period from 1970-1980. The roof of the second phase of the structure failed after high amounts of snow loading and drifting loads had occurred. Even though all three phases were designed similarly, the third phase had one thing slightly different which contributed greatly to the collapse. Specifically, the third phase of the structure was designed for storage and needed to be 1.5 meters (5 ft.) taller than the previous two phases. After a severe snow storm, two bays of the second phase collapsed. A large snow drift occurred against the 1.5 meter step between the structures from phase one and two, causing high local loading. It was reported that the ground snow load was not abnormal and had a return period of about 10 years, i.e., well below the 50-year interval in snow codes. The combination of the snow fall and winds caused the buildup of snow at the step of the roof leading to the failure (Pidgeon et al. 1986).

After investigating the factory roof collapse, several observations were made by Pidgeon et al. (1986). The first lesson learned from this case study is engineers must be aware that code provisions are a minimum standard and engineering judgment must be used to not only limit the cost of materials, but ensure the safety of structures. The engineer for this structure claimed that it would have been difficult to convince his client to make expensive modifications to the second phase when not required by the building code. Methods developed in performance-based snow

engineering could convince a building owner to make modifications to prevent the collapse of structures even though it is not required by building codes or standards. The second lesson learned is that the engineer should identify and minimize the risk of unintended consequences when faced with a decision. Even though material costs are major concern to building owners, engineers must identify risk and design accordingly (Pidgeon et al. 1986). Finally, when adding to another building the impact on neighboring structures must be considered. The engineer should have considered the consequences of drift loads occurring due to the roof step in the third phase and therefore, modified the design to mitigate risk of snow induced failure. Many of the lessons learned from this case study have been changed since the 1980's, but the study still shows how performance-based engineering methodology can be used to better inform decisions makers of snow related risks.

### *5.4 Village Square Building*

The investigative engineering firm, Knott Laboratory in Denver, CO, reviewed two roof failures and redesigned two similar structures that failed at Copper Mountain, CO. The two structures, similarly designed and built around the same time, failed within weeks of each other in late February and early March of 2008. After reviewing the reports for both structures it was determined that the failures were very similar and just one of the buildings was chosen to do a more in-depth study by constructing a model of the roof, described in the next Chapter. Additional information was provided by the property manager at Copper Mountain, Shedd Webster.

#### *5.4.1 Engineering Investigation*

The Village Square building is a six-story commercial building comprised mostly of condominiums, with a single story garden level of retail outlets. The garden level walkway roof

was severely damaged from sliding snow and ice from the upper six story building on February 19, 2008. Knott Laboratories inspected the structure on March 26th with a follow up on April 11th, 2008 to inspect and photograph damaged roof elements, shown in Figure 5.1. The majority of the bar joists were deflected and deformed and wide flange supporting beams were also visibly deflected (Knott Laboratory, 2008).

After Knott Laboratories' inspection, they recommended the roof structure be removed and replaced. This recommendation was based on visual inspections and after analyzing the roof structure in accordance with current building code requirements. Their analysis showed that the existing bar joists were stressed to 197 percent of the capacity under code load levels. The existing building code (IEBC) defines structural elements as "dangerous" when:

*"The stress in a member or portion thereof due to all factored dead and live loads is more than one and one third the nominal strength allowed in the International Building Code for new buildings of similar structure, purpose or location" (IEBC 2003).*

Based on the above observations Knott Laboratories recommended a new roof structure comprised of several new roof framing elements to prevent future failures (Knott Laboratory, 2008). The reconstruction was completed in July of 2009, approximately 15 months after the failure, at a total cost of $350,000 (Webster, 2010). This estimate of losses does not include the loss in revenue for businesses in the 15 months of closure and the loss of revenue to Copper Mountain during the closure.

**Figure 5.1-** Deflected (a) bar joists and (b) wide flange beams due to large snow loads in February 2008 (Knott Laboratory 2008).

In the redesign of the roof structure, several design changes were made. The joists were changed to a 12K1 Vulcraft joist and the joists were spaced at 24" o.c. as opposed to 44" o.c. The roof panels were not changed, but the reduction in joist spacing decreases the center-to-center distance making the failure of the panels or nonstructural components less likely. The W-beam was replaced with a W14x53 with stiffeners located at each of the column centerlines.

*5.4.2 Interview with Property Manager at Copper Mountain*

I met with Shedd Webster on Friday, January 21, 2010 to discuss the Knott Laboratory reports and to a take a tour of the roof structure. I asked Mr. Webster several questions about the weather conditions, warnings of structural failure, business closures, inspection after the collapse, and cost of repairs, along with other questions about the structural damage and repair. The first thing that I found interesting after meeting with Mr. Webster is that the two structures were built around the same time and then collapsed within days of each other. On the day of the Village Square failure the snow fell from a higher six story condominium onto the first story walkway roof. Mr. Webster stated that he believed that in addition to the weather conditions on the day of failure, the many years of sliding snow impacting the lower roof also contributed to the fatigue of the structure. The sliding snow load that caused the collapse was due to additional snowfall and then freezing due to cold temperatures at night. When warm temperatures occurred

during the day, the dense snow slid onto the lower roof leading to the large deformation and damage, shown in Figure 5.1. These rapidly changing conditions made the snow very unstable in essence the snow sliding off the upper roof occurred due to similar mechanisms that cause avalanches.

Due to the large amounts of snow at 10,000 feet Mr. Webster and his crew have to constantly maintain structures at Copper Mountain by removing excessive snow from roofs. Snow removal prevents snow from falling on pedestrians below and ice from forming at the eaves that can be very unsafe if it falls. Webster said that the snow had been cleared from the roof just days before and he mentioned that these events that caused the roof structural failure could not have been prevented and the walkway roof needed to be replaced in the near future. To clear the snow every time it snowed would be too costly and uneconomical. Instead, the roofs are cleared approximately every two weeks during the winter months.

After the structural damage, Mr. Webster and his crew inspected the damage along with the fire marshal. Mr. Webster's office is actually in one of the buildings that collapsed and said that the roof was severely damaged just feet from his desk where he was sitting. As mentioned before, commercial properties were primarily in the damaged area where the walkway roof structure was connected to steel I-beams and concrete walls inside the interior of the large mixed-use building. The fire marshal required these areas to be closed for many months due to severe damage preventing a second emergency exit for occupants. This closure created large economic setback for many businesses and left Copper Mountain employees displaced from their offices. In the Village Square building, restaurants and commercial retailers were the primary businesses affected from the roof failure. In the similar Mountain Plaza building, the Copper Mountain Resort employee offices had to be temporarily moved during the months of closure. In

addition to structural damage, there was also damage to much of the mechanical and electrical equipment. Sprinkler systems were severely deformed and had to be replaced and Copper Mountain Resort's computer server was also destroyed. Reconstruction of the roof took over a year to complete, including the structural investigations, obtaining building permits, redesign of the roof structure, and construction time.

The total cost to repair for both structures was $750,000, most of which was covered by the insurance company. However, the insurance company did require that snow fences be installed on the roof of the six-story condominium structure. The snow fences cost $55,000 for both buildings, and the cost was borne by the building owner, Copper Mountain Resorts. Mr. Webster, as well as insurer providers, has asked building owners, which are typically home owner associations, to install snow fences to prevent large chunks of snow and ice falling below, and some have done so and others have chosen not to.

Mr. Webster believes changes need to be made in the snow code provisions to prevent snow and ice from falling. He said even with the new buildings at Copper Mountain they still have problems with snow falling and ice forming at the eaves. He said a big part of this is due to architectural appeal, such as steep roofs that can cause snow sliding, but there is nothing in the standards to prevent architects from having designs that are at risk for forming ice dams and causing snow slides. In this type of high alpine terrain, snow melting methods, proper ventilation, and snow fences should be incorporated to prevent snow hazards while still maintaining the architectural appeal.

*5.5 Lessons from the Case Studies*

After reviewing these case studies on snow related structural failures, several conclusions were found. First, case studies have showed that designs motivated by saving the client money

in material cost and construction cost have contributed to snow related failures. Engineers tend to be motivated to design structures in the most cost-effective manner possible, but sometimes this leads to cost-saving at the expense of a well-designed structure. Second, in many of the cases the 50-year ground snow load specified in the code was not exceeded, but other factors such as snow drift, sliding snow or the age of the structure led to the failure. Older structures, constructed before the 1980's have also been shown to be susceptible to snow failure, as our snow load standards have greatly improved since the 1980's. Design requirements are a minimum standard and engineers need to consider other factors when making design decisions.

The following section describes the case study analysis for the Village Square walkway roof, where hazard curve for probability of exceedance for a given ground snow load can be used to inform decision makers, such as engineers and building owners, of snow related building failure risks.

## 6. ASSESSMENT OF VILLAGE SQUARE ROOF

The assessment methodology is illustrated here with analysis of a real structure that failed under large snow loads in February, 2008. This case study of an existing building is used as a preliminary demonstration and validation of the performance-based snow engineering methodology. In later parts of the project, the research team will systematically investigate a group of buildings with a variety of design features to quantify the influence of particular design features on the risk of snow-induced failure.

### *6.1 Structural Analysis Model*

The existing (pre-failure) structure of the Village Square walkway roof was modeled using MIDAS. MIDAS is a commercially available structural analysis and design software. All information about member sizes and dimensions was provided by Knott Laboratory (2008). Several assumptions were made in the model creation. Firstly, only a small section of the existing walkway roof, approximately 90 feet of the total 122 feet of roof, was modeled in MIDAS, as shown in Figure 6.1. A $4\frac{1}{2}$" x $4\frac{1}{2}$" x $\frac{3}{8}$" angle shape was used to support the roof joists in the background of the model. The angle shape was assumed to be fixed for rotation and displacement in the x, y and z-direction since the walkway roof is attached to an existing much larger (6 story) structure comprised of concrete frame elements, concrete block walls and steel I-beams. The trusses are modeled with a K-series rod joist system, running at 44 inches on center. Since the original manufacturer of the joists is unknown, the Vulcraft 16K2 joist was assumed for the model (Vulcraft 2007). As shown on drawings, a W16x26 beam supports the joist system of the walkway roof in the foreground of Figure 6.1. The two beams are connected at the center using a simple (zero- moment) connection. The beam is continuous over the other two supporting posts. The beam is supported by three HSS 4" x 4" x $\frac{1}{4}$" rectangular posts regularly

spaced at 30'-6" on center. The posts are assumed to be pinned at the base, allowing for rotation between the posts and the base plate/concrete foundation connection. Since only part of the structure was modeled, the boundary conditions on the right and left sides of the model in Figure 6.1 reflect the symmetry of the structure and are pinned to resist movement in the horizontal direction. All materials are modeled with linear-elastic behavior. This assumption is valid for snow loading scenarios that do not significantly stress bar joists or W- beams, but is not appropriate for predicting large deformations and buckling that may occur. The linear model is used here for illustration of the methodology and approach used in performance-based engineering. Future efforts will utilize non-linear modeling.

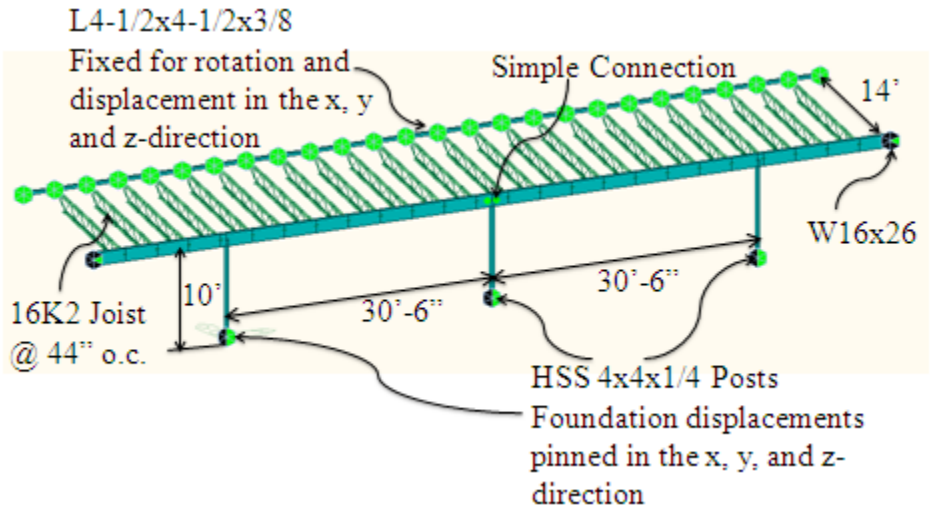


**Figure 6.1-** Existing walkway roof structure as modeled in MIDAS

*6.2 Loading and Results*

Three different loading conditions were applied in this analysis. First, the structure is modeled under ASCE 7-10 factored dead and snow loads. In the second load case, the structure is modeled under an estimated day of failure sliding snow load. In the third and final load case, the structure is modeled under the uniform probabilistic load models developed in Chapter 3.

*6.2.1 Code Loads*

The ASCE 7-10 code load case consists of the dead load (*D)* of roofing materials (shown in Figure 6.2), including the weight of metal roofing, plywood sheathing, wood roof framing, and metal decking, totaling 20 psf. The self-weight of the K-Series joists and other steel members is also inputted as dead load in the model.

The roof snow load is calculated from a ground snow load for Copper Mountain of 90 psf, resulting in design roof snow load of 76 psf (Summit County Building Inspection, 2010). These loads are combined with ASCE 7-10 provisions for sliding snow load from the upper roof structure for a total of 112 psf design roof snow load, denoted *S*. For simplicity, wind loads are not considered. The code snow load and dead loads were applied to the walkway roof structure uniformly.

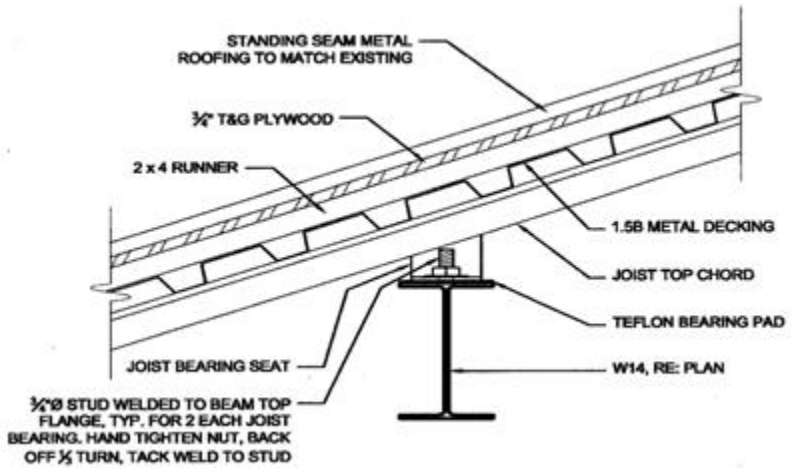


**Figure 6.2-** Roofing materials in the walkway roof that comprise the dead load (Knott Laboratory, 2008).

After applying the ASCE 7-10 loads to the model, the critical load combination was found to be *1.2D + 1.6S*. This load combination will be used in determining the failure modes in the walkway roof structure.

Deflections and stresses in the members were analyzed under factored code dead and snow loads to determine what members would fail first. Deflection in the W-flange beam and

the K-series joist, as shown in Figure 6.3, were examined first to see if the deflection requirements in ASCE 7-10 were exceeded. The maximum deflection in the building occurred in the W-flange beam at approximately 15 inches from the middle support. The maximum deflections of 1.92 in. exceeded the allowable maximum deflection in AISC for the W-section of 1/360 of the span length or 1.02 in. (1/360*30.5 ft.*12 in./ft. = 1.0 in.) by 92%. In addition, the maximum factored load that a 16K2 joist can support according to Vulcraft is 825 plf (Vulcraft, 2007). Assuming a 20 psf dead load and a 112 psf snow load the factored load is equal to 765 plf, 93% of the permitted loading. The bending moment distribution in the beam section under code-defined loads is shown in Figure 6.4.

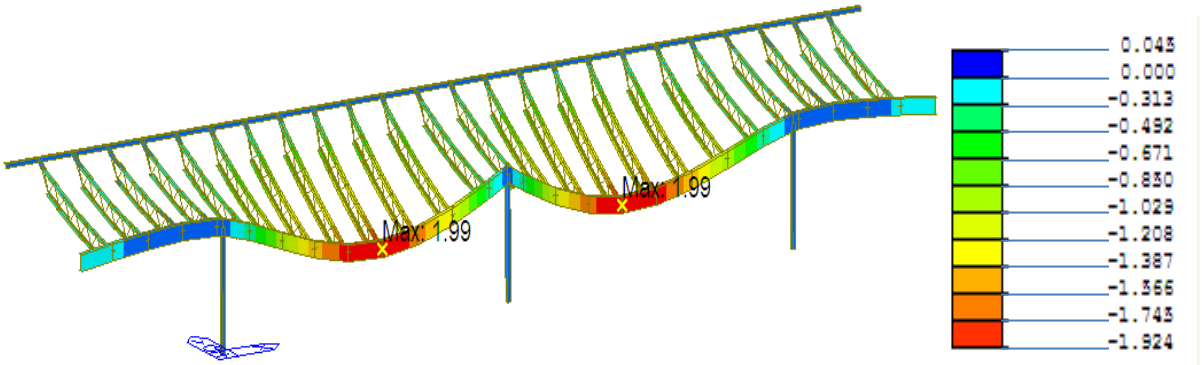


**Figure 6.3**- Displacement contour of the modeled roof system under ASCE 7-10 factored dead and snow load in units of inches.

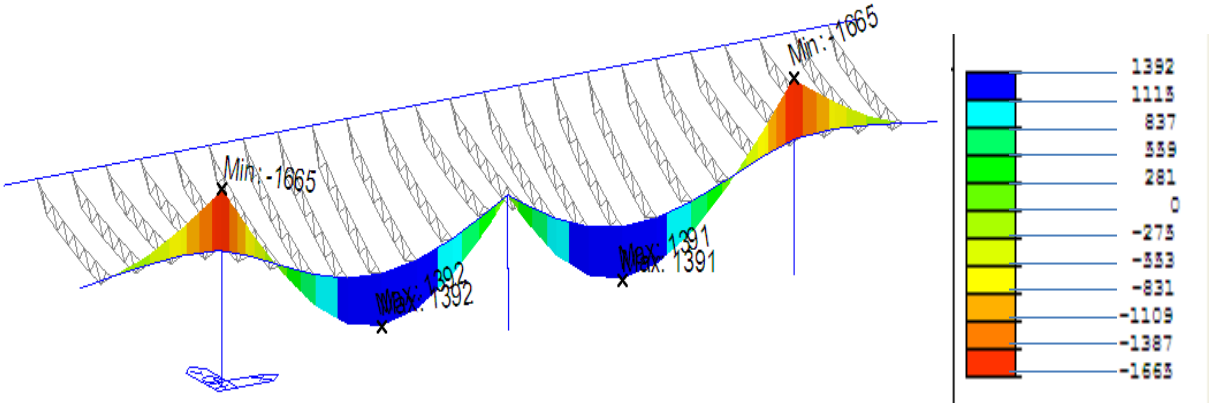


**Figure 6.4**- Maximum moment in the modeled roof system under ASCE 7-10 factored dead and snow load in units of kip-in.

We next considered increasing the snow loads to determine which failure modes might occur. For each type of failure, either deflection limits were compared to deflections recorded in the model or load requirements were compared to the loads applied in the model. The sequence of failure modes is reported in Table 6.1, the ratio of observed value in the model to code requirements are shown.

**Table 6.1-** Failure modes in Village Square walkway roof

| Order of Failure Modes | Description of Failure | Failure mode deflection or load governed | Exceedance of Code Requirements* |
|---|---|---|---|
| (1) | Deformation of steel joists | Deflection | 4.1 |
| (2) | Damage to nonstructural components | Deflection | 4.1 |
| (3) | Damage to 1.5Bx20Gauge roof panels | Deflection | 4.1 |
| (4) | Failure of the W beam | Load | 1.9 |
| (5) | Buckling of Columns | Load | 0.7 |
| (6) | Simple connection of the two W-beams to the middle post | Load | 0.2 |

*For deflection governed failure modes, this is the ratio of the actual deflection to the deflection limit. For the load governed failure modes, this is the ratio of the force in the element to the load limit (LRFD).

After running the analysis of the Village Square walkway roof under code loads, several observations were made. First, according to the manufacturer, neither the joists nor the roof panels used in the original design would meet current snow load requirements for deflection criteria. Non-structural components such as light fixtures, electrical and plumbing equipment were also a part of the ceiling in the walkway roof, as shown previously in Figure 5.1. Since these components were attached to the joists it is assumed that when the joists exceed the deflection limits that the non-structural components will no longer be functional, and may experience severe damage. Even though the roof panels can take a larger load than the steel joists, it is likely that deformations and possibly failure would occur in the roof panels if the joists exceed deflection limits. The W-beam meets code requirements for loads with a ratio of applied to capacity moment strength of 0.9, but fails to meet serviceability requirements. The

columns and connections are within AISC (2005) code requirements; when inspected by Knott Laboratories after the February 2008 failure, these components did not appear to have any damage.

*6.2.2 Day of Failure Loads*

This load case was developed to represent the snow load that occurred on the day of failure and the damages associated with that load. To start, the ground snow load for the day of failure had to be determined. Using water equivalent data for Copper Mountain, CO for the day of failure, February 19, 2008, from the National Water and Climate Center (2010) the ground snow load was determined using Equation *(1)*. This estimate is 71.2 psf of snow on the ground on that day. Then, the uniform probabilistic model developed in Chapter 3 was used to estimate the mean roof snow load on the upper roof. For a semi-sheltered, heated building with 71.2 psf of ground snow load, the snow load on the upper roof structure is estimated to be 29 psf. The snow sliding from the upper to the lower roof was assumed to be a 4'x4' block of snow that included 40% of the total upper roof snow load (i.e., a total sliding load of 4 ft. x 4 ft. x 0.4 x 186 lb.). This assumed was made since the spacing of the joists in the model is approximately four feet. Only 40% of the load was assumed to slide based on the 40% assumption for sliding snow load in ASCE 7-10. Knowing that the snow fell approximately 50 feet (five stories of 10 feet each) on to the lower roof the time of falling was calculated as 1.8 seconds. This load was then applied using a time function load in MIDAS. The time function load was applied to several nodes of the joist, where the snow from the upper roof most likely landed.

This sliding snow load represents the loading conditions on the day of failure. It was assumed that there was no snow on the lower roof when the slide occurred on the day of failure, because the snow load would be small in comparison to the sliding snow load from the upper

roof and much of it had probably already slid off. Figure 6.5 shows the deflections in the W-flange beam and in the K-series joists due to the sliding snow load.

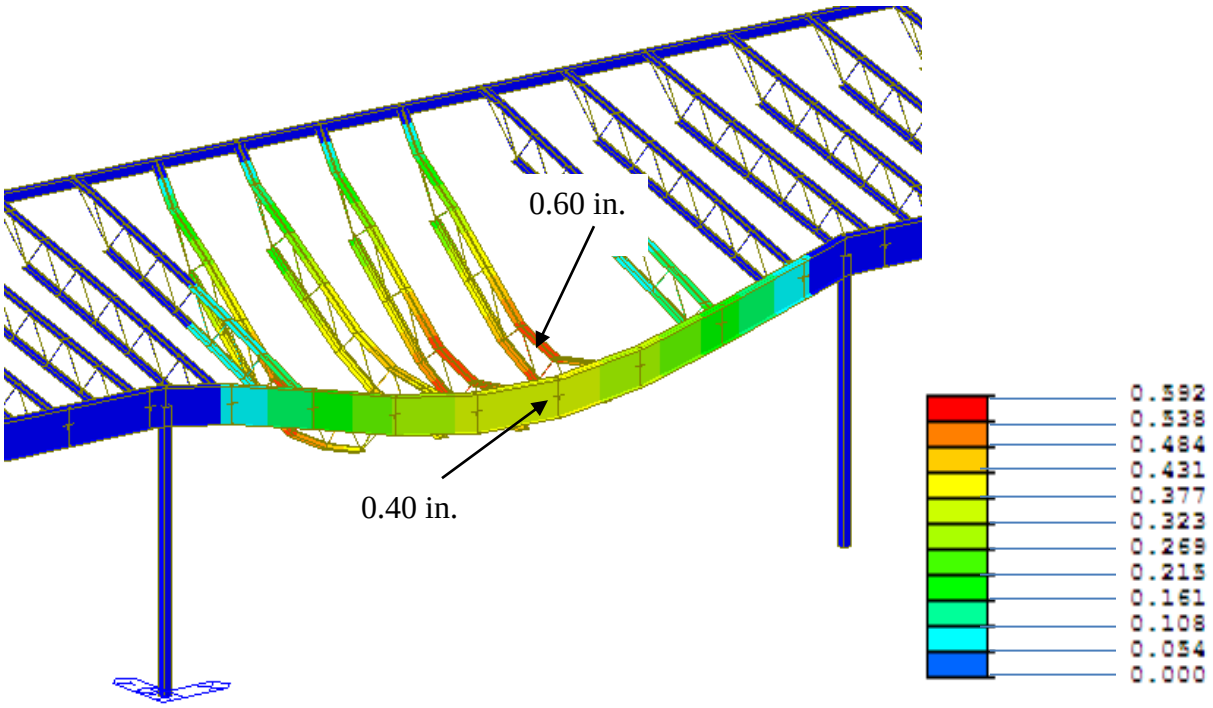


**Figure 6.5-** Maximum deflections in inches, observed in the K-series joists and the W-flange beam under simulated day of failure snow loads.

Under this simulated day of failure load the K-series joists, as shown, would exceed the deflection limits in AISC of 0.5 in. (1/360*14 ft. = 0.47 in.). Large deformations are also observed in the W-flange beam. These do not exceed the deflection limits in AISC, but if a larger piece of snow were to fall, therefore damaging more joists the deflection in the W-flange beam would be larger. The displaced shape shown in Figure 6.5 under the simulated load shows a similar shape to that photographed by Knott Laboratories in Figure 5.1.

Although the building manager commented that he thought the damage was due to an accumulation of damage in the joists over the years since construction, deformations to the joists and W-flange beam were likely due to a large chunk of snow and ice sliding from the upper roof, and damaging the members upon impact, as modeled here. It is unlikely that many years of

sliding snow would contribute to the deformations observed in the walkway roof structure. Steel has not been shown to deteriorate in this manner, showing that the loads that occurred on the day of failure were different from previous sliding snow loads (Knott Laboratories 2008). Replacing the W-flange beam and spacing the joists closer together, as the building owner did, will reduce damage due to snow in the future.

*6.2.3 Probabilistic Load Models*

In the third load case, the probabilistic uniform load models described in Chapter 3 are applied to the structure. In order to determine how the structural response varies with ground snow loads, ten different levels of ground snow loads varying from 10 psf to 100 psf are considered and reported in Table 6.2. Each ground snow load is inputted into roof load probability models to generate 10,000 realizations of the roof snow load that represent the uncertainty in roof snow loading for the given value of ground snow load. The average roof snow load for each ground load value is included in Table 6.2. Each loading realization is applied as a uniform load across the entire modeled roof.

**Table 6.2-** Deflections predicted in the Village Square walkway roof for different ground snow loads.

| Ground Snow Load (psf) | Avg. Roof Load (psf) | Avg. Maximum Deflection in Beam (in.) |
|---|---|---|
| 10 | 8 | 0.32 |
| 20 | 13 | 0.37 |
| 30 | 15 | 0.38 |
| 40 | 19 | 0.42 |
| 50 | 24 | 0.46 |
| 60 | 28 | 0.50 |
| 70 | 33 | 0.54 |
| 80 | 37 | 0.58 |
| 90 | 42 | 0.63 |
| 100 | 48 | 0.68 |

Ten representative roof snow load realizations for each ground snow load level were then applied to the structure and the structural responses, including maximum deflection of the critical W-beam, were recorded. Each of these different loading scenarios leads to a different prediction of structural response, as illustrated in Figure 6.6. The variability in roof deflection associated with each level of ground snow load is due to uncertainties in the prediction of roof snow load. To compute the average maximum deflection, the response under each loading realization is weighted according to its relative likelihood of occurring, according to the histogram obtained from the Monte Carlo simulation model. Besides roof deflection, other structural response parameters of interest include the ratio of demand stress to yield stress in critical members.

Figure 6.6 (a) shows an average maximum roof deflection of 0.63" at a ground snow load of 90 psf. The maximum roof deflection occurs in the wide-flange beam. The probability that the deflection will exceed the AISC limit of 1/360 of 1.0" increases with larger ground snow loads. The probability of exceeding a deflection of 1.0" in the wide-flange beam can be related to ground snow load in an inverse cumulative distribution function, *i.e., P[Deflection > 1.0" | GSL]*. For 100 psf ground snow load, we predict a 17% probability that deflections in the beam exceed 1.0", assuming a lognormal distribution. A ground snow load of 160 psf would be required for the average deflection to exceed the limit specified in AISC. Figure 6.6 (b) shows an average maximum bending stress in the wide-flange beam of the 12.8 ksi for a ground snow load of 100 psf. The bending stress can be compared to requirements for stress demand in AISC for the existing wide-flange beam in the structure.

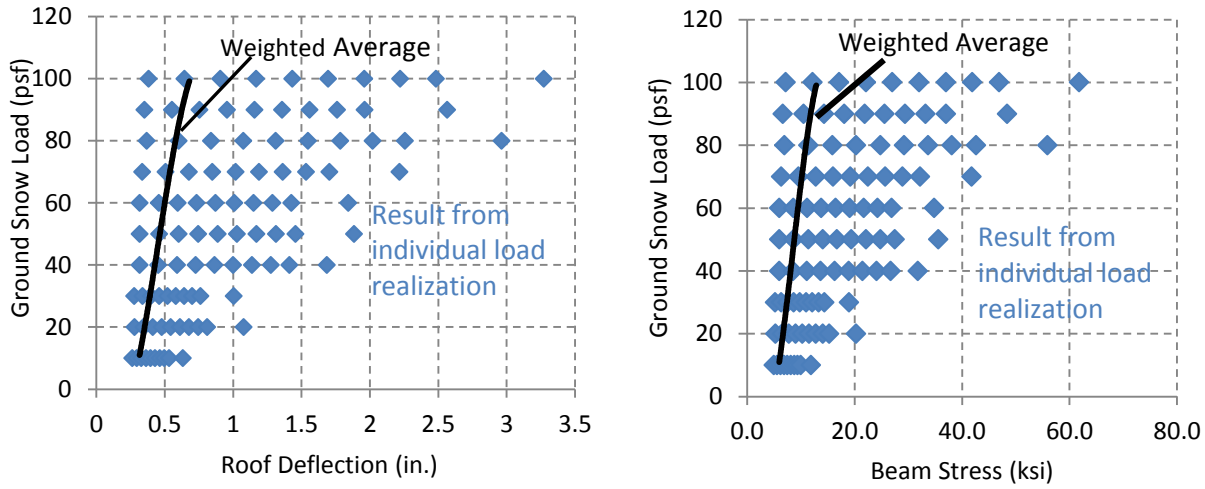


**Figure 6.6-** Predicted (a) maximum roof deflection and (b) maximum beam stress as a function of ground snow load for case study structure under uniform snow loads.

To determine the mean annual frequency of roof deflection exceeding 1.0", the cumulative distribution function can be integrated with a ground snow hazard curve (*P[GSL]*) for the case study site. The ground snow hazard curve, included in Figure 6.7 (a), represents the annual probability that a particular ground snow load is exceeded at a particular site. This curve has been generated using historic snow load data for Copper Mountain, Colorado (National Water and Climate Center, 2010).

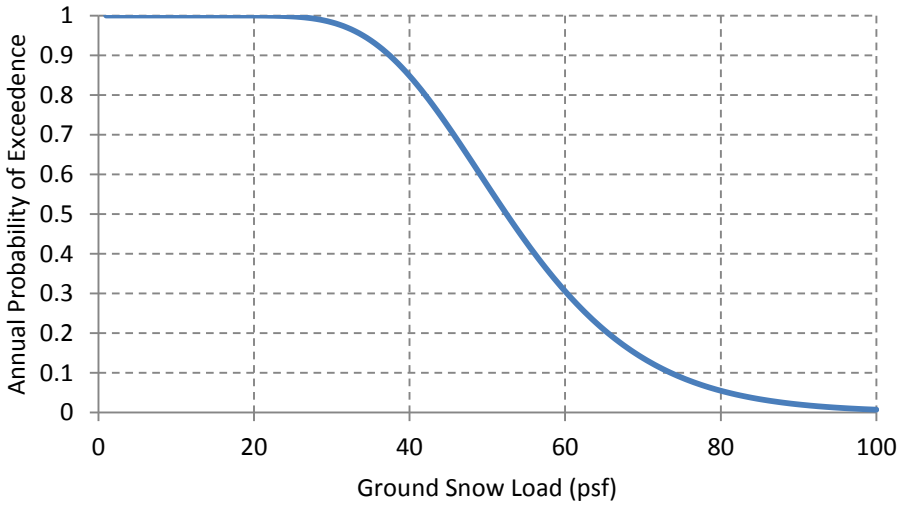

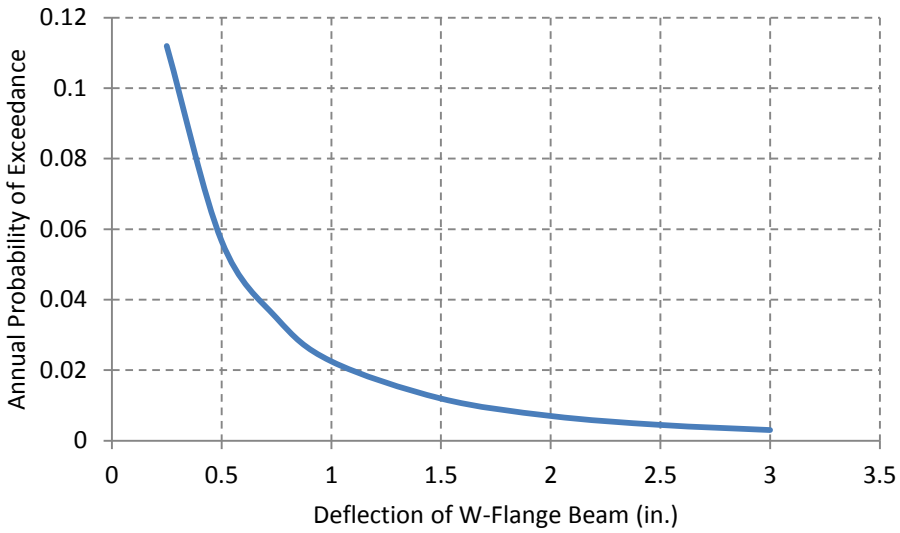


**Figure 6.7-** Ground snow load hazard curve for the walkway roof structure at Copper Mountain, CO showing (a) annual probability of ground snow load being exceeded, (b) the annual probability of deflection limits being exceeded for a given ground snow load.

The probabilistic loading model used in this analysis can be used for other case studies to develop similar hazard curves for annual exceedance of deflection or annual exceedance of beam stress. The annual probability of exceedance for various deflections for the walkway roof structure is shown in Figure 6.7 (b). This type of information can be used to inform building owners of risks to the structure if a certain ground snow load occurs.

## 7. CONCLUSIONS

Determining accurate roof snow loads from ground snow load values has been a difficult task for engineers due to variation in climate, ground snow loads and roof systems. Building codes and standards use a 50-year mean recurrence interval for the ground snow load and convert the value to a design roof snow load that has a 2% chance of being exceeded in any given winter. In most cases, building codes are conservative and overestimate uniform roof snow loads, and the mean recurrence interval on the average is closer to 75 years. Even though drift load design values are conservative also, the uncertainty in drift loads is much larger than uniform loads and therefore account for 75% of snow related structural failures (O'Rourke et al. 1982).

For performance-based engineering, models of roof snow load that predict the mean roof snow load, as well as the uncertainty in that prediction are needed to develop event based snow loads. The models are based on a known ground snow load and account for building and weather specific information. The metrics used in performance-based engineering use the uncertainty and load values for a snow event in order to quantify the risk of hazards occurring. Therefore, two probabilistic models were developed in this study to predict roof snow load from a ground snow load for a particular event. The models were developed by accounting for parameters in the order that were most influential in the overall conversion of ground to roof snow load and adjusting the ground snow load at each step based on importance. For example, exposure of the structure was found to be the most influential and therefore was used first in the model. After adjusting the ground snow load for the exposure parameter, the thermal parameter was input next and so on for the other terms used. The first model developed for uniform loads, can be used for most structures where the formation of drifts is unlikely. The second model

developed for non-uniform or drifting loads is used for structures with obstructions such as multilevel roofs or parapet roofs located in regions where snow densities are low and high winds transport the snow to form a surcharge load. In the United States, regions such as the Northeast and the Northern plains are likely to have roofs that form drifts. The models differ from current design equations where the models estimate a value for the roof snow load for one event or specified ground snow level, rather than the 2% or 50-year mean recurrence design value. Therefore, the uniform model and the non-uniform model predict a smaller mean roof snow load than those required by ASCE 7-10 for a ground snow load of 25 psf for the uniform model and 30 psf for the non-uniform model.

The Monte Carlo simulation used in the analysis gives a mean uniform load of 15 psf for an unheated structure, semi-sheltered exposure rating, metal roof with a slope of 14˚ and a ground snow load of 25 psf. ASCE 7-10 gives a design snow load of 21 psf for the same roof structure. The model predicts a higher conversion factor for lower ground snow loads taking into account the climatic factor, which is not considered in American design standards, but has been shown based on data to have an effect on the overall conversion factor. The lognormal standard deviation in the overall conversion factor for the model was lower than the overall conversion factor in the data, 0.28 compared to 0.62. When predicted roof snow loads using the model were compared to actual recorded roof snow loads the mean bias ratio for all the buildings was found to be 1.01 showing the model predicts comparable roof snow loads to the recoded roof snow loads with a smaller variance. The non-uniform model showed similar results, where the mean maximum drift load found using the model for a 30 psf ground snow load was found to be 42 psf, compared to a maximum design drift load using ASCE 7-10 for the same structural parameters of 64 psf. Again, the non-uniform model had a smaller variance in overall

conversion factor with a lognormal standard deviation of 0.62 compared to 0.85 for the data. However, the variance in the non-uniform model was larger than the uniform model (0.62 for the non-uniform versus 0.28 for the uniform model) showing the greater difficulty in predicting drift loads.

Applications of the probabilistic load models are illustrated by calculating deflections and stresses for a case study building. The case study building in this study was a walkway roof structure located at Copper Mountain, CO that failed in early 2008 due to large sliding snow loads from an upper roof structure. In the study, probability of exceeding deflections in the roof system was found for various ground snow loads. It was found that there is a 17% probability that a deflection of 1.0 in. can occur in the main supporting W-flange beam of the walkway roof structure. Lastly, a ground snow load hazard curve for the site that shows the annual probability of various ground snow loads being exceeded was developed. Combining the ground snow load hazard curve with the annual probability of various deflections being exceeded, building owners or other stakeholders can use the curves to determine risk of failure or damage.

Further analysis is needed in this newly developed framework of performance-based engineering in snow design. This study showed some areas where data are lacking and further research is needed to improve the models developed. For the uniform model, having a better understanding of thermal conditions and roofing material would improve the model. In this study, the data used had limited variation in thermal parameters and limited roofing materials and slope. In addition, having more metal buildings in the study would improve the roof snow load predictions for these structures. Recording roof and ground snow load data for other light weight metal buildings such as grocery stores and retailers could show how roof snow loads affect metal buildings. Wind speed and other historical weather data in the non-uniform model

would improve drift snow load predictions as well. This would increase the number of exposure categories used in the model and provide incite on the affect snow transport theory has on drift predictions.

Lastly, the case study used in this report can further be modeled by developing hazard curves showing the risk of collapse for a group of buildings with different design features. Buildings such as large, lightweight steel structures used for warehouses and manufacturing facilities have been shown to be vulnerable to snow induced collapse and could be modeled similar to the one used in this study. Developing hazard curves for these structures that might be at risk of snow induced failures and providing decision makers with the consequences in terms of economic losses will help building owners decide whether to invest in retrofitting roofs to mitigate these risks.

## NOTATION LIST

| | |
|---|---|
| $C_e$ | exposure conversion factor (ASCE 7-10) |
| $C_m$ | ratio of maximum roof load to maximum ground load in a single winter season |
| $C_s$ | slope conversion factor (ASCE 7-10) |
| $C_t$ | thermal conversion factor (ASCE 7-10) |
| $C_v$ | ratio of roof to ground snow loads for a particular visit |
| $D$ | dead load (ASCE 7-10) |
| $D$ | magnitude of the drift load in psf (ASCE 7-10) |
| $D_e$ | exposure conversion factor in non-uniform drift model |
| $D_{gd}$ | ground density factor in non-uniform drift model |
| $D_l$ | upper roof length conversion factor in non-uniform drift model |
| $DR$ | drift ratio of total drift surcharge to ground snow load |
| $DSL$ | drift snow load predicted by the non-uniform drift model |
| $D_t$ | thermal conversion factor in non-uniform drift model |
| $d_w$ | water equivalent depth of snow in inches (in.) |
| $E$ | earthquake load (ASCE 7-10) |
| $E$ | exposure conversion factor (CRREL Report, 1982) |
| $F$ | fetch distance or the distance of the windward snow source in feet |
| $Fp_g$ | cumulative distribution function of the yearly maximum ground snow load |
| $GSD$ | ground snow density measured |
| $GSL$ | ground snow load measured |
| $h_d$ | drift height in feet (ASCE 7-10) |
| $h_g$ | ground snow depth of snow in inches (in.) |

| | |
|---|---|
| $h_r$ | roof snow depth of snow in inches (in.) |
| $K_e$ | exposure conversion factor in uniform model |
| $K_{gs}$ | ground snow load conversion factor in uniform model |
| $K_{log}$ | mean exponent of the lognormal mean for each factor |
| $K_{sm}$ | slope and material conversion factor in uniform model |
| $K_t$ | thermal conversion factor in uniform model |
| $K_v$ | ratio of roof to ground snow loads for a particular visit for uniform model |
| $I$ | importance factor (ASCE 7-10) |
| $L$ | live load (ASCE 7-10) |
| $L_d$ | total drift surcharge with units of pounds per square foot |
| $L_r$ | live roof load (ASCE 7-10) |
| $l_u$ | upper roof length in feet (ASCE 7-10) |
| $N$ | the return period for the ground snow load level of interest (e.g. 50 years) |
| $p_g$ | the N-year ground snow load in pounds per square foot (psf) |
| $P_r$ | roof snow load in pounds per square foot (psf) |
| *RSD* | roof snow density predicted by the non-uniform drift model |
| *RSL* | roof snow load predicted by the uniform model |
| $S$ | snow load for design equal to $P_r$ *(ASCE 7-10)* |
| $T$ | thermal conversion factor (CRREL Report, 1982) |
| $w$ | width or horizontal extent of drift load in feet (ASCE 7-10) |
| $W$ | wind load (ASCE 7-10) |
| $\gamma_g$ | density of ground snow in pounds per cubic feet (pcf) |
| $\gamma_r$ | density of roof snow in pounds per cubic feet (pcf) |

| | |
|---|---|
| $\lambda_g$ | lognormal mean of the ground snow load |
| $\zeta_g$ | lognormal variance of the ground snow load |
| $\Phi$ | the standard normal integral |
| $\mu$ | mean value for each factor |
| $\sigma$ | standard deviation for each factor |
| $\sigma_{ln}$ | lognormal standard deviation for each factor |
| $\beta$ | snowdrift coefficient based on length to width ratio proposed for ASCE |

## REFERENCES


American Institute of Steel Construction Inc. AISC, (2005) "Manual for Steel Construction, 13th edition".

American Society of Civil Engineers (2010) "Minimum design loads for buildings and other structures". ASCE 7-10, Reston, VA.

Auren, M. and O'Rourke, M. (1997) "Snow Loads on Gable Roofs". Journal of Structural Engineering, 123, (12), 1645-1651.

Bennett, R. (1988) "Snow Load Factors for LRFD". Journal of Structural Engineering, 114, (10), 2371-2382.

Buska, J. and Tobiasson, W. (2001) "Minimizing the adverse effects of snow and ice on roofs". International Conference on Building Envelope Systems and Technologies (ICBEST), Ottawa, Canada.

DeGaetano, A. and O'Rourke, M. (2003) "A Climatological Measure of Extreme Snowdrift Loading on Building Roofs". Journal of Applied Meteorology, 43, 134-144.

DeGaetano, A., Schmidlin, T. and Wilks, D. (1997) "Evaluation of East Coast Snow Loads Following January 1996 Storms". Journal of Performance of Construction Performance, 90-94.

Delatte, N. and Martin, R. (2001) "Another Look at Hartford Civic Center Coliseum Collapse". Journal of Performance of Construction Performance, 31-36.

Ellingwood, B. and O'Rourke M. (1985) "Probabilistic models of snow loads on structures". Structural Safety, 2, 291-299.

Geis, J., Strobel, K. and Liel, A. (2010) "Snow-Induced Building Failures". Department of Civil, Environmental and Architectural Engineering, University of Colorado, Boulder, CO.

International Existing Building Code IEBC, (2003) "International Code Council", Chapter 2.

Irwin, P., Gamble, S. and Taylor, D. (1995) "Effects of roof size, heat transfer, and climate on snow loads: studies for the 1995 IBC". Canadian Journal of Civil Engineering, 22, 770-784.

Knott Laboratory, LLC (2008) "Village Square Investigation of Roof Snow Load Damage".

Lee, K. and Rosowsky, D. (2005) "Site-specific snow load models and hazard curves for probabilistic design". Natural Hazards Review, 109-120.

Meloysund, V., Liso, K., Hygen, H., Hoiseth, K. and Liera, B. (2007) "Effects of wind exposure on roof snow loads". Building and Environment, 42, 3276-3736.

Meloysund, V., Liso, K., Siem, J. and Apeland, K. (2006) "Increased snow loads and wind actions on existing buildings: Reliability of the Norwegian building stock". Journal of Structural Engineering, 132, (11), 1813-1820.

Moehle, J. and Deierlein, G. (2004) "A framework methodology for performance-based earthquake engineering". 13th World Conference on Earthquake Engineering, Vancover, B.C., Canada.

National Water and Climate Center (2010), United States Department of Agriculture, http://www.wcc.nrcs.usda.gov/ftpref/data/snow/snotel/table/history/colorado/06k24s_s.txt, accessed on February 2, 2011.

O'Rourke, M. (2007) "Snow Loads- Guide to the Snow Load Provisions of ASCE 7-05". American Society of Civil Engineers.

O'Rourke, M. and De Angelis, C. (2002) "Snow drifts at windward roof steps". Journal of Structural Engineering, 128, 1330-1336.

O'Rourke, M., DeGaetano, A. and Tokarczyk, J. (2005) "Analytical simulation of snow drift loading". Journal of Structural Engineering, 131, 660-667.

O'Rourke, M., Koch, P. and Redfield, R. (1983) "Analysis of roof snow load case studies- Uniform loads". US Army Corps of Engineers, CRREL Report 83-1.

O'Rourke, M., Speck, R. and Stiefel, U. (1985) "Drift Snow Loads on Multilevel Roofs". Journal of Structural Engineering, 111, (2), 290-305.

O'Rourke, M. and Stiefel, U. (1983) "Roof Snow Loads for Structural Design". Journal of Structural Engineering, 109, (7), 1527-1537.

Pidgeon, N., Blocley, D and Turner, B.A. (1986) "Design Practice and Snow Loading – Lessons from a Roof Collapse". Structural Engineer, Part A, 64A, 57-71.

Summit County Building Inspection. *Codes and Amendments*, <http:// www.co.summit.co.us/Building Insp/documents/MASTERMATRIX_013.pdf>, 2010.

Takahashi, T and Ellingwood, R. (2004) "Reliability-based assessment of roofs in Japan subjected to extreme snows: incorporation of site-specific data". Engineering Structures, (27), 89–95

Tobiasson, W. and Greatorex, A. (1996) "Database and methodology for conducting site specific snow load case studies for the United States". U.S. Army Cold Regions Research and Engineering Laboratory Report, Hanover, N.H.

Tobiasson, W. and Redfield, R. (1983) “Snow Loads for the United States”. U.S. Army Cold Regions Research and Engineering Laboratory Report, Hanover, N.H.

Von Bradsky, P. (1980) “Three Roof Snow Load Studies”, Rensselaer Polytechnic Institute, Master of Engineering Thesis.

Vulcraft (2007) “Steel Joists & Joist Girders” Catalog 5.

## APPENDIX A

Uniform Roof Snow Load Data

| Roof Structure No. | Exposure Rating | Slope | Roof Material | Heating Parameter | Ground Snow Load (psf) | Pred. Roof Snow Load (psf) | Actual Roof Snow Load (psf) | Bias Equation *(16)* |
|---|---|---|---|---|---|---|---|---|
| 25 | 2 | 33 | 2 | 2 | 28.3 | 13.1 | 13.4 | 1.02 |
| | 2 | 33 | 2 | 2 | 29.2 | 13.2 | 3.5 | 0.27 |
| | 2 | 33 | 2 | 2 | 37.2 | 14.9 | 9.6 | 0.64 |
| | 2 | 33 | 2 | 2 | 45.7 | 18.3 | 3.3 | 0.18 |
| | 2 | 33 | 2 | 2 | 19.0 | 11.1 | 16.1 | 1.45 |
| 26-1 | 2 | 14 | 4 | 1 | 29.2 | 14.8 | 5.9 | 0.40 |
| | 2 | 14 | 4 | 1 | 37.2 | 16.7 | 8.8 | 0.53 |
| | 2 | 14 | 4 | 1 | 45.7 | 20.5 | 4.8 | 0.23 |
| | 2 | 14 | 4 | 1 | 14.3 | 10.3 | 18.0 | 1.74 |
| 26-2 | 2 | 28 | 4 | 1 | 29.2 | 14.8 | 8.2 | 0.56 |
| | 2 | 28 | 4 | 1 | 37.2 | 16.7 | 7.3 | 0.44 |
| | 2 | 28 | 4 | 1 | 45.7 | 20.5 | 2.4 | 0.12 |
| | 2 | 28 | 4 | 1 | 14.3 | 10.3 | 18.0 | 1.74 |
| 27 | 2 | 34 | 2 | 1 | 28.3 | 14.7 | 10.3 | 0.70 |
| | 2 | 34 | 2 | 1 | 29.2 | 14.8 | 6.3 | 0.43 |
| | 2 | 34 | 2 | 1 | 37.2 | 16.7 | 9.5 | 0.57 |
| | 2 | 34 | 2 | 1 | 45.7 | 20.5 | 21.8 | 1.07 |
| | 2 | 34 | 2 | 1 | 15.5 | 10.9 | 21.7 | 2.00 |
| 28-1 | 2 | 34 | 2 | 1 | 45.7 | 20.5 | 2.2 | 0.11 |
| | 2 | 34 | 2 | 1 | 15.5 | 10.9 | 18.2 | 1.67 |
| 28-2 | 2 | 9 | 2 | 1 | 45.7 | 20.5 | 2.2 | 0.11 |
| | 2 | 9 | 2 | 1 | 15.5 | 10.9 | 20.6 | 1.90 |
| 35-1 | 3 | 25 | 2 | 2 | 17.2 | 8.2 | 1.5 | 0.18 |
| | 3 | 25 | 2 | 2 | 13.5 | 7.0 | 7.5 | 1.08 |
| 35-2 | 3 | 16 | 2 | 1 | 17.2 | 9.2 | 2.0 | 0.21 |
| | 3 | 16 | 2 | 1 | 13.5 | 7.8 | 17.4 | 2.23 |
| 40-1 | 3 | 0 | 3 | 2 | 3.0 | 1.9 | 2.0 | 1.06 |
| | 3 | 0 | 3 | 2 | 4.7 | 2.8 | 0.5 | 0.18 |
| | 3 | 0 | 3 | 2 | 13.4 | 6.9 | 14.0 | 2.03 |
| 40-2 | 3 | 0 | 3 | 2 | 3.0 | 1.9 | 1.7 | 0.91 |
| | 3 | 0 | 3 | 2 | 13.4 | 6.9 | 14.6 | 2.11 |
| 42 | 3 | 0 | 4 | 2 | 2.6 | 1.6 | 0.8 | 0.50 |
| | 3 | 0 | 4 | 2 | 3.2 | 2.0 | 2.0 | 1.00 |
| | 3 | 0 | 4 | 2 | 10.3 | 5.6 | 17.3 | 3.06 |
| 43 | 3 | 0 | 3 | 2 | 2.5 | 1.6 | 1.8 | 1.15 |
| | 3 | 0 | 3 | 2 | 14.6 | 7.4 | 15.1 | 2.04 |
| 56 | 3 | 15 | 2 | 2 | 15.4 | 7.7 | 3.9 | 0.51 |
| | 3 | 15 | 2 | 2 | 20.9 | 9.3 | 5.7 | 0.62 |
| | 3 | 15 | 2 | 2 | 36.5 | 11.6 | 3.1 | 0.27 |
| | 3 | 15 | 2 | 2 | 34.8 | 10.5 | 11.3 | 1.07 |
| | 3 | 15 | 2 | 2 | 36.7 | 11.6 | 2.1 | 0.18 |

| Roof Structure No. | Exposure Rating | Slope | Roof Material | Heating Parameter | Ground Snow Load (psf) | Pred. Roof Snow Load (psf) | Actual Roof Snow Load (psf) | Bias Equation *(16)* |
|---|---|---|---|---|---|---|---|---|
| 57 | 3 | 12 | 2 | 2 | 13.6 | 7.0 | 0.0 | 0.00 |
| | 3 | 12 | 2 | 2 | 20.4 | 9.1 | 0.7 | 0.08 |
| | 3 | 12 | 2 | 2 | 25.0 | 10.0 | 2.6 | 0.26 |
| | 3 | 12 | 2 | 2 | 42.7 | 13.5 | 0.0 | 0.00 |
| | 3 | 12 | 2 | 2 | 31.2 | 10.6 | 0.0 | 0.00 |
| 58 | 3 | 12 | 2 | 2 | 8.3 | 4.7 | 3.1 | 0.66 |
| | 3 | 12 | 2 | 2 | 17.9 | 8.5 | 0.0 | 0.00 |
| | 3 | 12 | 2 | 2 | 30.7 | 10.5 | 0.0 | 0.00 |
| | 3 | 12 | 2 | 2 | 12.0 | 6.4 | 0.0 | 0.00 |
| | 3 | 12 | 2 | 2 | 28.4 | 10.4 | 0.0 | 0.00 |
| 59 | 3 | 12 | 2 | 2 | 18.1 | 8.5 | 0.0 | 0.00 |
| | 3 | 12 | 2 | 2 | 17.9 | 8.5 | 4.2 | 0.50 |
| | 3 | 12 | 2 | 2 | 35.5 | 11.3 | 4.2 | 0.37 |
| | 3 | 12 | 2 | 2 | 46.7 | 14.8 | 2.3 | 0.15 |
| | 3 | 12 | 2 | 2 | 22.8 | 9.7 | 0.0 | 0.00 |
| 60 | 3 | 27 | 2 | 2 | 19.4 | 8.9 | 1.9 | 0.21 |
| | 3 | 27 | 2 | 2 | 16.5 | 8.0 | 1.9 | 0.23 |
| | 3 | 27 | 2 | 2 | 39.4 | 12.5 | 4.6 | 0.37 |
| | 3 | 27 | 2 | 2 | 28.1 | 10.4 | 3.3 | 0.32 |
| | 3 | 27 | 2 | 2 | 36.7 | 11.6 | 0.0 | 0.00 |
| 61 | 3 | 12 | 2 | 2 | 20.6 | 9.2 | 7.3 | 0.79 |
| | 3 | 12 | 2 | 2 | 23.0 | 9.7 | 6.8 | 0.70 |
| | 3 | 12 | 2 | 2 | 25.7 | 10.1 | 8.8 | 0.87 |
| | 3 | 12 | 2 | 2 | 38.7 | 12.3 | 0.0 | 0.00 |
| 62 | 3 | 18 | 2 | 2 | 20.9 | 9.3 | 14.4 | 1.56 |
| | 3 | 18 | 2 | 2 | 20.8 | 9.2 | 28.3 | 3.07 |
| | 3 | 18 | 2 | 2 | 24.8 | 10.0 | 19.8 | 1.98 |
| | 3 | 18 | 2 | 2 | 34.5 | 10.5 | 18.2 | 1.73 |
| | 3 | 18 | 2 | 2 | 55.8 | 17.7 | 17.5 | 0.99 |
| | 3 | 18 | 2 | 2 | 18.1 | 8.5 | 7.8 | 0.91 |
| | 3 | 18 | 2 | 2 | 23.4 | 9.8 | 5.2 | 0.53 |
| | 3 | 18 | 2 | 2 | 26.1 | 10.2 | 13.0 | 1.28 |
| | 3 | 18 | 2 | 2 | 31.2 | 10.6 | 18.2 | 1.73 |
| | 3 | 18 | 2 | 2 | 36.4 | 11.5 | 18.2 | 1.58 |
| | 3 | 18 | 2 | 2 | 23.4 | 9.8 | 13.0 | 1.33 |
| 63 | 3 | 12 | 2 | 2 | 18.2 | 8.6 | 1.9 | 0.22 |
| | 3 | 12 | 2 | 2 | 20.6 | 9.2 | 1.9 | 0.20 |
| | 3 | 12 | 2 | 2 | 29.3 | 10.5 | 4.6 | 0.44 |
| | 3 | 12 | 2 | 2 | 21.9 | 9.5 | 0.0 | 0.00 |
| 64 | 1 | 12 | 2 | 2 | 20.9 | 14.7 | 14.0 | 0.95 |
| | 1 | 12 | 2 | 2 | 24.0 | 15.7 | 20.2 | 1.28 |
| | 1 | 12 | 2 | 2 | 31.2 | 16.8 | 25.8 | 1.53 |
| 65 | 1 | 28 | 2 | 2 | 13.1 | 10.9 | 13.4 | 1.23 |
| | 1 | 28 | 2 | 2 | 20.6 | 14.6 | 14.8 | 1.01 |
| | 1 | 28 | 2 | 2 | 26.0 | 16.2 | 21.0 | 1.30 |
| | 1 | 28 | 2 | 2 | 49.8 | 25.1 | 18.8 | 0.75 |

| Roof Structure No. | Exposure Rating | Slope | Roof Material | Heating Parameter | Ground Snow Load (psf) | Pred. Roof Snow Load (psf) | Actual Roof Snow Load (psf) | Bias Equation *(16)* |
|---|---|---|---|---|---|---|---|---|
| 66 | 1 | 17 | 2 | 2 | 8.7 | 7.8 | 9.3 | 1.18 |
| | 1 | 17 | 2 | 2 | 21.1 | 14.8 | 15.6 | 1.05 |
| | 1 | 17 | 2 | 2 | 36.6 | 18.5 | 21.1 | 1.14 |
| | 1 | 17 | 2 | 2 | 39.0 | 19.7 | 23.3 | 1.19 |
| | 1 | 17 | 2 | 2 | 36.2 | 18.3 | 17.8 | 0.97 |
| 67 | 1 | 32 | 2 | 2 | 6.3 | 5.9 | 4.1 | 0.69 |
| | 1 | 32 | 2 | 2 | 15.8 | 12.5 | 14.0 | 1.12 |
| | 1 | 32 | 2 | 2 | 27.0 | 16.4 | 26.6 | 1.62 |
| | 1 | 32 | 2 | 2 | 50.0 | 25.2 | 13.5 | 0.53 |
| | 1 | 32 | 2 | 2 | 38.5 | 19.4 | 5.6 | 0.29 |
| 68 | 1 | 22 | 2 | 2 | 20.6 | 14.6 | 14.0 | 0.96 |
| | 1 | 22 | 2 | 2 | 35.0 | 16.7 | 23.0 | 1.37 |
| | 1 | 22 | 2 | 2 | 37.0 | 18.7 | 28.4 | 1.52 |
| | 1 | 22 | 2 | 2 | 49.1 | 24.8 | 17.5 | 0.71 |
| | 1 | 22 | 2 | 2 | 36.2 | 18.3 | 23.7 | 1.30 |
| 69 | 1 | 0 | 4 | 1 | 26.3 | 18.2 | 26.3 | 1.45 |
| | 1 | 0 | 4 | 1 | 25.7 | 18.0 | 25.7 | 1.42 |
| | 1 | 0 | 4 | 1 | 26.0 | 18.1 | 28.7 | 1.58 |
| | 1 | 0 | 4 | 1 | 15.6 | 13.8 | 15.6 | 1.13 |
| | 1 | 0 | 4 | 1 | 20.8 | 16.4 | 18.3 | 1.11 |
| | 1 | 0 | 4 | 1 | 20.8 | 16.4 | 20.9 | 1.27 |
| | 1 | 0 | 4 | 1 | 20.9 | 16.4 | 18.3 | 1.11 |
| | 1 | 0 | 4 | 1 | 23.5 | 17.4 | 26.0 | 1.49 |
| 70 | 2 | 38 | 2 | 2 | 13.1 | 8.6 | 9.9 | 1.15 |
| | 2 | 38 | 2 | 2 | 18.2 | 10.8 | 20.0 | 1.85 |
| | 2 | 38 | 2 | 2 | 36.4 | 14.6 | 26.3 | 1.80 |
| | 2 | 38 | 2 | 2 | 33.8 | 13.3 | 24.6 | 1.85 |
| 71 | 3 | 19 | 2 | 2 | 12.9 | 6.7 | 7.8 | 1.16 |
| | 3 | 19 | 2 | 2 | 20.6 | 9.2 | 6.0 | 0.65 |
| | 3 | 19 | 2 | 2 | 36.4 | 11.5 | 12.4 | 1.07 |
| | 3 | 19 | 2 | 2 | 54.4 | 17.2 | 18.9 | 1.10 |
| 72 | 2 | 19 | 2 | 2 | 10.4 | 7.2 | 9.9 | 1.37 |
| | 2 | 19 | 2 | 2 | 13.0 | 8.6 | 14.0 | 1.63 |
| | 2 | 19 | 2 | 2 | 45.3 | 18.1 | 17.3 | 0.96 |
| | 2 | 19 | 2 | 2 | 51.5 | 20.6 | 0.0 | 0.00 |
| 73 | 3 | 23 | 2 | 1 | 23.0 | 10.8 | 24.9 | 2.30 |
| | 3 | 23 | 2 | 1 | 52.8 | 18.7 | 49.9 | 2.66 |
| | 3 | 23 | 2 | 1 | 19.4 | 9.9 | 22.5 | 2.26 |
| | 3 | 23 | 2 | 1 | 53.2 | 18.8 | 40.6 | 2.15 |
| | 3 | 23 | 2 | 1 | 41.6 | 14.7 | 20.8 | 1.41 |
| | 3 | 23 | 2 | 1 | 57.4 | 20.3 | 20.9 | 1.03 |
| | 3 | 23 | 2 | 1 | 41.7 | 14.8 | 20.8 | 1.41 |
| | 3 | 23 | 2 | 1 | 78.7 | 27.9 | 26.0 | 0.93 |
| | 3 | 23 | 2 | 1 | 62.4 | 22.1 | 34.1 | 1.54 |

| Roof Structure No. | Exposure Rating | Slope | Roof Material | Heating Parameter | Ground Snow Load (psf) | Pred. Roof Snow Load (psf) | Actual Roof Snow Load (psf) | Bias Equation *(16)* |
|---|---|---|---|---|---|---|---|---|
| 77 | 2 | 17 | 2 | 2 | 15.6 | 9.8 | 14.2 | 1.45 |
| | 2 | 17 | 2 | 2 | 28.6 | 13.2 | 7.8 | 0.59 |
| | 2 | 17 | 2 | 2 | 28.7 | 13.2 | 7.8 | 0.59 |
| | 2 | 17 | 2 | 2 | 26.0 | 12.8 | 7.8 | 0.61 |
| | 2 | 17 | 2 | 2 | 57.2 | 22.9 | 7.8 | 0.34 |
| | 2 | 17 | 2 | 2 | 36.4 | 14.6 | 10.4 | 0.71 |
| 78 | 3 | 14 | 2 | 2 | 29.9 | 10.5 | 37.1 | 3.53 |
| | 3 | 14 | 2 | 2 | 15.6 | 7.7 | 10.4 | 1.34 |
| | 3 | 14 | 2 | 2 | 23.4 | 9.8 | 13.0 | 1.33 |
| | 3 | 14 | 2 | 2 | 28.5 | 10.4 | 20.8 | 1.99 |
| | 3 | 14 | 2 | 2 | 36.4 | 11.5 | 18.2 | 1.58 |
| | 3 | 14 | 2 | 2 | 31.2 | 10.6 | 18.2 | 1.73 |
| | 3 | 14 | 2 | 2 | 31.2 | 10.6 | 26.0 | 2.46 |
| 79 | 2 | 24 | 2 | 2 | 15.6 | 9.8 | 7.8 | 0.80 |
| | 2 | 24 | 2 | 2 | 28.5 | 13.2 | 7.8 | 0.59 |
| | 2 | 24 | 2 | 2 | 36.4 | 14.6 | 10.4 | 0.71 |
| | 2 | 24 | 2 | 2 | 31.2 | 13.3 | 13.0 | 0.97 |
| | 2 | 24 | 2 | 2 | 31.2 | 13.3 | 18.3 | 1.37 |
| 80 | 2 | 21 | 2 | 2 | 41.4 | 16.6 | 25.0 | 1.51 |
| | 2 | 21 | 2 | 2 | 20.8 | 11.6 | 13.0 | 1.12 |
| | 2 | 21 | 2 | 2 | 26.1 | 12.9 | 10.4 | 0.81 |
| | 2 | 21 | 2 | 2 | 44.1 | 17.7 | 15.6 | 0.88 |
| | 2 | 21 | 2 | 2 | 31.2 | 13.3 | 18.2 | 1.37 |
| | 2 | 21 | 2 | 2 | 26.1 | 12.9 | 36.0 | 2.80 |
| | 2 | 21 | 2 | 2 | 44.2 | 17.7 | 18.2 | 1.03 |
| 81 | 3 | 22 | 2 | 2 | 20.8 | 9.2 | 7.8 | 0.84 |
| | 3 | 22 | 2 | 2 | 20.8 | 9.2 | 10.4 | 1.13 |
| | 3 | 22 | 2 | 2 | 26.1 | 10.2 | 15.6 | 1.53 |
| | 3 | 22 | 2 | 2 | 23.3 | 9.8 | 13.0 | 1.33 |
| 82 | 3 | 20 | 2 | 2 | 23.3 | 9.8 | 5.2 | 0.53 |
| | 3 | 20 | 2 | 2 | 26.1 | 10.2 | 2.6 | 0.26 |
| | 3 | 20 | 2 | 2 | 26.0 | 10.2 | 26.0 | 2.56 |
| 83 | 3 | 0 | 4 | 2 | 15.6 | 7.7 | 22.5 | 2.90 |
| | 3 | 0 | 4 | 2 | 26.1 | 10.2 | 0.0 | 0.00 |
| | 3 | 0 | 4 | 2 | 28.7 | 10.4 | 0.0 | 0.00 |
| 87 | 3 | 20 | 2 | 2 | 23.5 | 9.8 | 5.4 | 0.55 |
| | 3 | 20 | 2 | 2 | 23.3 | 9.8 | 10.4 | 1.06 |
| | 3 | 20 | 2 | 2 | 28.7 | 10.4 | 10.4 | 0.99 |
| 88 | 3 | 13 | 2 | 2 | 26.0 | 10.2 | 13.0 | 1.28 |
| | 3 | 13 | 2 | 2 | 26.1 | 10.2 | 26.0 | 2.55 |
| | 3 | 13 | 2 | 2 | 33.7 | 10.6 | 18.3 | 1.73 |
| | 3 | 13 | 2 | 2 | 36.3 | 11.5 | 18.2 | 1.58 |
| 89 | 2 | 10 | 2 | 2 | 25.5 | 12.8 | 11.9 | 0.94 |
| | 2 | 10 | 2 | 2 | 36.5 | 14.6 | 15.6 | 1.06 |
| | 2 | 10 | 2 | 2 | 36.5 | 14.6 | 7.8 | 0.53 |
| | 2 | 10 | 2 | 2 | 46.8 | 18.7 | 12.1 | 0.65 |

| Roof Structure No. | Exposure Rating | Slope | Roof Material | Heating Parameter | Ground Snow Load (psf) | Pred. Roof Snow Load (psf) | Actual Roof Snow Load (psf) | Bias Equation *(16)* |
|---|---|---|---|---|---|---|---|---|
| 90 | 1 | 28 | 2 | 2 | 15.6 | 12.3 | 10.4 | 0.84 |
| | 1 | 28 | 2 | 2 | 20.8 | 14.7 | 18.2 | 1.24 |
| | 1 | 28 | 2 | 2 | 20.8 | 14.7 | 15.6 | 1.06 |
| | 1 | 28 | 2 | 2 | 20.9 | 14.7 | 15.6 | 1.06 |
| | 1 | 28 | 2 | 2 | 23.5 | 15.6 | 15.6 | 1.00 |
| 91 | 1 | 23 | 2 | 1 | 15.6 | 13.8 | 13.0 | 0.95 |
| | 1 | 23 | 2 | 1 | 20.8 | 16.4 | 13.1 | 0.79 |
| | 1 | 23 | 2 | 1 | 20.8 | 16.4 | 18.3 | 1.11 |
| | 1 | 23 | 2 | 1 | 20.9 | 16.4 | 18.3 | 1.11 |
| | 1 | 23 | 2 | 1 | 23.5 | 17.4 | 18.2 | 1.05 |
| 94 | 2 | 0 | 3 | 2 | 48.3 | 19.4 | 14.5 | 0.75 |
| | 2 | 0 | 3 | 2 | 92.7 | 37.1 | 57.4 | 1.55 |
| 95 | 3 | 56 | 2 | 2 | 92.7 | 29.4 | 54.5 | 1.85 |
| | 3 | 56 | 2 | 2 | 147.9 | 46.9 | 82.1 | 1.75 |
| 96 | 3 | 18 | 2 | 2 | 18.9 | 8.7 | 10.4 | 1.19 |
| | 3 | 18 | 2 | 2 | 68.4 | 21.7 | 39.7 | 1.83 |
| | 3 | 18 | 2 | 2 | 13.4 | 6.9 | 0.0 | 0.00 |
| | 3 | 18 | 2 | 2 | 23.4 | 9.8 | 0.0 | 0.00 |
| | 3 | 18 | 2 | 2 | 52.5 | 16.7 | 0.0 | 0.00 |
| 97 | 2 | 45 | 1 | 1 | 32.3 | 12.8 | 10.8 | 0.84 |
| | 2 | 45 | 1 | 1 | 68.4 | 26.3 | 55.8 | 2.12 |
| | 2 | 45 | 1 | 1 | 124.8 | 48.0 | 98.7 | 2.05 |
| 98 | 3 | 27 | 2 | 1 | 31.7 | 11.8 | 24.3 | 2.05 |
| | 3 | 27 | 2 | 1 | 68.4 | 24.3 | 43.8 | 1.80 |
| 99 | 3 | 0 | 3 | 2 | 18.8 | 8.7 | 14.2 | 1.62 |
| | 3 | 0 | 3 | 2 | 50.2 | 15.9 | 0.0 | 0.00 |
| 100 | 3 | 45 | 1 | 1 | 18.8 | 8.4 | 1.7 | 0.20 |
| | 3 | 45 | 1 | 1 | 50.2 | 15.3 | 31.9 | 2.08 |
| 101 | 3 | 45 | 1 | 1 | 18.8 | 8.4 | 8.3 | 0.99 |
| | 3 | 45 | 1 | 1 | 50.2 | 15.3 | 0.0 | 0.00 |
| 102 | 3 | 2 | 4 | 2 | 31.3 | 10.6 | 16.1 | 1.52 |
| | 3 | 2 | 4 | 2 | 107.5 | 34.1 | 40.1 | 1.18 |
| 103 | 1 | 5 | 4 | 2 | 2.1 | 2.1 | 4.3 | 2.01 |
| | 1 | 5 | 4 | 2 | 16.9 | 13.0 | 12.6 | 0.97 |
| | 1 | 5 | 4 | 2 | 23.5 | 15.6 | 15.0 | 0.96 |
| | 1 | 5 | 4 | 2 | 28.4 | 16.6 | 17.0 | 1.02 |
| | 1 | 5 | 4 | 2 | 27.3 | 16.4 | 12.9 | 0.78 |
| 104 | 1 | 7 | 1 | 1 | 18.2 | 14.3 | 11.4 | 0.80 |
| | 1 | 7 | 1 | 1 | 23.5 | 16.4 | 11.9 | 0.72 |
| | 1 | 7 | 1 | 1 | 28.4 | 17.4 | 0.0 | 0.00 |
| | 1 | 7 | 1 | 1 | 27.3 | 17.3 | 14.3 | 0.83 |
| 105 | 2 | 34 | 2 | 2 | 28.4 | 13.2 | 0.0 | 0.00 |
| | 2 | 34 | 2 | 2 | 27.3 | 13.0 | 15.9 | 1.22 |
| 106 | 2 | 0 | 3 | 2 | 28.4 | 13.2 | 0.0 | 0.00 |
| | 2 | 0 | 3 | 2 | 27.3 | 13.0 | 24.0 | 1.84 |

| Roof Structure No. | Exposure Rating | Slope | Roof Material | Heating Parameter | Ground Snow Load (psf) | Pred. Roof Snow Load (psf) | Actual Roof Snow Load (psf) | Bias Equation *(16)* |
|---|---|---|---|---|---|---|---|---|
| 107 | 2 | 2 | 2 | 2 | 28.4 | 13.2 | 17.3 | 1.32 |
| | 2 | 2 | 2 | 2 | 27.3 | 13.0 | 15.3 | 1.18 |
| 118-1 | 3 | 23 | 2 | 2 | 12.0 | 6.4 | 0.0 | 0.00 |
| | 3 | 23 | 2 | 2 | 15.0 | 7.5 | 0.0 | 0.00 |
| 118-2 | 3 | 23 | 2 | 2 | 12.0 | 6.4 | 6.3 | 0.98 |
| | 3 | 23 | 2 | 2 | 15.0 | 7.5 | 0.0 | 0.00 |
| 119-1 | 3 | 23 | 2 | 2 | 12.0 | 6.4 | 0.0 | 0.00 |
| | 3 | 23 | 2 | 2 | 15.0 | 7.5 | 0.0 | 0.00 |
| | 3 | 23 | 2 | 2 | 22.4 | 9.6 | 0.0 | 0.00 |
| 119-2 | 3 | 23 | 2 | 2 | 12.0 | 6.4 | 0.0 | 0.00 |
| | 3 | 23 | 2 | 2 | 15.0 | 7.5 | 0.0 | 0.00 |
| 120 | 3 | 0 | 2 | 2 | 12.0 | 6.4 | 9.2 | 1.44 |
| | 3 | 0 | 2 | 2 | 15.0 | 7.5 | 5.2 | 0.68 |
| 125 | 3 | 0 | 3 | 2 | 12.1 | 6.4 | 3.7 | 0.57 |
| | 3 | 0 | 3 | 2 | 13.0 | 6.8 | 11.7 | 1.72 |
| 128 | 2 | 0 | 4 | 2 | 12.2 | 8.2 | 3.0 | 0.36 |
| | 2 | 0 | 4 | 2 | 14.4 | 9.3 | 6.0 | 0.64 |
| 130-1 | 3 | 6 | 1 | 2 | 3.6 | 2.1 | 0.0 | 0.00 |
| | 3 | 6 | 1 | 2 | 8.3 | 4.5 | 0.0 | 0.00 |
| | 3 | 6 | 1 | 2 | 7.4 | 4.0 | 0.0 | 0.00 |
| | 3 | 6 | 1 | 2 | 1.8 | 1.1 | 0.0 | 0.00 |
| 130-2 | 3 | 6 | 1 | 1 | 3.6 | 2.3 | 1.9 | 0.81 |
| | 3 | 6 | 1 | 1 | 8.3 | 5.0 | 2.3 | 0.47 |
| | 3 | 6 | 1 | 1 | 7.4 | 4.5 | 2.4 | 0.54 |
| | 3 | 6 | 1 | 1 | 1.8 | 1.2 | 3.3 | 2.81 |
| 131 | 3 | 0 | 4 | 2 | 2.9 | 1.8 | 3.4 | 1.88 |
| | 3 | 0 | 4 | 2 | 5.2 | 3.1 | 3.1 | 1.00 |
| | 3 | 0 | 4 | 2 | 9.6 | 5.3 | 0.0 | 0.00 |
| | 3 | 0 | 4 | 2 | 0.7 | 0.5 | 1.8 | 3.77 |
| 132 | 3 | 18 | 1 | 2 | 4.0 | 2.3 | 3.2 | 1.40 |
| | 3 | 18 | 1 | 2 | 6.9 | 3.8 | 7.6 | 2.00 |
| | 3 | 18 | 1 | 2 | 8.8 | 4.6 | 7.0 | 1.51 |
| | 3 | 18 | 1 | 2 | 2.3 | 1.4 | 2.3 | 1.66 |
| 133 | 3 | 0 | 4 | 2 | 3.0 | 1.9 | 1.8 | 0.95 |
| | 3 | 0 | 4 | 2 | 8.3 | 4.7 | 3.5 | 0.74 |
| | 3 | 0 | 4 | 2 | 2.0 | 1.3 | 2.5 | 2.00 |
| 135 | 3 | 0 | 3 | 2 | 5.5 | 3.3 | 3.7 | 1.13 |
| | 3 | 0 | 3 | 2 | 7.2 | 4.2 | 5.0 | 1.18 |
| | 3 | 0 | 3 | 2 | 7.6 | 4.4 | 4.4 | 0.99 |
| | 3 | 0 | 3 | 2 | 2.0 | 1.3 | 1.9 | 1.49 |
| 137 | 3 | 3 | 4 | 2 | 4.2 | 2.5 | 3.1 | 1.20 |
| | 3 | 3 | 4 | 2 | 7.4 | 4.3 | 2.6 | 0.61 |
| | 3 | 3 | 4 | 2 | 7.9 | 4.6 | 3.8 | 0.82 |
| | 3 | 3 | 4 | 2 | 2.9 | 1.8 | 2.2 | 1.23 |

| Roof Structure No. | Exposure Rating | Slope | Roof Material | Heating Parameter | Ground Snow Load (psf) | Pred. Roof Snow Load (psf) | Actual Roof Snow Load (psf) | Bias Equation *(16)* |
|---|---|---|---|---|---|---|---|---|
| 138 | 2 | 45 | 2 | 2 | 5.0 | 3.8 | 2.7 | 0.70 |
| | 2 | 45 | 2 | 2 | 8.2 | 5.9 | 2.9 | 0.49 |
| | 2 | 45 | 2 | 2 | 7.5 | 5.5 | 4.8 | 0.88 |
| | 2 | 45 | 2 | 2 | 1.8 | 1.4 | 0.7 | 0.48 |
| 140-3 | 3 | 0 | 4 | 2 | 2.2 | 1.4 | 1.1 | 0.74 |
| | 3 | 0 | 4 | 2 | 3.8 | 2.3 | 3.1 | 1.35 |
| | 3 | 0 | 4 | 2 | 9.6 | 5.4 | 2.2 | 0.41 |
| | 3 | 0 | 4 | 2 | 2.0 | 1.3 | 1.7 | 1.32 |
| 141-1 | 2 | 28 | 2 | 2 | 10.5 | 7.3 | 12.6 | 1.74 |
| | 2 | 28 | 2 | 2 | 7.1 | 5.2 | 7.5 | 1.44 |
| | 2 | 28 | 2 | 2 | 6.8 | 5.0 | 5.0 | 0.99 |
| | 2 | 28 | 2 | 2 | 9.0 | 6.4 | 9.3 | 1.45 |
| | 2 | 28 | 2 | 2 | 10.4 | 7.2 | 5.9 | 0.81 |
| | 2 | 28 | 2 | 2 | 10.1 | 7.0 | 3.7 | 0.52 |
| 141-2 | 2 | 26 | 2 | 2 | 10.5 | 7.3 | 10.9 | 1.51 |
| | 2 | 26 | 2 | 2 | 7.1 | 5.2 | 7.5 | 1.44 |
| | 2 | 26 | 2 | 2 | 6.8 | 5.0 | 5.0 | 0.99 |
| | 2 | 26 | 2 | 2 | 9.0 | 6.4 | 11.1 | 1.73 |
| | 2 | 26 | 2 | 2 | 10.4 | 7.2 | 7.3 | 1.02 |
| | 2 | 26 | 2 | 2 | 10.1 | 7.0 | 3.7 | 0.52 |
| 142-1 | 2 | 16 | 2 | 2 | 8.8 | 6.3 | 7.6 | 1.20 |
| | 2 | 16 | 2 | 2 | 7.3 | 5.4 | 5.7 | 1.06 |
| | 2 | 16 | 2 | 2 | 8.2 | 5.9 | 8.6 | 1.46 |
| 142-2 | 2 | 24 | 2 | 2 | 7.3 | 5.4 | 6.7 | 1.24 |
| | 2 | 24 | 2 | 2 | 8.2 | 5.9 | 6.0 | 1.02 |
| 142-3 | 2 | 4 | 2 | 2 | 7.3 | 5.4 | 7.6 | 1.42 |
| | 2 | 4 | 2 | 2 | 8.2 | 5.9 | 5.2 | 0.87 |
| 143 | 2 | 24 | 2 | 2 | 9.4 | 6.6 | 5.4 | 0.81 |
| | 2 | 24 | 2 | 2 | 7.6 | 5.5 | 3.7 | 0.67 |
| | 2 | 24 | 2 | 2 | 7.2 | 5.3 | 5.3 | 1.00 |
| | 2 | 24 | 2 | 2 | 7.3 | 5.4 | 2.2 | 0.40 |
| 144 | 2 | 27 | 2 | 2 | 9.4 | 6.6 | 4.9 | 0.74 |
| | 2 | 27 | 2 | 2 | 7.6 | 5.5 | 6.5 | 1.18 |
| | 2 | 27 | 2 | 2 | 7.2 | 5.3 | 5.3 | 1.01 |
| | 2 | 27 | 2 | 2 | 7.3 | 5.4 | 2.8 | 0.52 |
| 145 | 3 | 11 | 2 | 2 | 7.8 | 4.5 | 4.7 | 1.03 |
| | 3 | 11 | 2 | 2 | 7.4 | 4.3 | 5.4 | 1.27 |
| | 3 | 11 | 2 | 2 | 7.7 | 4.4 | 5.7 | 1.29 |
| 146-1 | 2 | 35 | 2 | 2 | 7.3 | 5.3 | 5.8 | 1.10 |
| | 2 | 35 | 2 | 2 | 7.6 | 5.5 | 3.7 | 0.66 |
| | 2 | 35 | 2 | 2 | 8.4 | 6.0 | 3.1 | 0.51 |
| 146-3 | 2 | 17 | 2 | 2 | 7.3 | 5.3 | 7.6 | 1.43 |
| | 2 | 17 | 2 | 2 | 7.6 | 5.5 | 7.4 | 1.33 |
| | 2 | 17 | 2 | 2 | 8.4 | 6.0 | 3.1 | 0.51 |

| Roof Structure No. | Exposure Rating | Slope | Roof Material | Heating Parameter | Ground Snow Load (psf) | Pred. Roof Snow Load (psf) | Actual Roof Snow Load (psf) | Bias Equation *(16)* |
|---|---|---|---|---|---|---|---|---|
| 147-2 | 3 | 9 | 2 | 2 | 10.7 | 5.9 | 3.7 | 0.63 |
| | 3 | 9 | 2 | 2 | 7.6 | 4.4 | 7.4 | 1.68 |
| | 3 | 9 | 2 | 2 | 9.0 | 5.1 | 2.5 | 0.50 |
| | 3 | 9 | 2 | 2 | 8.5 | 4.8 | 5.8 | 1.19 |
| | 3 | 9 | 2 | 2 | 10.7 | 5.9 | 2.6 | 0.45 |
| 149-2 | 2 | 0 | 4 | 2 | 7.2 | 5.3 | 1.0 | 0.19 |
| | 2 | 0 | 4 | 2 | 13.7 | 8.9 | 0.8 | 0.09 |
| | 2 | 0 | 4 | 2 | 8.0 | 5.8 | 0.0 | 0.00 |
| | 2 | 0 | 4 | 2 | 8.5 | 6.1 | 11.9 | 1.94 |
| | 2 | 0 | 4 | 2 | 8.5 | 6.1 | 1.7 | 0.28 |
| 150-2 | 2 | 0 | 3 | 2 | 8.6 | 6.2 | 4.2 | 0.67 |
| | 2 | 0 | 3 | 2 | 6.0 | 4.5 | 1.8 | 0.39 |
| | 2 | 0 | 3 | 2 | 7.1 | 5.2 | 2.3 | 0.43 |
| 150-3 | 2 | 8 | 3 | 2 | 8.6 | 6.2 | 3.5 | 0.56 |
| | 2 | 8 | 3 | 2 | 6.0 | 4.5 | 1.2 | 0.26 |
| | 2 | 8 | 3 | 2 | 7.1 | 5.2 | 2.3 | 0.43 |
| 154 | 3 | 0 | 3 | 2 | 7.5 | 4.3 | 4.2 | 0.97 |
| | 3 | 0 | 3 | 2 | 3.6 | 2.2 | 3.0 | 1.35 |
| | 3 | 0 | 3 | 2 | 8.0 | 4.6 | 1.3 | 0.28 |
| | 3 | 0 | 3 | 2 | 7.1 | 4.1 | 4.0 | 0.98 |
| | 3 | 0 | 3 | 2 | 10.7 | 5.8 | 2.0 | 0.35 |
| | 3 | 0 | 3 | 2 | 12.1 | 6.4 | 4.0 | 0.62 |
| | 3 | 0 | 3 | 2 | 13.1 | 6.8 | 9.4 | 1.38 |
| | 3 | 0 | 3 | 2 | 13.9 | 7.1 | 2.9 | 0.41 |
| 165 | 1 | 30 | 2 | 2 | 9.2 | 8.2 | 10.0 | 1.21 |
| | 1 | 30 | 2 | 2 | 12.1 | 10.2 | 12.0 | 1.17 |
| | 1 | 30 | 2 | 2 | 9.0 | 8.1 | 4.8 | 0.60 |
| 166 | 2 | 27 | 2 | 2 | 8.1 | 5.9 | 6.7 | 1.15 |
| | 2 | 27 | 2 | 2 | 11.1 | 7.6 | 11.9 | 1.57 |
| | 2 | 27 | 2 | 2 | 8.3 | 6.0 | 3.8 | 0.63 |
| 167 | 2 | 25 | 2 | 2 | 9.1 | 6.4 | 3.9 | 0.61 |
| | 2 | 25 | 2 | 2 | 7.9 | 5.7 | 4.0 | 0.70 |
| 168 | 2 | 22 | 2 | 2 | 7.7 | 5.6 | 8.2 | 1.45 |
| | 2 | 22 | 2 | 2 | 12.8 | 8.5 | 4.8 | 0.56 |
| 169 | 2 | 21 | 2 | 2 | 7.2 | 5.3 | 8.3 | 1.57 |
| | 2 | 21 | 2 | 2 | 10.9 | 7.5 | 3.5 | 0.46 |
| 170 | 2 | 25 | 2 | 2 | 5.7 | 4.3 | 7.4 | 1.73 |
| | 2 | 25 | 2 | 2 | 10.5 | 7.3 | 3.8 | 0.53 |
| 171-1 | 2 | 18 | 1 | 1 | 16.5 | 10.7 | 14.7 | 1.37 |
| | 2 | 18 | 1 | 1 | 26.1 | 13.5 | 0.0 | 0.00 |
| | 2 | 18 | 1 | 1 | 18.7 | 11.5 | 17.8 | 1.54 |
| | 2 | 18 | 1 | 1 | 32.8 | 14.0 | 24.6 | 1.75 |
| | 2 | 18 | 1 | 1 | 40.4 | 17.0 | 37.6 | 2.21 |

| Roof Structure No. | Exposure Rating | Slope | Roof Material | Heating Parameter | Ground Snow Load (psf) | Pred. Roof Snow Load (psf) | Actual Roof Snow Load (psf) | Bias Equation *(16)* |
|---|---|---|---|---|---|---|---|---|
| 171-2 | 2 | 21 | 2 | 1 | 16.5 | 11.4 | 16.1 | 1.42 |
| | 2 | 21 | 2 | 1 | 26.1 | 14.4 | 13.7 | 0.95 |
| | 2 | 21 | 2 | 1 | 18.7 | 12.3 | 17.8 | 1.45 |
| | 2 | 21 | 2 | 1 | 32.8 | 14.9 | 33.9 | 2.27 |
| | 2 | 21 | 2 | 1 | 40.4 | 18.1 | 37.6 | 2.08 |
| 172 | 1 | 11 | 1 | 1 | 16.5 | 13.4 | 17.1 | 1.27 |
| | 1 | 11 | 1 | 1 | 26.1 | 17.0 | 0.0 | 0.00 |
| | 1 | 11 | 1 | 1 | 18.7 | 14.5 | 21.3 | 1.47 |
| | 1 | 11 | 1 | 1 | 32.8 | 17.7 | 35.4 | 2.00 |
| | 1 | 11 | 1 | 1 | 40.4 | 21.4 | 43.0 | 2.01 |
| 173 | 1 | 5 | 1 | 1 | 16.5 | 13.4 | 18.5 | 1.38 |
| | 1 | 5 | 1 | 1 | 26.1 | 17.0 | 0.0 | 0.00 |
| 174 | 2 | 5 | 2 | 1 | 12.3 | 9.2 | 6.5 | 0.70 |
| | 2 | 5 | 2 | 1 | 24.9 | 14.1 | 0.0 | 0.00 |
| | 2 | 5 | 2 | 1 | 19.3 | 12.5 | 22.5 | 1.80 |
| | 2 | 5 | 2 | 1 | 36.3 | 16.2 | 20.2 | 1.24 |
| | 2 | 5 | 2 | 1 | 36.9 | 16.5 | 28.2 | 1.71 |
| 175 | 2 | 0 | 2 | 1 | 12.3 | 9.2 | 7.4 | 0.80 |
| | 2 | 0 | 2 | 1 | 24.9 | 14.1 | 0.0 | 0.00 |
| 176 | 1 | 34 | 2 | 1 | 11.1 | 10.7 | 14.7 | 1.37 |
| | 1 | 34 | 2 | 1 | 25.3 | 17.9 | 8.5 | 0.48 |
| | 1 | 34 | 2 | 1 | 23.1 | 17.3 | 23.8 | 1.38 |
| | 1 | 34 | 2 | 1 | 35.4 | 20.0 | 46.8 | 2.34 |
| | 1 | 34 | 2 | 1 | 49.6 | 28.0 | 38.0 | 1.36 |
| 177 | 1 | 0 | 1 | 1 | 15.5 | 12.9 | 13.5 | 1.05 |
| | 1 | 0 | 1 | 1 | 22.3 | 16.0 | 11.7 | 0.73 |
| | 1 | 0 | 1 | 1 | 19.0 | 14.7 | 18.5 | 1.26 |
| | 1 | 0 | 1 | 1 | 29.5 | 17.6 | 27.7 | 1.58 |
| | 1 | 0 | 1 | 1 | 38.7 | 20.5 | 24.7 | 1.20 |
| 185 | 3 | 32 | 2 | 1 | 9.9 | 6.1 | 10.1 | 1.64 |
| | 3 | 32 | 2 | 1 | 23.0 | 10.8 | 14.6 | 1.35 |
| | 3 | 32 | 2 | 1 | 19.7 | 10.0 | 10.7 | 1.06 |
| 187 | 3 | 37 | 2 | 1 | 8.6 | 5.4 | 5.2 | 0.96 |
| | 3 | 37 | 2 | 1 | 24.2 | 11.1 | 0.0 | 0.00 |
| | 3 | 37 | 2 | 1 | 23.7 | 11.0 | 0.0 | 0.00 |
| 188 | 3 | 0 | 2 | 1 | 9.3 | 5.8 | 4.3 | 0.75 |
| | 3 | 0 | 2 | 1 | 24.2 | 11.1 | 9.8 | 0.88 |
| 190-1 | 1 | 14 | 2 | 1 | 10.9 | 10.5 | 9.8 | 0.93 |
| | 1 | 14 | 2 | 1 | 19.8 | 16.0 | 11.0 | 0.69 |
| | 1 | 14 | 2 | 1 | 20.8 | 16.4 | 10.1 | 0.61 |
| 190-2 | 1 | 23 | 2 | 1 | 10.9 | 10.5 | 9.8 | 0.93 |
| | 1 | 23 | 2 | 1 | 19.8 | 16.0 | 16.5 | 1.03 |
| | 1 | 23 | 2 | 1 | 20.8 | 16.4 | 13.4 | 0.82 |
| 190-3 | 1 | 7 | 2 | 1 | 10.9 | 10.5 | 9.8 | 0.93 |
| | 1 | 7 | 2 | 1 | 19.8 | 16.0 | 18.3 | 1.15 |
| | 1 | 7 | 2 | 1 | 20.8 | 16.4 | 13.4 | 0.82 |

| Roof Structure No. | Exposure Rating | Slope | Roof Material | Heating Parameter | Ground Snow Load (psf) | Pred. Roof Snow Load (psf) | Actual Roof Snow Load (psf) | Bias Equation *(16)* |
|---|---|---|---|---|---|---|---|---|
| 192 | 3 | 32 | 2 | 2 | 9.3 | 5.2 | 5.8 | 1.11 |
| | 3 | 32 | 2 | 2 | 21.6 | 9.4 | 7.6 | 0.81 |
| | 3 | 32 | 2 | 2 | 17.7 | 8.4 | 3.0 | 0.36 |
| 193 | 3 | 10 | 2 | 1 | 8.6 | 5.4 | 9.1 | 1.68 |
| | 3 | 10 | 2 | 1 | 20.8 | 10.3 | 3.5 | 0.33 |
| 194 | 3 | 32 | 2 | 1 | 13.1 | 7.6 | 13.7 | 1.80 |
| | 3 | 32 | 2 | 1 | 27.7 | 11.6 | 11.9 | 1.03 |
| | 3 | 32 | 2 | 1 | 28.0 | 11.6 | 14.0 | 1.21 |
| 195 | 3 | 17 | 2 | 2 | 9.8 | 5.4 | 6.6 | 1.21 |
| | 3 | 17 | 2 | 2 | 18.7 | 8.7 | 6.3 | 0.72 |
| 197 | 1 | 23 | 2 | 1 | 6.3 | 6.6 | 7.8 | 1.18 |
| | 1 | 23 | 2 | 1 | 15.3 | 13.6 | 15.6 | 1.15 |
| | 1 | 23 | 2 | 1 | 13.0 | 12.1 | 12.8 | 1.05 |
| 198 | 1 | 16 | 1 | 1 | 5.9 | 5.9 | 6.0 | 1.02 |
| | 1 | 16 | 1 | 1 | 15.8 | 13.1 | 8.9 | 0.68 |
| | 1 | 16 | 1 | 1 | 13.8 | 11.9 | 10.5 | 0.89 |
| 199 | 3 | 13 | 2 | 2 | 9.3 | 5.2 | 5.0 | 0.97 |
| | 3 | 13 | 2 | 2 | 24.3 | 9.9 | 10.4 | 1.05 |
| | 3 | 13 | 2 | 2 | 20.8 | 9.2 | 9.8 | 1.06 |
| 200 | 1 | 25 | 2 | 1 | 10.9 | 10.5 | 17.1 | 1.63 |
| | 1 | 25 | 2 | 1 | 17.5 | 14.9 | 22.4 | 1.51 |
| | 1 | 25 | 2 | 1 | 22.4 | 17.0 | 22.0 | 1.29 |
| 201-1 | 1 | 5 | 1 | 1 | 12.4 | 11.0 | 0.0 | 0.00 |
| | 1 | 5 | 1 | 1 | 20.8 | 15.4 | 0.0 | 0.00 |
| | 1 | 5 | 1 | 1 | 19.3 | 14.8 | 18.8 | 1.26 |
| | 1 | 5 | 1 | 1 | 36.3 | 19.2 | 13.3 | 0.69 |
| | 1 | 5 | 1 | 1 | 36.9 | 19.6 | 13.8 | 0.71 |
| 201-2 | 1 | 28 | 2 | 1 | 12.4 | 11.7 | 0.0 | 0.00 |
| | 1 | 28 | 2 | 1 | 20.8 | 16.4 | 0.0 | 0.00 |
| | 1 | 28 | 2 | 1 | 19.3 | 15.8 | 18.8 | 1.19 |
| | 1 | 28 | 2 | 1 | 36.3 | 20.5 | 13.3 | 0.65 |
| | 1 | 28 | 2 | 1 | 36.9 | 20.8 | 13.8 | 0.66 |
| 201-3 | 1 | 0 | 2 | 1 | 12.4 | 11.7 | 0.0 | 0.00 |
| | 1 | 0 | 2 | 1 | 20.8 | 16.4 | 0.0 | 0.00 |
| | 1 | 0 | 2 | 1 | 19.3 | 15.8 | 18.8 | 1.19 |
| | 1 | 0 | 2 | 1 | 36.3 | 20.5 | 20.5 | 1.00 |
| | 1 | 0 | 2 | 1 | 36.9 | 20.8 | 24.9 | 1.20 |
| 204 | 2 | 0 | 1 | 1 | 18.3 | 11.4 | 18.8 | 1.65 |
| | 2 | 0 | 1 | 1 | 33.3 | 14.0 | 16.1 | 1.15 |
| | 2 | 0 | 1 | 1 | 36.3 | 15.3 | 13.9 | 0.91 |
| 205 | 3 | 40 | 1 | 1 | 15.0 | 7.2 | 6.7 | 0.92 |
| | 3 | 40 | 1 | 1 | 23.5 | 9.4 | 7.1 | 0.75 |
| | 3 | 40 | 1 | 1 | 31.3 | 10.2 | 7.4 | 0.73 |
| 206 | 3 | 9 | 1 | 1 | 15.0 | 7.9 | 14.0 | 1.77 |
| | 3 | 9 | 1 | 1 | 23.5 | 10.3 | 13.8 | 1.34 |
| | 3 | 9 | 1 | 1 | 31.3 | 11.1 | 6.2 | 0.56 |

| Roof Structure No. | Exposure Rating | Slope | Roof Material | Heating Parameter | Ground Snow Load (psf) | Pred. Roof Snow Load (psf) | Actual Roof Snow Load (psf) | Bias Equation *(16)* |
|---|---|---|---|---|---|---|---|---|
| 207 | 3 | 27 | 2 | 1 | 18.9 | 9.8 | 12.5 | 1.28 |
| | 3 | 27 | 2 | 1 | 34.4 | 11.8 | 8.4 | 0.71 |
| | 3 | 27 | 2 | 1 | 33.6 | 11.8 | 12.5 | 1.06 |
| 208 | 3 | 10 | 1 | 1 | 18.9 | 9.2 | 15.0 | 1.63 |
| | 3 | 10 | 1 | 1 | 34.4 | 11.1 | 8.2 | 0.74 |
| | 3 | 10 | 1 | 1 | 33.6 | 11.1 | 5.2 | 0.46 |
| 209 | 3 | 34 | 2 | 1 | 19.3 | 9.9 | 18.8 | 1.89 |
| | 3 | 34 | 2 | 1 | 51.5 | 18.2 | 20.1 | 1.10 |
| | 3 | 34 | 2 | 1 | 38.1 | 13.5 | 12.6 | 0.93 |
| | 3 | 10 | 2 | 1 | 19.3 | 9.9 | 18.8 | 1.89 |
| | 3 | 10 | 2 | 1 | 51.5 | 18.2 | 21.8 | 1.19 |
| | 3 | 10 | 2 | 1 | 38.1 | 13.5 | 9.0 | 0.67 |
| 210 | 2 | 25 | 1 | 1 | 18.7 | 10.5 | 19.3 | 1.83 |
| | 2 | 25 | 1 | 1 | 45.9 | 17.7 | 30.9 | 1.75 |
| | 2 | 25 | 1 | 1 | 58.9 | 22.7 | 46.7 | 2.06 |
| 211 | 1 | 34 | 2 | 1 | 24.5 | 17.7 | 28.0 | 1.58 |
| | 1 | 34 | 2 | 1 | 36.3 | 20.5 | 34.8 | 1.70 |
| | 1 | 34 | 2 | 1 | 52.8 | 29.8 | 40.1 | 1.34 |
| 212 | 2 | 40 | 2 | 2 | 26.6 | 12.9 | 40.6 | 3.14 |
| | 2 | 40 | 2 | 2 | 21.1 | 11.7 | 8.6 | 0.73 |
| | 2 | 40 | 2 | 2 | 36.4 | 14.6 | 11.5 | 0.79 |
| | 2 | 40 | 2 | 2 | 43.4 | 17.4 | 4.7 | 0.27 |

## APPENDIX B

Drift Loads using the Non-Uniform Model

| Roof Structure No. | Heating Parameter | Exposure Rating | length of upper roof (ft) | Ground Snow Load (psf) | Roof Snow Load | Actual Roof Snow Load | Bias Equation *(16)* |
|---|---|---|---|---|---|---|---|
| 10 | 2 | 3 | 32 | 15.0 | 51.7 | 92.1 | 1.78 |
| | 2 | 3 | 32 | 4.6 | 31.2 | 20.8 | 0.67 |
| | 2 | 3 | 32 | 5.7 | 33.1 | 64.2 | 1.94 |
| | 2 | 3 | 32 | 7.9 | 50.1 | 72.3 | 1.44 |
| | 2 | 3 | 32 | 10.8 | 68.6 | 75.6 | 1.10 |
| | 2 | 3 | 32 | 19.0 | 109.8 | 81.7 | 0.74 |
| 11 | 2 | 3 | 70 | 4.4 | 39.2 | 31.3 | 0.80 |
| | 2 | 3 | 70 | 8.0 | 64.4 | 36.0 | 0.56 |
| | 2 | 3 | 70 | 4.2 | 29.2 | 32.9 | 1.13 |
| | 2 | 3 | 70 | 5.0 | 43.4 | 39.8 | 0.92 |
| | 2 | 3 | 70 | 25.6 | 207.6 | 50.0 | 0.24 |
| 13 | 2 | 3 | 100 | 3.4 | 35.4 | 54.9 | 1.55 |
| | 2 | 3 | 100 | 1.2 | 13.3 | 30.2 | 2.26 |
| | 2 | 3 | 100 | 8.4 | 79.3 | 49.1 | 0.62 |
| | 2 | 3 | 100 | 2.3 | 24.4 | 41.8 | 1.71 |
| | 2 | 3 | 100 | 14.8 | 115.2 | 43.4 | 0.38 |
| 14 | 2 | 3 | 60 | 2.5 | 22.6 | 1.4 | 0.06 |
| | 2 | 3 | 60 | 9.0 | 68.6 | 43.2 | 0.63 |
| | 2 | 3 | 60 | 8.7 | 62.7 | 52.7 | 0.84 |
| 15 | 2 | 3 | 240 | 4.4 | 49.3 | 39.0 | 0.79 |
| | 2 | 3 | 240 | 12.6 | 113.2 | 52.4 | 0.46 |
| | 2 | 3 | 240 | 14.3 | 98.9 | 60.0 | 0.61 |
| | 2 | 3 | 240 | 5.5 | 57.8 | 80.0 | 1.39 |
| | 2 | 3 | 240 | 10.9 | 101.3 | 77.3 | 0.76 |
| 16 | 2 | 3 | 80 | 6.0 | 49.6 | 43.6 | 0.88 |
| | 2 | 3 | 80 | 9.1 | 72.9 | 68.7 | 0.94 |
| | 2 | 3 | 80 | 2.4 | 20.8 | 33.6 | 1.62 |
| | 2 | 3 | 80 | 34.3 | 112.2 | 51.8 | 0.46 |
| | 2 | 3 | 80 | 7.5 | 57.9 | 25.0 | 0.43 |
| | 2 | 3 | 80 | 9.7 | 77.4 | 61.7 | 0.80 |
| | 2 | 3 | 80 | 10.9 | 90.9 | 59.2 | 0.65 |
| 19 | 2 | 3 | 656 | 7.0 | 74.1 | 61.7 | 0.83 |
| | 2 | 3 | 656 | 11.7 | 93.9 | 105.9 | 1.13 |
| | 2 | 3 | 656 | 7.2 | 62.9 | 63.3 | 1.01 |
| | 2 | 3 | 656 | 9.3 | 88.1 | 92.7 | 1.05 |
| | 2 | 3 | 656 | 11.1 | 93.6 | 98.3 | 1.05 |
| 143 | 1 | 2 | 44 | 7.6 | 4.7 | 20.8 | 4.42 |
| | 1 | 2 | 44 | 7.2 | 3.7 | 7.0 | 1.88 |
| | 1 | 2 | 44 | 7.3 | 5.3 | 7.2 | 1.35 |
| 144 | 2 | 2 | 47 | 7.2 | 9.2 | 7.1 | 0.78 |
| | 2 | 2 | 47 | 6.7 | 12.1 | 8.3 | 0.68 |
| | 2 | 2 | 47 | 8.4 | 13.7 | 0.0 | 0.00 |

| Roof Structure No. | Heating Parameter | Exposure Rating | length of upper roof (ft) | Ground Snow Load (psf) | Roof Snow Load | Actual Roof Snow Load | Bias Equation *(16)* |
|---|---|---|---|---|---|---|---|
| 145 | 1 | 3 | 45 | 7.8 | 23.1 | 8.2 | 0.35 |
| | 1 | 3 | 45 | 7.4 | 15.5 | 7.1 | 0.46 |
| | 1 | 3 | 45 | 7.7 | 22.3 | 7.8 | 0.35 |
| | 1 | 3 | 45 | 8.4 | 23.0 | 7.4 | 0.32 |
| 146 | 2 | 2 | 46 | 7.3 | 11.2 | 10.9 | 0.98 |
| | 2 | 2 | 46 | 8.4 | 14.4 | 7.4 | 0.51 |
| 147 | 2 | 3 | 15 | 15.2 | 59.1 | 14.1 | 0.24 |
| | 2 | 3 | 15 | 10.7 | 50.7 | 5.5 | 0.11 |
| | 2 | 3 | 15 | 10.7 | 50.7 | 14.1 | 0.28 |
| 148 | 1 | 2 | 50 | 10.1 | 7.1 | 7.8 | 1.10 |
| | 1 | 2 | 50 | 8.8 | 6.2 | 14.6 | 2.36 |
| | 1 | 2 | 50 | 9.9 | 6.5 | 15.5 | 2.39 |
| 150 | 2 | 2 | 24 | 6.0 | 7.8 | 3.5 | 0.45 |
| | 2 | 2 | 24 | 7.1 | 10.1 | 2.7 | 0.27 |
| 156 | 2 | 2 | 50 | 7.3 | 12.7 | 15.8 | 1.24 |
| | 2 | 2 | 50 | 8.1 | 11.2 | 36.8 | 3.27 |
| | 2 | 2 | 50 | 13.6 | 21.3 | 48.3 | 2.26 |
| | 2 | 2 | 50 | 16.9 | 26.0 | 48.9 | 1.88 |
| | 2 | 2 | 50 | 8.0 | 13.5 | 13.3 | 0.99 |
| | 2 | 2 | 50 | 13.3 | 16.6 | 6.8 | 0.41 |
| 160 | 2 | 3 | 100 | 7.6 | 73.4 | 57.6 | 0.79 |
| 177 | 1 | 1 | 8 | 22.3 | 8.4 | 18.9 | 2.26 |
| | 1 | 1 | 8 | 19.0 | 10.8 | 18.5 | 1.71 |
| 187 | 1 | 3 | 20 | 8.6 | 17.2 | 6.0 | 0.35 |
| | 1 | 3 | 20 | 24.2 | 51.8 | 15.1 | 0.29 |
| | 1 | 3 | 20 | 23.7 | 43.3 | 15.5 | 0.36 |
| | 1 | 3 | 29 | 8.6 | 18.5 | 6.0 | 0.33 |
| | 1 | 3 | 29 | 24.2 | 55.8 | 19.3 | 0.35 |

Drift Height using the Non-Uniform Model

| Roof Structure No. | Ground Snow Density (pcf) | Roof Snow Density (pcf) | Drift Height (ft) | Actual Drift Height (ft) | Bias in Drift Height | $C_d$ |
|---|---|---|---|---|---|---|
| 10 | 30.0 | 23.1 | 2.24 | 3.21 | 1.43 | 3.45 |
| | 6.9 | 13.5 | 2.31 | 2.21 | 0.96 | 6.78 |
| | 13.7 | 16.3 | 2.03 | 3.67 | 1.81 | 5.80 |
| | 10.0 | 14.8 | 3.39 | 4.82 | 1.42 | 6.33 |
| | 10.0 | 14.8 | 4.64 | 4.67 | 1.01 | 6.33 |
| | 13.7 | 16.3 | 6.73 | 4.08 | 0.61 | 5.80 |
| 11 | 6.2 | 13.2 | 2.97 | 2.79 | 0.94 | 8.93 |
| | 10.6 | 15.0 | 4.28 | 2.50 | 0.58 | 8.10 |
| | 16.8 | 17.6 | 1.66 | 2.63 | 1.59 | 6.94 |
| | 7.5 | 13.8 | 3.16 | 2.46 | 0.78 | 8.68 |
| | 10.6 | 15.0 | 13.81 | 2.50 | 0.18 | 8.10 |
| 13 | 6.2 | 13.2 | 2.68 | 2.67 | 0.99 | 10.55 |
| | 3.1 | 11.9 | 1.12 | 2.42 | 2.16 | 11.23 |
| | 11.2 | 15.3 | 5.19 | 2.38 | 0.46 | 9.44 |
| | 5.6 | 13.0 | 1.88 | 3.73 | 1.98 | 10.68 |
| | 18.7 | 18.4 | 6.26 | 2.25 | 0.36 | 7.78 |
| 14 | 2.5 | 11.7 | 1.94 | 2.29 | 1.18 | 9.04 |
| | 10.6 | 15.0 | 4.56 | 3.00 | 0.66 | 7.61 |
| | 13.1 | 16.1 | 3.90 | 2.42 | 0.62 | 7.17 |
| 15 | 3.1 | 11.9 | 4.14 | 1.25 | 0.30 | 11.23 |
| | 13.1 | 16.1 | 7.05 | 4.00 | 0.57 | 9.02 |
| | 22.5 | 20.0 | 4.95 | 4.00 | 0.81 | 6.94 |
| | 6.2 | 13.2 | 4.37 | 4.00 | 0.91 | 10.55 |
| | 11.9 | 15.6 | 6.50 | 3.75 | 0.58 | 9.29 |
| 16 | 11.9 | 15.6 | 3.18 | 2.79 | 0.88 | 8.34 |
| | 13.7 | 16.3 | 4.46 | 3.15 | 0.71 | 7.98 |
| | 9.4 | 14.5 | 1.43 | 2.00 | 1.40 | 8.83 |
| | 37.4 | 26.1 | 4.29 | 3.60 | 0.84 | 3.27 |
| | 15.0 | 16.9 | 3.43 | 3.08 | 0.90 | 7.72 |
| | 13.7 | 16.3 | 4.74 | 3.08 | 0.65 | 7.98 |
| | 11.9 | 15.6 | 5.84 | 2.96 | 0.51 | 8.34 |
| 19 | 6.2 | 13.2 | 5.61 | 6.17 | 1.10 | 10.55 |
| | 17.5 | 17.9 | 5.25 | 4.58 | 0.87 | 8.05 |
| | 14.4 | 16.6 | 3.79 | 4.83 | 1.28 | 8.73 |
| | 11.2 | 15.3 | 5.76 | 4.50 | 0.78 | 9.44 |
| | 15.6 | 17.1 | 5.47 | 4.92 | 0.90 | 8.47 |
| 143 | 15.1 | 16.9 | 0.28 | 1.33 | 4.79 | 0.62 |
| | 21.6 | 19.6 | 0.19 | 0.33 | 1.75 | 0.52 |
| | 8.8 | 14.3 | 0.37 | 0.83 | 2.24 | 0.72 |
| 144 | 21.6 | 19.6 | 0.47 | 0.33 | 0.71 | 1.27 |
| | 8.0 | 14.0 | 0.86 | 0.83 | 0.97 | 1.81 |
| | 12.6 | 15.9 | 0.86 | 0.00 | 0.00 | 1.63 |

| Roof Structure No. | Ground Snow Density (pcf) | Roof Snow Density (pcf) | Drift Height (ft) | Actual Drift Height (ft) | Bias in Drift Height | $C_d$ |
|---|---|---|---|---|---|---|
| 145 | 9.4 | 14.5 | 1.59 | 0.83 | 0.53 | 2.94 |
| | 22.1 | 19.8 | 0.78 | 0.33 | 0.43 | 2.10 |
| | 10.3 | 14.9 | 1.49 | 0.83 | 0.56 | 2.88 |
| | 12.6 | 15.9 | 1.45 | 0.58 | 0.40 | 2.73 |
| 146 | 14.5 | 16.7 | 0.67 | 0.83 | 1.24 | 1.54 |
| | 10.1 | 14.8 | 0.97 | 0.75 | 0.77 | 1.71 |
| 147 | 22.8 | 20.1 | 2.94 | 0.67 | 0.23 | 3.89 |
| | 16.1 | 17.3 | 2.93 | 0.25 | 0.09 | 4.72 |
| | 16.1 | 17.3 | 2.93 | 0.67 | 0.23 | 4.72 |
| 148 | 12.1 | 15.7 | 0.45 | 0.71 | 1.57 | 0.70 |
| | 11.7 | 15.5 | 0.40 | 1.25 | 3.12 | 0.71 |
| | 14.8 | 16.8 | 0.39 | 0.75 | 1.95 | 0.65 |
| 150 | 14.3 | 16.6 | 0.47 | 0.25 | 0.53 | 1.31 |
| | 10.6 | 15.0 | 0.67 | 0.25 | 0.37 | 1.43 |
| 156 | 11.0 | 15.2 | 0.83 | 1.25 | 1.50 | 1.73 |
| | 19.5 | 18.7 | 0.60 | 1.75 | 2.92 | 1.38 |
| | 14.8 | 16.8 | 1.27 | 2.67 | 2.10 | 1.57 |
| | 15.6 | 17.1 | 1.52 | 3.00 | 1.97 | 1.54 |
| | 12.0 | 15.6 | 0.86 | 0.83 | 0.97 | 1.69 |
| | 22.8 | 20.1 | 0.83 | 0.25 | 0.30 | 1.25 |
| 160 | 10.1 | 14.8 | 4.95 | 4.50 | 0.91 | 9.68 |
| 177 | 22.3 | 19.9 | 0.42 | 0.67 | 1.58 | 0.38 |
| | 6.0 | 13.1 | 0.83 | 2.50 | 3.03 | 0.57 |
| 187 | 17.2 | 17.8 | 0.97 | 0.33 | 0.35 | 2.00 |
| | 14.5 | 16.7 | 3.11 | 0.83 | 0.27 | 2.14 |
| | 20.3 | 19.1 | 2.27 | 0.83 | 0.37 | 1.83 |
| | 17.2 | 17.8 | 1.04 | 0.33 | 0.32 | 2.15 |
| | 14.5 | 16.7 | 3.35 | 1.42 | 0.42 | 2.31 |

**APPENDIX C**

ASCE 7 Drift Load Calculations

Gable Roof Design Example

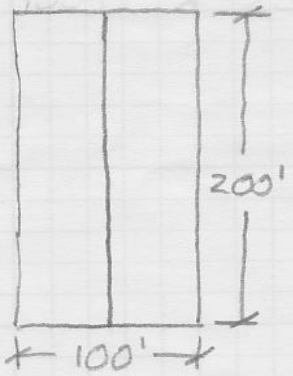


$L = 200'$
$W = 50'$
$0.5/12$
$\theta = 2.386°$

$P_g = 30$ psf
$C_t = 1.0$
$C_e = 1.0$
$I = 1.0$
$C_s = 1.0$

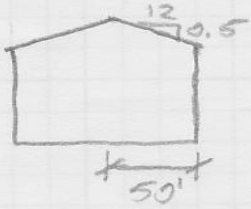


ASCE 95

$$P_s = 0.7 (1.0)(1.0)(1.0)(1.0)(30) = 21 \text{ psf}$$
$$C_s \quad C_e \quad C_t \quad I \quad P_g$$

$\gamma = 0.13(21) + 14 = 16.7$ pcf $\leq 30$ pcf

unbalanced load is not considered

$P_{total} = P_r = 21$ psf

ASCE 02

$P_s = 21$ psf

$B = 1.5 - 0.025(30) = 0.75$

$$\frac{1.2\left[1 + (0.75/2)\right] 21}{1.0} = 34.7 \text{ psf}$$

$P_{total} = 34.7$ psf

ASCE 05

$P_r = 0.3(21) = 6.3$ psf

$$\frac{h_d \gamma}{\sqrt{s}} = \frac{2.4(16.7)}{\sqrt{24}} = 8.18$$

$8/3\, h_d \sqrt{s} = 8/3(2.4)(\sqrt{24}) = 31.3$

$P_{total} = 29.2$ psf

## Lower Roof snowdrifts

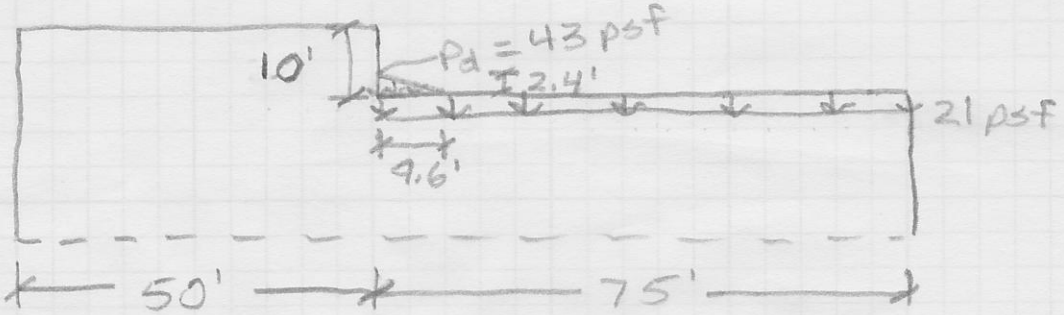


$P_g = 30$ psf
$C_t = 1.0$
$C_e = 1.0$
$I = 1.0$

$$P_f = 0.7(C_e)(C_t)(I)(P_g)$$
$$= 0.7(1.0)(1.0)(1.0)(30)$$
$$= 21 \text{ psf}$$

ASCE 7-02

$$h_d = 0.42 \sqrt[3]{l_u}\sqrt[4]{P_g + 10} - 1.5$$
$$= 0.42 \sqrt[3]{50}\sqrt[4]{30 + 10} - 1.5$$
$$h_d = 2.39 \text{ feet}$$
$$w = 4h_d = 9.6 \text{ feet}$$
$$\gamma = 0.13P_g + 14$$
$$= 0.13(30) + 14 = 17.9 \text{ pcf}$$
$$P_d = 17.9(2.39) = \underline{42.8 \text{ psf}}$$

ASCE 7-05

From figure 7-9
$h_d = 2.4$ feet
$w = 4(2.4) = 9.6$ feet
$\gamma = 0.13(30) + 14 = 17.9$ pcf
$P_d = 17.9(2.4) = \underline{43.0 \text{ psf}}$